Advanced High-Order Algorithms for High-Fidelity Simulation of Unsteady Flow

Prof. Antony Jameson

Department of Aeronautics & Astronautics

– *Aerospace Computing Laboratory* –

Stanford University

jameson@baboon.stanford.edu

AFOSR Computational Mathematics Program Review Meeting

August 1st, 2012, Arlington, VA

Outline

I. Current & Future Trends
- The Current Status of CFD
- The Future of CFD (?)
- Large-Eddy Simulation

II. The Aerospace Computing Lab

III. Overview of Numerical Methods
- Typical Requirements of CFD
- Classic Numerical Methods
- A Review of the Literature
- A Review of the Literature from ACL

IV. The FR Methodology
- Introduction
- The Flux Reconstruction Scheme
- The FR Scheme Graphically Illustrated
- The Energy Stability of the FR Scheme
- ESFR Schemes
- ESFR Schemes for 2nd-Order PDEs
- ESFR Schemes on Triangles
- Non-Linear Properties of the ESFR Schemes

V. Applications
- Numerical Dissipation
- High-Order Boundaries
- Maximum Time Step *vs.* Accuracy
- 3D Unsteady Flow over a Sphere
- Transitional Flow over SD7003 Airfoil
- Study of Flapping Wing Sections

VI. Structural LES Modeling
- Explicit Filtering in the SD Element
- The Restriction-Prolongation Filter
- Discrete Filters by Gauss Quadrature
- Discrete Filters for Arbitrary Points

VII. LES Computations
- Wall-Resolved Turbulent Channel Flow
- Wall-Modeling Strategy
- Wall-Modeled Turbulent Channel Flow
- Flow past a Square Cylinder

VIII. Conclusions and Summary

Outline

I. Current & Future Trends

- The Current Status of CFD
- The Future of CFD (?)
- Large-Eddy Simulation

II. The Aerospace Computing Lab

III. Overview of Numerical Methods

- Typical Requirements of CFD
- Classic Numerical Methods
- A Review of the Literature
- A Review of the Literature from ACL

IV. The FR Methodology

- Introduction
- The Flux Reconstruction Scheme
- The FR Scheme Graphically Illustrated
- The Energy Stability of the FR Scheme
- ESFR Schemes
- ESFR Schemes for 2nd-Order PDEs
- ESFR Schemes on Triangles
- Non-Linear Properties of the ESFR Schemes

V. Applications

- Numerical Dissipation
- High-Order Boundaries
- Maximum Time Step *vs.* Accuracy
- 3D Unsteady Flow over a Sphere
- Transitional Flow over SD7003 Airfoil
- Study of Flapping Wing Sections

VI. Structural LES Modeling

- Explicit Filtering in the SD Element
- The Restriction-Prolongation Filter
- Discrete Filters by Gauss Quadrature
- Discrete Filters for Arbitrary Points

VII. LES Computations

- Wall-Resolved Turbulent Channel Flow
- Wall-Modeling Strategy
- Wall-Modeled Turbulent Channel Flow
- Flow past a Square Cylinder

VIII. Conclusions

The Current Status of CFD

- Worldwide commercial and government codes are based on algorithms developed in the ‘80s and ‘90s
- These codes can handle complex geometry but are generally limited to 2^{nd} order accuracy
- They cannot handle turbulence without modeling
- Unsteady simulations are very expensive, and questions over accuracy remain

The Future of CFD (?)

CFD has been on a plateau for the past 15 years

- Representations of current state of the art:
  - Formula 1 cars
  - Complete aircrafts
- The majority of current CFD methods are not adequate for vortex dominated and transitional flows:
  - Rotorcraft
  - High-lift systems
  - Formation flying

Large-Eddy Simulation

The number of DoF for an LES of turbulent flow over an airfoil scales as **$Re_c^{1.8}$ (resp. $Re_c^{0.4}$) if the inner layer is resolved (resp. modeled)**

Rapid advances in computer hardware should make LES feasible within the foreseeable future for industrial problems at high Reynolds numbers. To realize this goal requires

- high-order algorithms for unstructured meshes (complex geometries)
- Sub-Grid Scale models applicable to wall bounded flows
- massively parallel implementation

Chapman (1979), AIAA J. 17(12)

Outline

I. Current & Future Trends
- The Current Status of CFD
- The Future of CFD (?)
- Large-Eddy Simulation

II. The Aerospace Computing Lab

III. Overview of Numerical Methods
- Typical Requirements of CFD
- Classic Numerical Methods
- A Review of the Literature
- A Review of the Literature from ACL

IV. The FR Methodology
- Introduction
- The Flux Reconstruction Scheme
- The FR Scheme Graphically Illustrated
- The Energy Stability of the FR Scheme
- ESFR Schemes
- ESFR Schemes for 2nd-Order PDEs
- ESFR Schemes on Triangles
- Non-Linear Properties of the ESFR Schemes

V. Applications
- Numerical Dissipation
- High-Order Boundaries
- Maximum Time Step *vs.* Accuracy
- 3D Unsteady Flow over a Sphere
- Transitional Flow over SD7003 Airfoil
- Study of Flapping Wing Sections

VI. Structural LES Modeling
- Explicit Filtering in the SD Element
- The Restriction-Prolongation Filter
- Discrete Filters by Gauss Quadrature
- Discrete Filters for Arbitrary Points

VII. LES Computations
- Wall-Resolved Turbulent Channel Flow
- Wall-Modeling Strategy
- Wall-Modeled Turbulent Channel Flow
- Flow past a Square Cylinder

VIII. Conclusions and Summary

Acknowledgement

The current research is a combined effort by

- *Postdocs*: Charlie Liang, Peter Vincent, Guido Lodato
- *Ph.D. students*: Sachin Premasuthan, Kui Ou, Patrice Castonguay, David Williams, Yves Allenau, Lala Li, Manuel Lopez, and Andy Chan

It is made possible by the support of

- the *Airforce Office of Scientific Research* under grant FA9550-10-1-0418 by Dr. Fariba Fahroo
- the *National Science Foundation* under grants 0708071 and 0915006 monitored by Dr. Leland Jameson

Typical Requirements of CFD

Traditional numerical schemes for engineering problems are too dissipative and do not provide sufficient accuracy for LES and DNS

• **Accuracy:**	solution must be right
• **Small numerical dissipation:**	unsteady flow features
• **Unstructured grids:**	complex geometries
• **Numerical flux:**	wave propagation problems
• **High resolution capabilities:**	transitional and turbulent flows
• **Efficiency:**	code parallelism
• **...**	

Classic Numerical Methods

Finite Difference

- Structured
- High-order
- Numerical flux

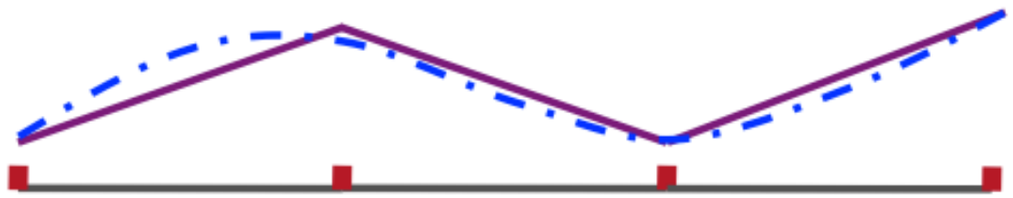

Finite Volume

- Unstructured
- Low-order
- Numerical flux

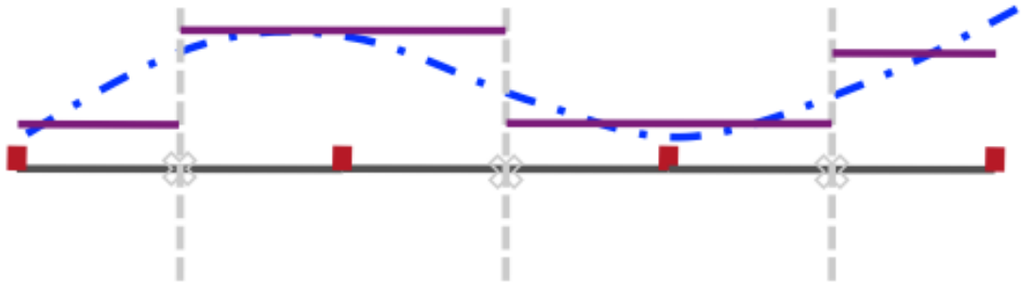

Continuous FE

- Unstructured
- High-order
- No numerical flux

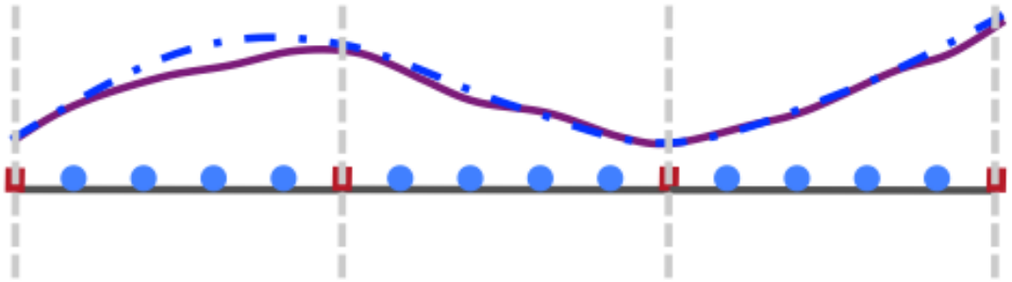

Classic Numerical Methods

Finite Difference

- Structured
- High-order
- Numerical flux

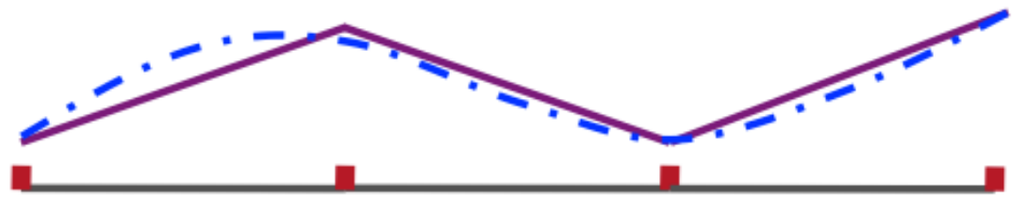

Finite Volume

- Unstructured
- Low-order
- Numerical flux

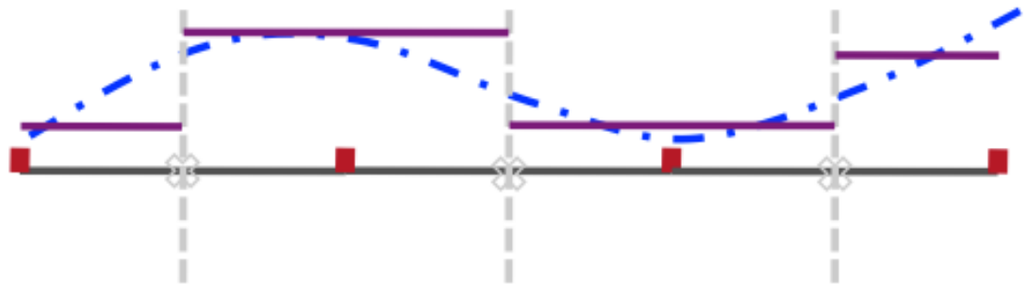

Continuous FE

- Unstructured
- High-order
- No numerical flux

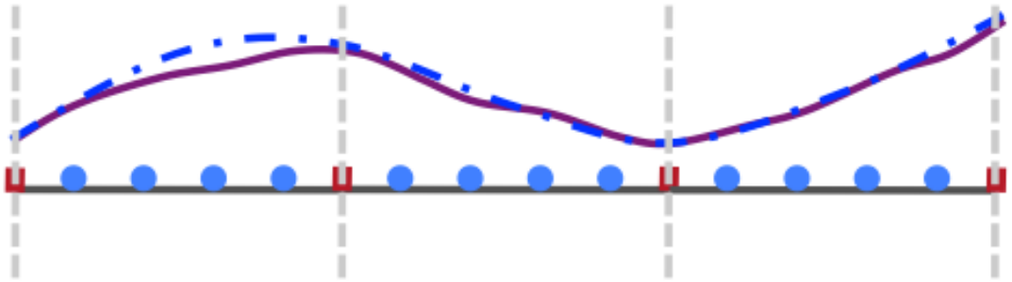

Disontinuous FE

- Unstructured
- High-order
- Numerical flux

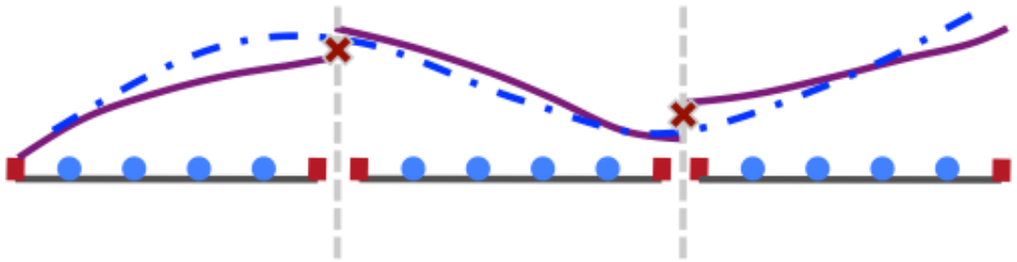

A Review of the Literature

Past Research on DG Schemes:

- Modern development of DG schemes for hyperbolic conservation laws stems from the work of Cockburn & Shu [1989a,1989b,1990,1998,2001]

Recent Research:

Attempts to reduce complexity and avoid quadrature:

- Spectral Difference (SD) scheme by Kopriva & Kolias [1996], Liu, Vinokur & Wang [2006]
- Nodal Discontinuous Galerkin (NDG) scheme by Atkins & Shu [1998], Hesthaven & Warburton [2007]
- Flux Reconstruction (FR) scheme by Huynh [2007,2009]

Cockburn, et al. (1989). J. Comput. Phys., 84(1); Cockburn, Shu (1989). Math. Comput., 52; Cockburn, et al. (1990). Math. Comput., 54(190); Cockburn, Shu (1998). J. Comput. Phys., 141; Cockburn, Shu (2001). J. Sci. Comput., 16; Kopriva, Kolias (1996). J. Comput. Phys., 125(1); Liu, et al. (2006). J. Comput. Phys., 216(2); Atkins, Shu (1998). AIAA J., 36(5); Hesthaven, Warburton, (Springer Verlag, 2007); Huynh, (2007). AIAA P., 2007-4079; Huynh, (2009) AIAA P., 2009-403

Outline

I. Current & Future Trends
- The Current Status of CFD
- The Future of CFD (?)
- Large-Eddy Simulation

II. The Aerospace Computing Lab

III. Overview of Numerical Methods
- Typical Requirements of CFD
- Classic Numerical Methods
- A Review of the Literature
- A Review of the Literature from ACL

IV. The FR Methodology
- Introduction
- The Flux Reconstruction Scheme
- The FR Scheme Graphically Illustrated
- The Energy Stability of the FR Scheme
- ESFR Schemes
- ESFR Schemes for 2nd-Order PDEs
- ESFR Schemes on Triangles
- Non-Linear Properties of the ESFR Schemes

V. Applications
- Numerical Dissipation
- High-Order Boundaries
- Maximum Time Step *vs.* Accuracy
- 3D Unsteady Flow over a Sphere
- Transitional Flow over SD7003 Airfoil
- Study of Flapping Wing Sections

VI. Structural LES Modeling
- Explicit Filtering in the SD Element
- The Restriction-Prolongation Filter
- Discrete Filters by Gauss Quadrature
- Discrete Filters for Arbitrary Points

VII. LES Computations
- Wall-Resolved Turbulent Channel Flow
- Wall-Modeling Strategy
- Wall-Modeled Turbulent Channel Flow
- Flow past a Square Cylinder

VIII. Conclusions and Summary

Introduction

- **The following presentation emphasizes development of Huynh's FR approach, and energy stability**
- **Energy stability analysis versus Fourier stability analysis**
  - Energy method is more general and rigorous
  - Energy method enables stability proofs for all orders of accuracy
  - Energy method applies to non-uniform meshes
  - *Fourier analysis provides more detailed information about the distribution of dispersive and diffusive errors*
  - *Fourier analysis identifies super accuracy for linear problems*

The Energy Stable FR scheme (ESFR):

- **Until recently, stable FR schemes identified on an ad hoc basis**
- **We have identified a range of correction functions that guarantee linear stability for all orders of accuracy**
- **Achieved by extending Jameson's proof of stability of an SD scheme for the linear advection equation for all orders of accuracy**

The Flux Reconstruction Scheme

The solution is locally represented by Lagrange polynomial of degree $n-1$ on the solution points:

$$u_h = \sum_{j=1}^{n} u_j l_j(x) \qquad f_h^D = \sum_{j=1}^{n} f_j^D l_j(x)$$

The flux is discontinuous and needs to be corrected in a suitable way

$$\Delta_L = \widetilde{f}_L - f_h^D(-1) \qquad \Delta_R = \widetilde{f}_R - f_h^D(1)$$

$$h_L(-1) = 1, \quad h_L(1) = 0 \qquad h_R(1) = 1, \quad h_R(-1) = 0$$

The continuous flux is obtained from the discontinuous counterpart by adding the correction functions of degree n weighted by the flux corrections

$$f_h^C = \sum_{j=1}^{n} f_j^D l_j(x) + h_L(x)\Delta_L + h_R(x)\Delta_R$$

The continuous flux is finally differentiated at the solution points and the solution is advanced in time

$$\frac{\partial u_i}{\partial t} + \left[\sum_{j=1}^{n} f_j^D \frac{\mathrm{d}l_j}{\mathrm{d}x}(x_i) + \Delta_L \frac{\mathrm{d}h_L}{\mathrm{d}x}(x_i) + \Delta_R \frac{\mathrm{d}h_R}{\mathrm{d}x}(x_i) \right] = 0$$

Huynh, (2007). AIAA P., 2007-4079; Huynh, (2009) AIAA P., 2009-403

The FR Scheme Graphically Illustrated

The solution is locally represented by Lagrange polynomial of degree *n*-1 on the *n* solution points:

$$u_h = \sum_{j=1}^{n} u_j l_j(x)$$

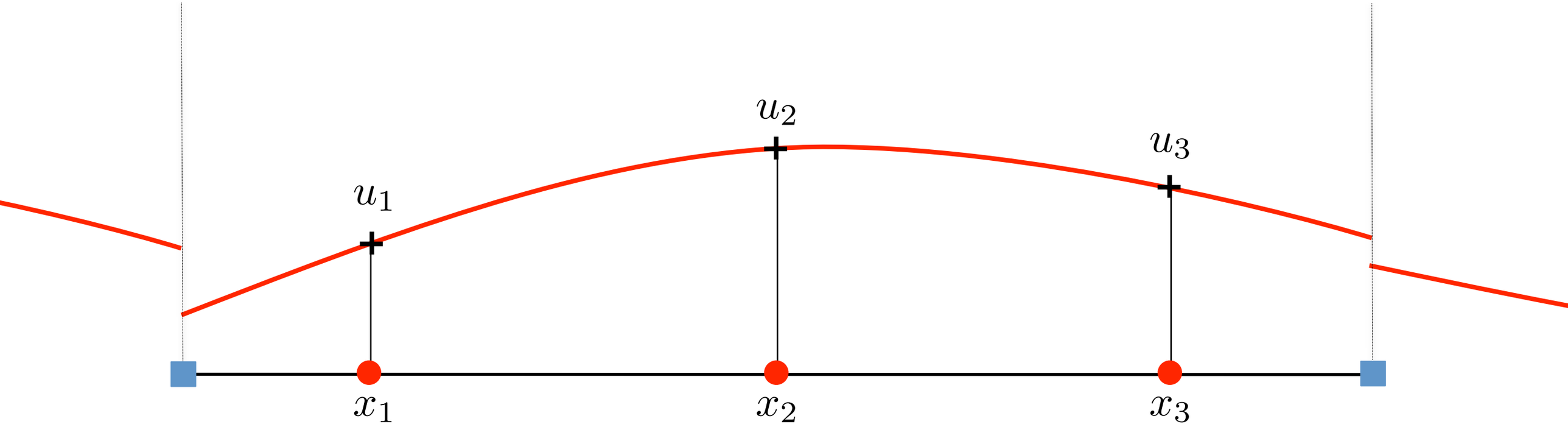

Huynh, (2007). AIAA P., 2007-4079; Huynh, (2009) AIAA P., 2009-403

The FR Scheme Graphically Illustrated

The discontinuous flux is constructed

$$f_h^D = \sum_{j=1}^{n} f_j^D l_j(x)$$

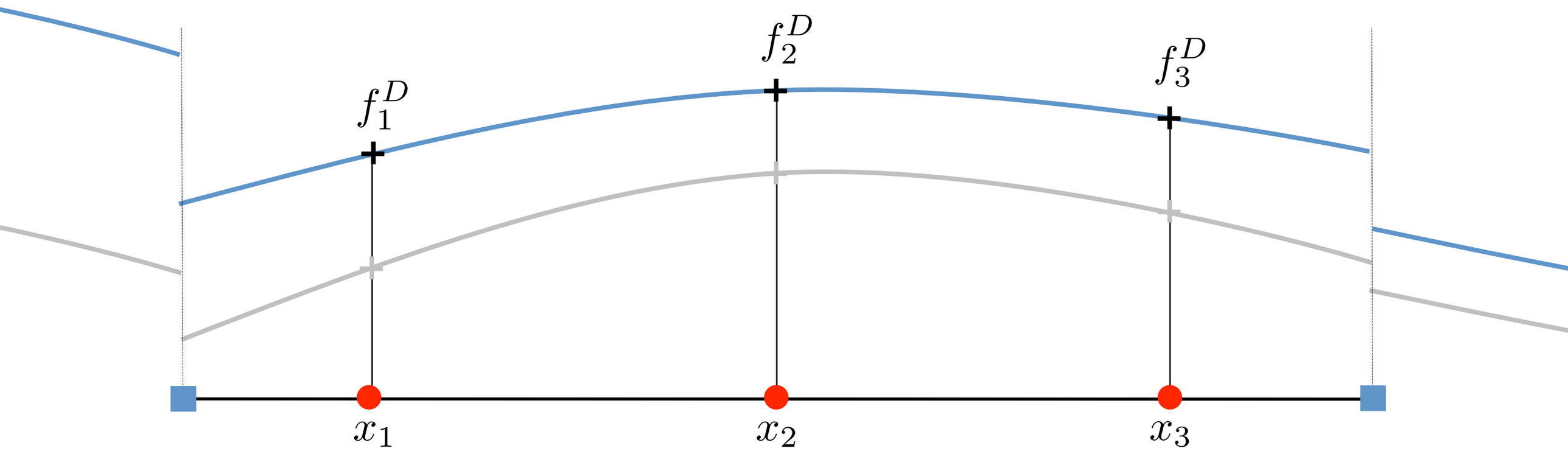

Huynh, (2007). AIAA P., 2007-4079; Huynh, (2009) AIAA P., 2009-403

The FR Scheme Graphically Illustrated

Solution is evaluated at element boundaries

$$u_L = \sum_{j=1}^{n} u_j l_j(-1) \qquad u_R = \sum_{j=1}^{n} u_j l_j(+1)$$

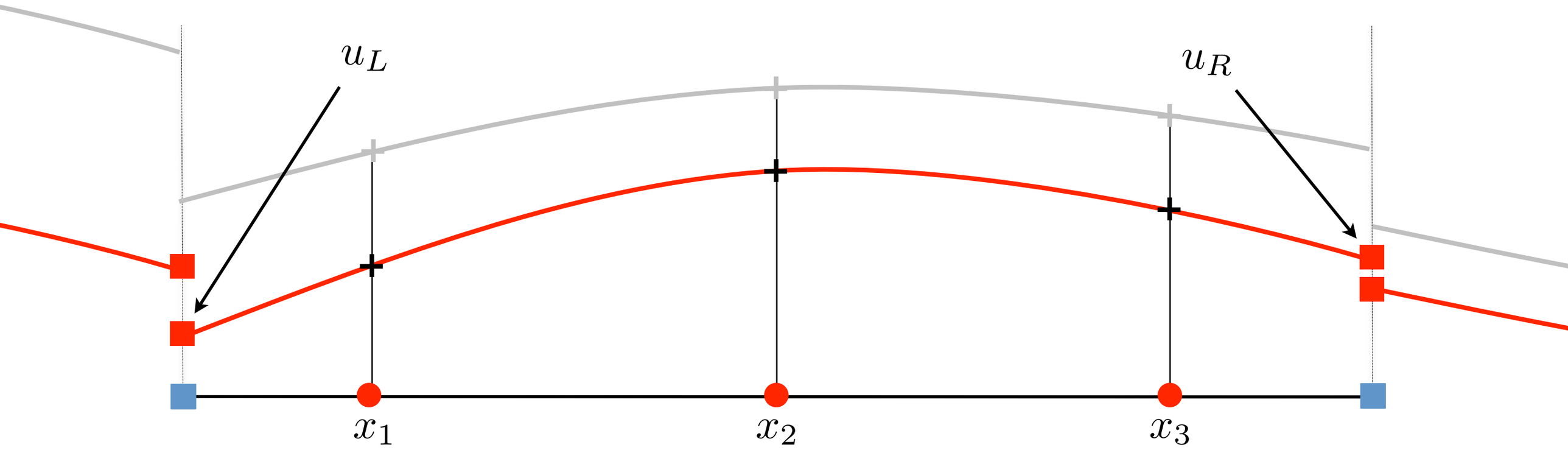

Huynh, (2007). AIAA P., 2007-4079; Huynh, (2009) AIAA P., 2009-403

The FR Scheme Graphically Illustrated

The common interface flux is computed from multiply defined values at each interface (FV-type numerical flux such as approximate Riemann flux)

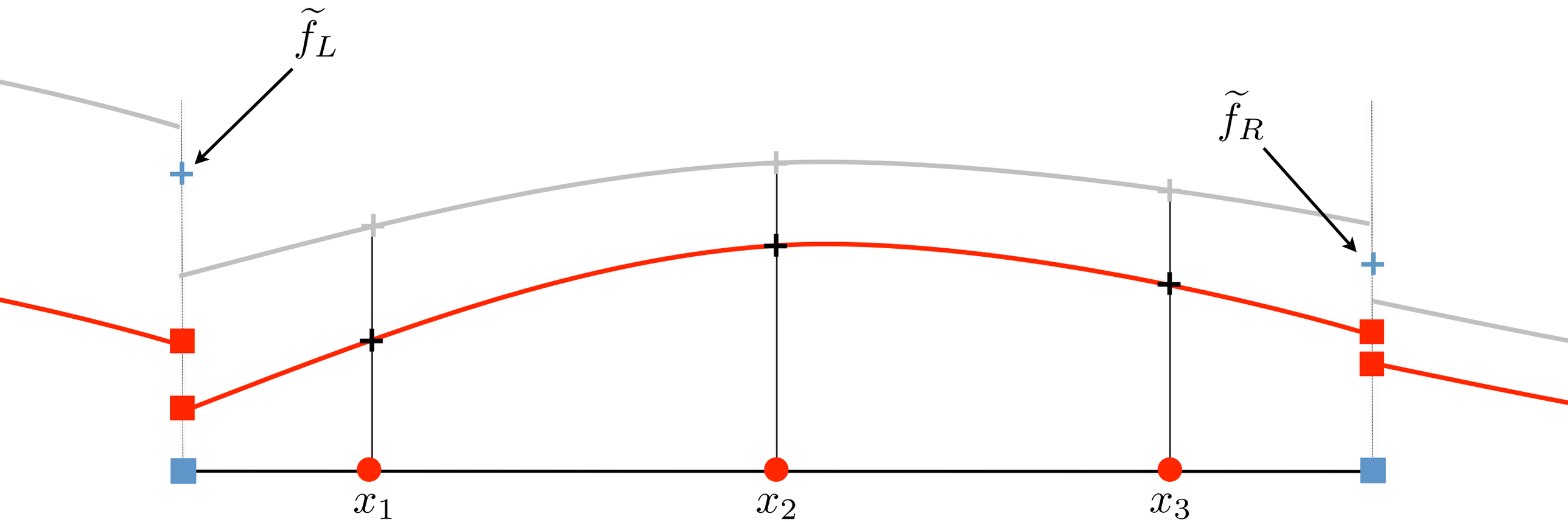

Huynh, (2007). AIAA P., 2007-4079; Huynh, (2009) AIAA P., 2009-403

The FR Scheme Graphically Illustrated

The common interface flux is computed from multiply defined values at each interface (FV-type numerical flux such as approximate Riemann flux)

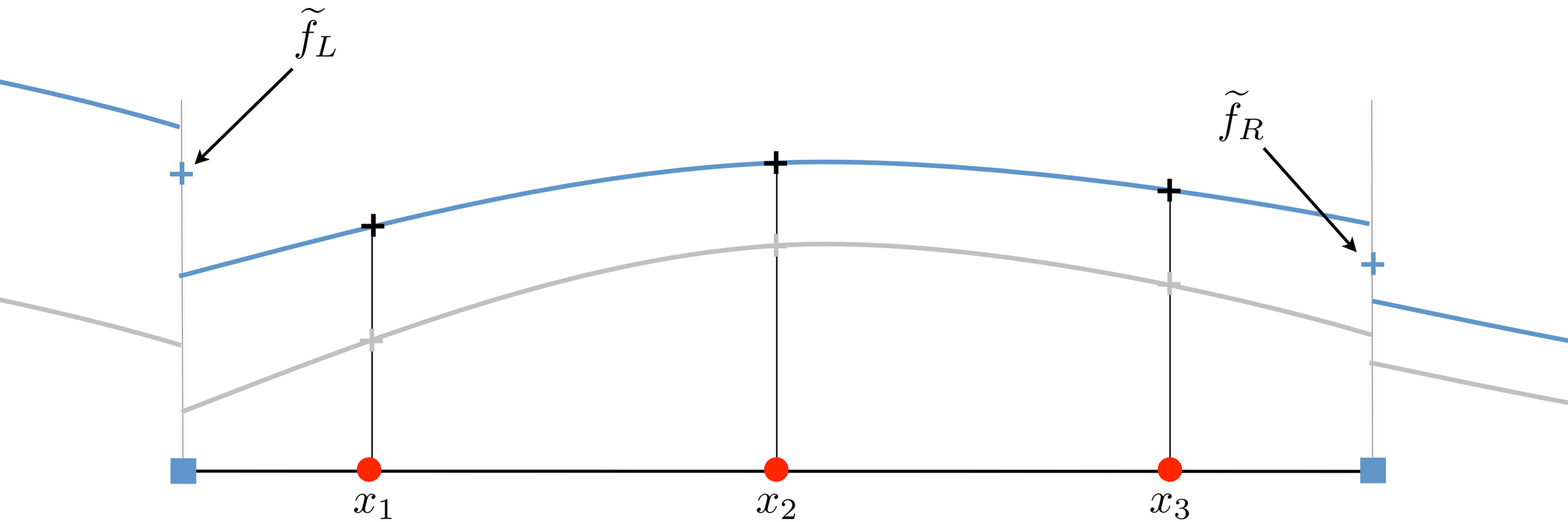

Huynh, (2007). AIAA P., 2007-4079; Huynh, (2009) AIAA P., 2009-403

The FR Scheme Graphically Illustrated

Correction functions of degree *n* are introduced

$$h_L(-1) = 1, \quad h_L(1) = 0$$

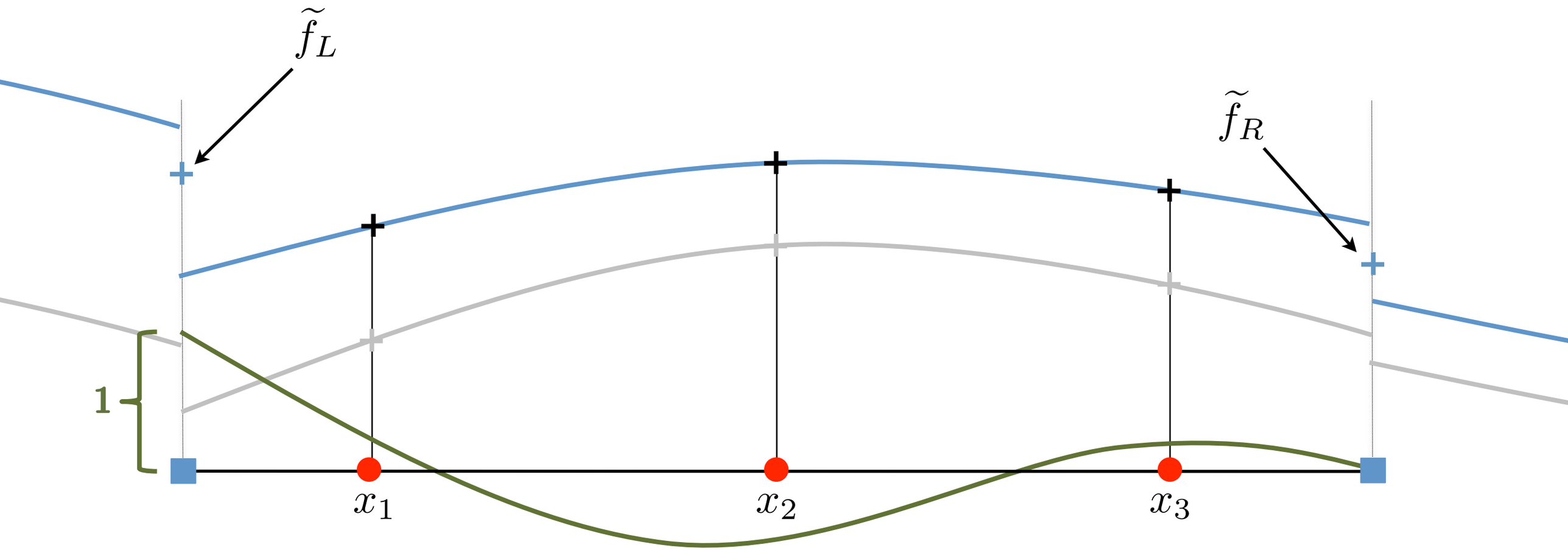

Huynh, (2007). AIAA P., 2007-4079; Huynh, (2009) AIAA P., 2009-403

The FR Scheme Graphically Illustrated

The correction functions are scaled

$$\Delta_L = \widetilde{f}_L - f_h^D(-1)$$

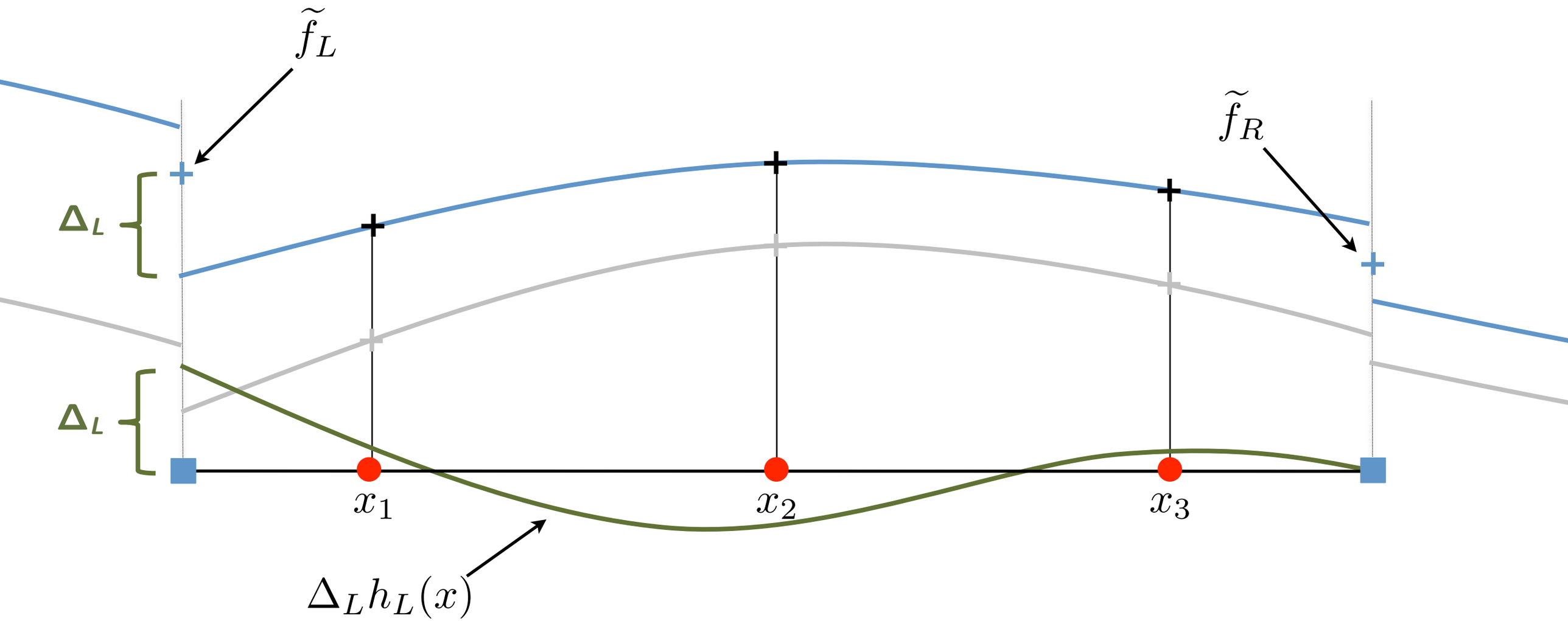

Huynh, (2007). AIAA P., 2007-4079; Huynh, (2009) AIAA P., 2009-403

The FR Scheme Graphically Illustrated

The correction is added to the discontinuous flux

$$f_h^* = \sum_{j=1}^{n} f_j^D l_j(x) + h_L(x)\Delta_L$$

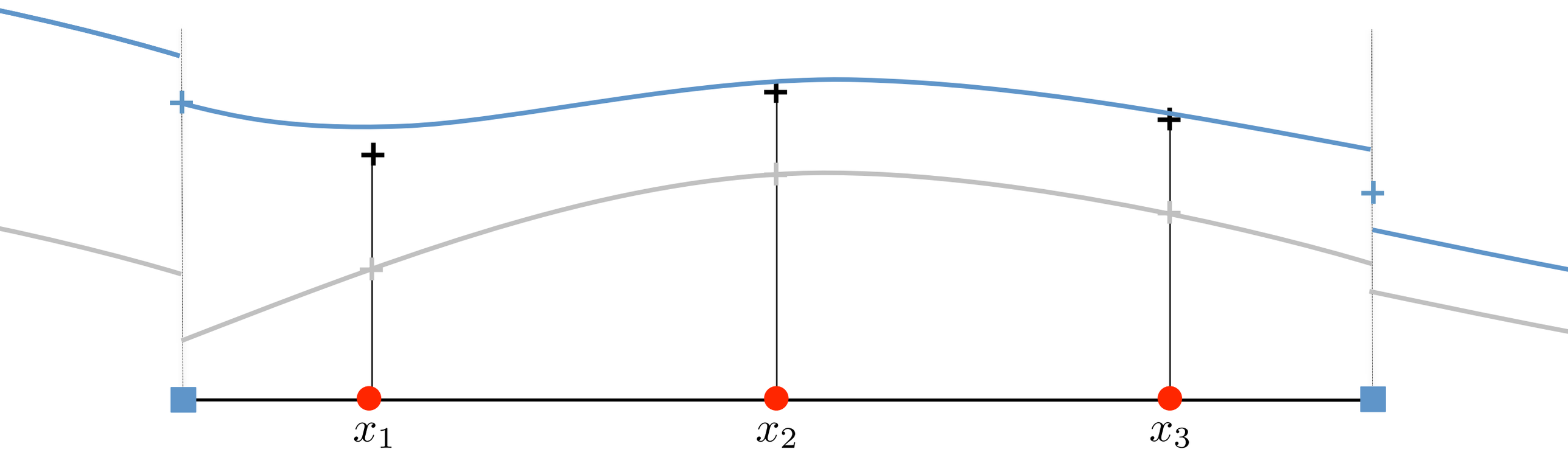

Huynh, (2007). AIAA P., 2007-4079; Huynh, (2009) AIAA P., 2009-403

The FR Scheme Graphically Illustrated

The right boundary is corrected the same way

$$h_R(1) = 1, \quad h_R(-1) = 0$$

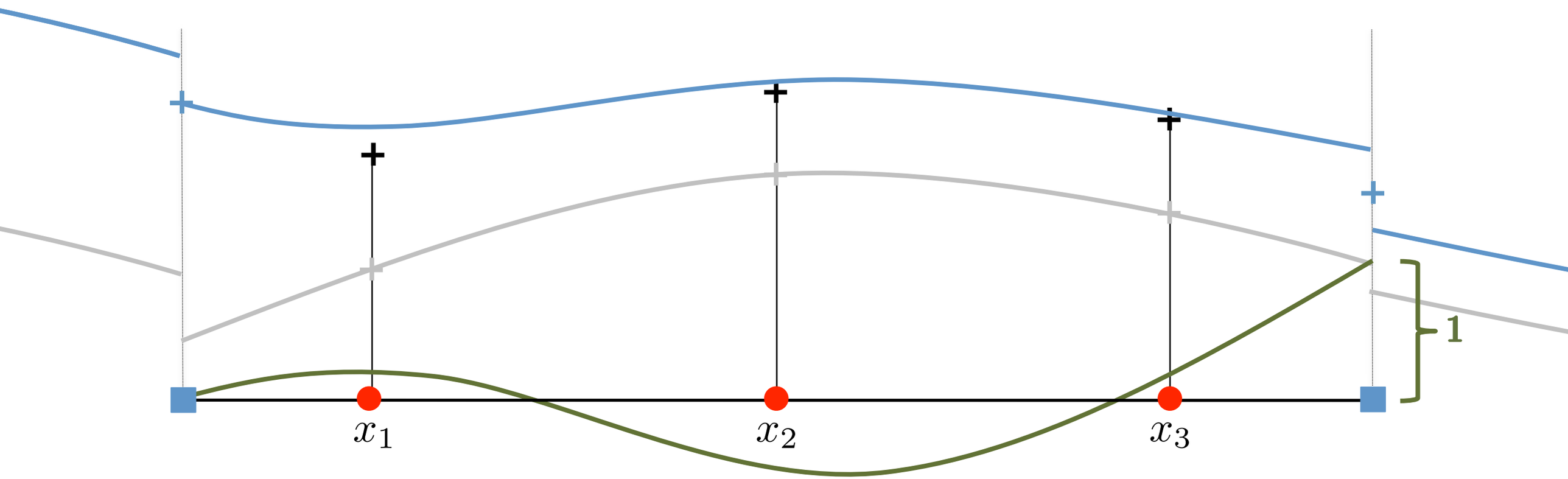

Huynh, (2007). AIAA P., 2007-4079; Huynh, (2009) AIAA P., 2009-403

The FR Scheme Graphically Illustrated

The correction is scaled...

$$\Delta_R = \widetilde{f}_R - f_h^D(+1)$$

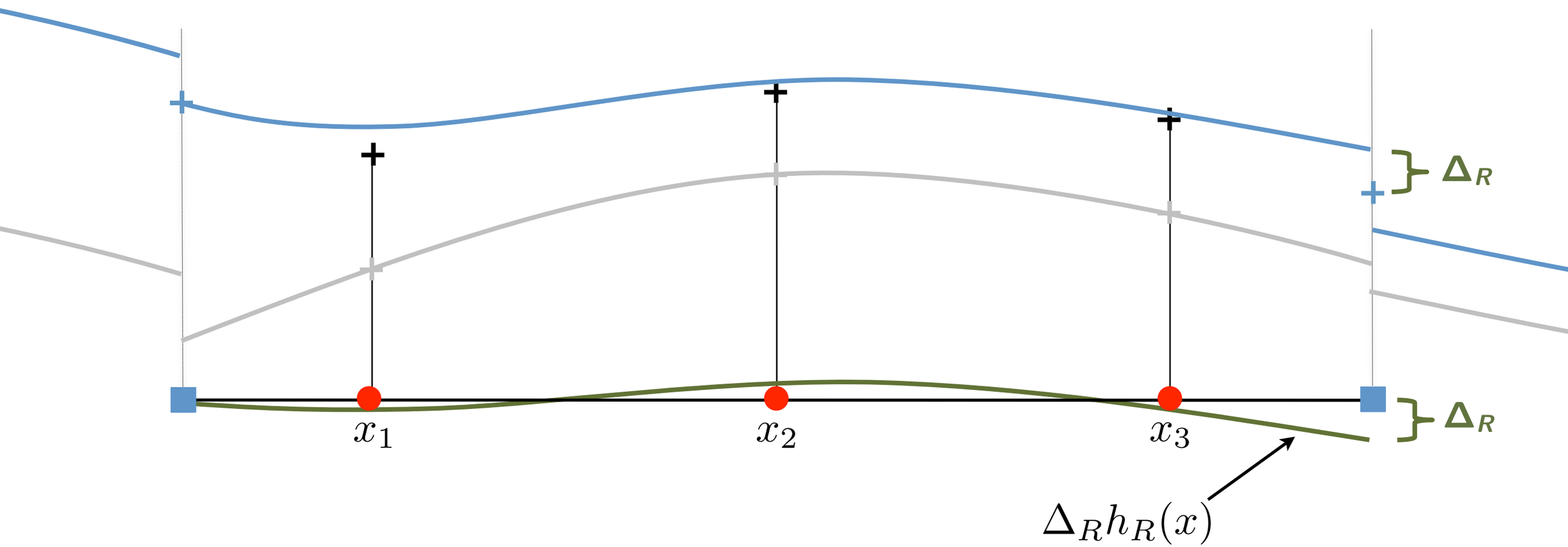

Huynh, (2007). AIAA P., 2007-4079; Huynh, (2009) AIAA P., 2009-403

The FR Scheme Graphically Illustrated

And added to the discontinuous flux

$$f_h^C = \sum_{j=1}^{n} f_j^D l_j(x) + h_L(x)\Delta_L + h_R(x)\Delta_R$$

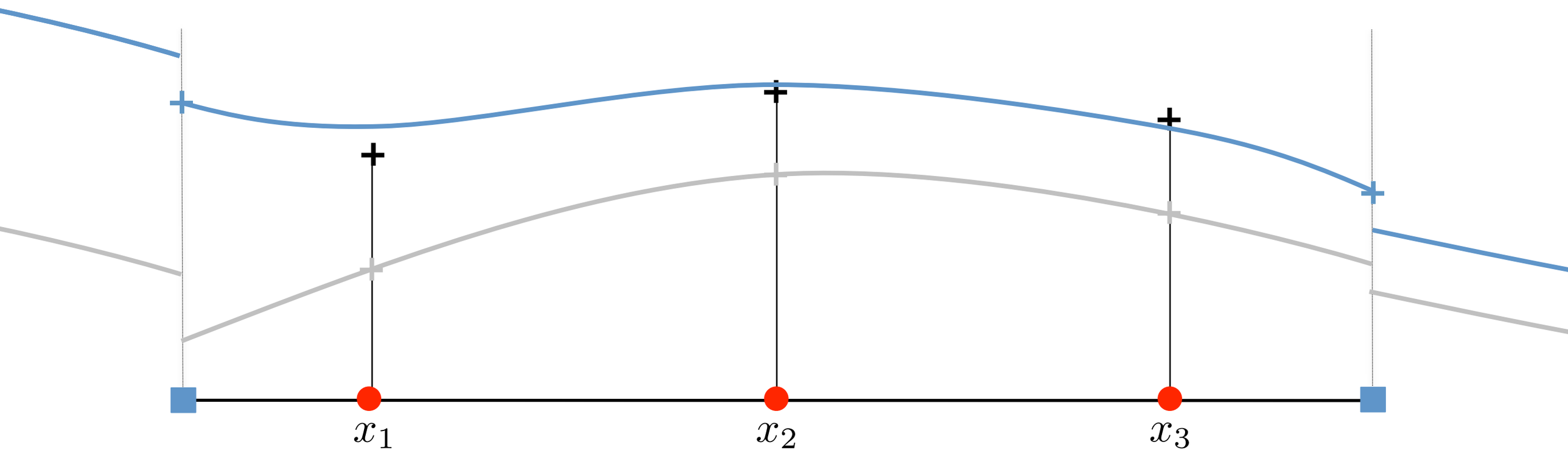

Huynh, (2007). AIAA P., 2007-4079; Huynh, (2009) AIAA P., 2009-403

The FR Scheme Graphically Illustrated

Total approximate continuous flux

$$f_h^C = \sum_{j=1}^{n} f_j^D l_j(x) + h_L(x)\Delta_L + h_R(x)\Delta_R$$

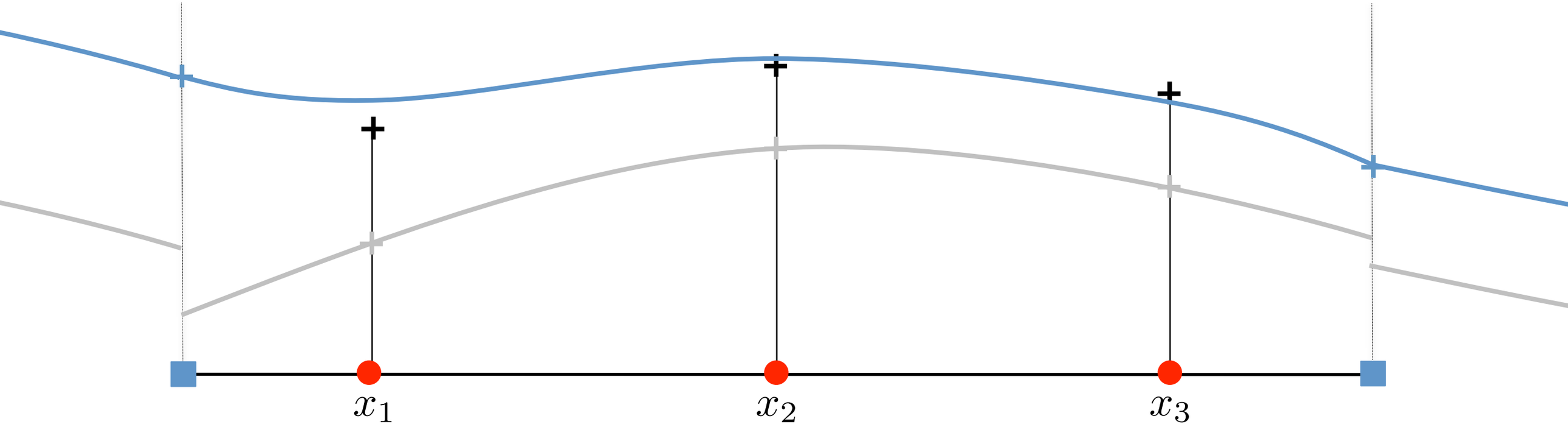

Huynh, (2007). AIAA P., 2007-4079; Huynh, (2009) AIAA P., 2009-403

The FR Scheme Graphically Illustrated

The divergence of the flux is evaluated at the solution points

$$\frac{\partial f^C}{\partial x}(x_i) = \sum_{j=1}^{n} f_j^D \frac{\mathrm{d}l_j}{\mathrm{d}x}(x_i) + \Delta_L \frac{\mathrm{d}h_L}{\mathrm{d}x}(x_i) + \Delta_R \frac{\mathrm{d}h_R}{\mathrm{d}x}(x_i)$$

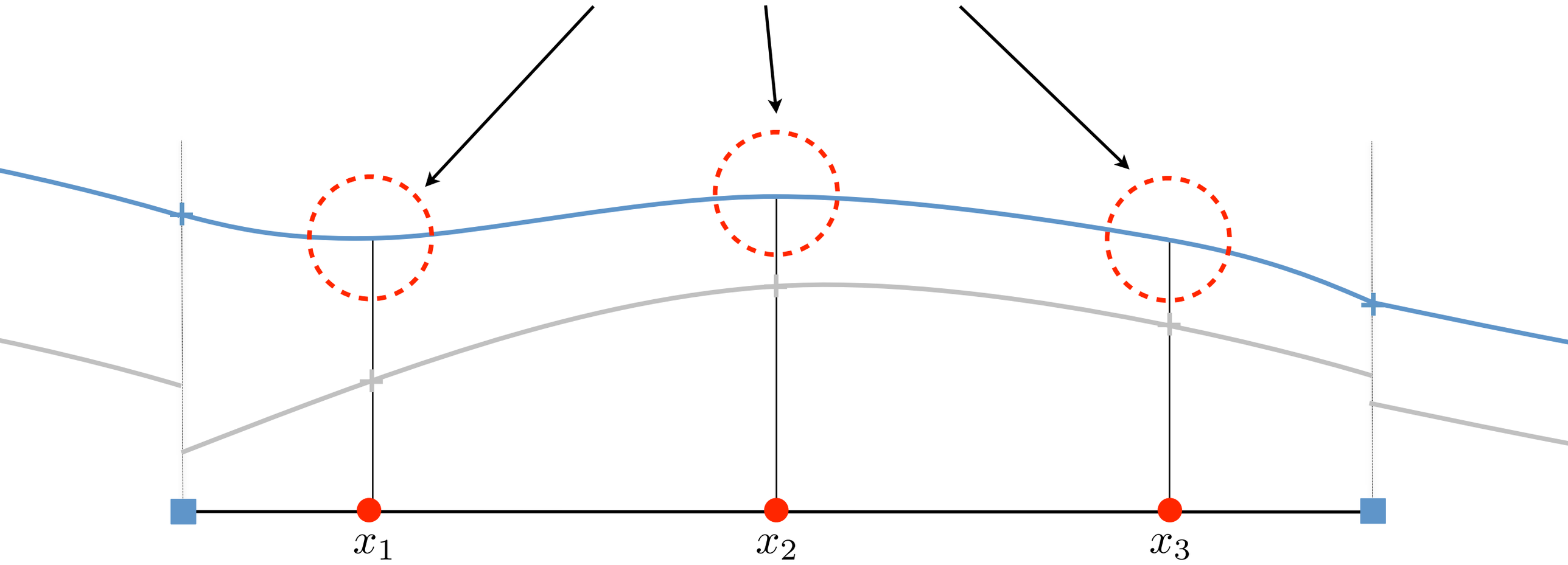

Huynh, (2007). AIAA P., 2007-4079; Huynh, (2009) AIAA P., 2009-403

The FR Scheme Graphically Illustrated

The solution is advanced in time

$$\frac{\partial u_i}{\partial t} + \left[\sum_{j=1}^{n} f_j^D \frac{\mathrm{d}l_j}{\mathrm{d}x}(x_i) + \Delta_L \frac{\mathrm{d}h_L}{\mathrm{d}x}(x_i) + \Delta_R \frac{\mathrm{d}h_R}{\mathrm{d}x}(x_i) \right] = 0$$

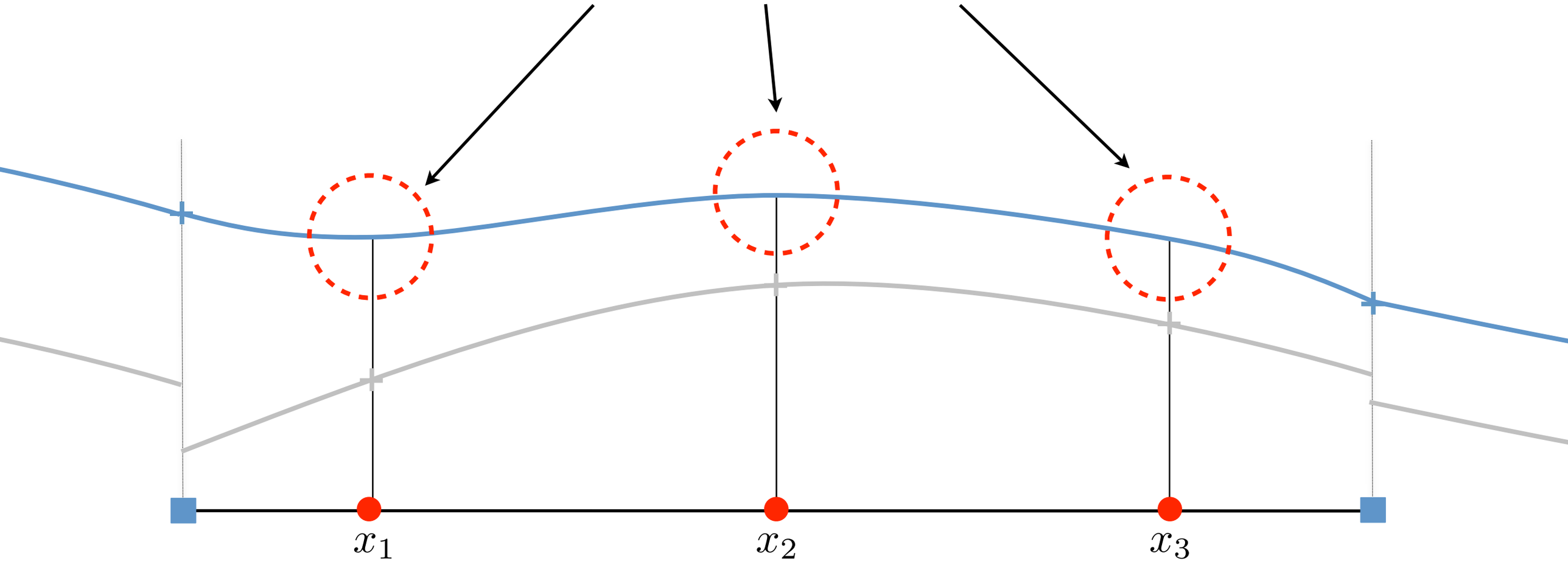

Huynh, (2007). AIAA P., 2007-4079; Huynh, (2009) AIAA P., 2009-403

Energy Stability of the FR Scheme

The FR method defines a family of energy stable schemes in the norm

$$||U^{\delta D}||_{p,2} = \left[\sum_{n=1}^{N}\int_{x_n}^{x_{n+1}} (U_n^{\delta D})^2 + \frac{c}{2}(J_n)^{2p}\left(\frac{\partial^p U_n^{\delta D}}{\partial x^p}\right)^2 \mathrm{d}x\right]^{1/2}$$

The schemes have the form

$$\frac{\partial u_i}{\partial t} + \left[\sum_{j=1}^{n} f_j^D \frac{\mathrm{d}l_j}{\mathrm{d}x}(x_i) + \Delta_L \frac{\mathrm{d}h_L}{\mathrm{d}x}(x_i) + \Delta_R \frac{\mathrm{d}h_R}{\mathrm{d}x}(x_i)\right] = 0$$

where the correction functions in terms of Legendre polynomials are

$$h_L = \frac{(-1)^p}{2}\left[L_p - \left(\frac{\eta_p(c)L_{p-1} + L_{p+1}}{1+\eta_p(c)}\right)\right]$$

$$h_R = \frac{(+1)^p}{2}\left[L_p + \left(\frac{\eta_p(c)L_{p-1} + L_{p+1}}{1+\eta_p(c)}\right)\right]$$

with a single parameter c

$$\eta_p(c) = \frac{c(2p+1)(a_p p!)^2}{2}$$

Vincent, et al. (2010). J. Sci. Comput., 47(1); Vincent, et al. (2011). J. Comput. Phys., 230(22)

ESFR Schemes

If correction functions $h_L(\xi)$ (and $h_R(\xi)$ by symmetry) satisfy

$$\int_{-1}^{1} h_L \frac{\mathrm{d}l_i}{\mathrm{d}\xi}\mathrm{d}\xi - c\left(\frac{\mathrm{d}^p l_i}{\mathrm{d}\xi^p}\right)\left(\frac{\mathrm{d}^{p+1} h_L}{\mathrm{d}\xi^{p+1}}\right) = 0 \qquad \forall i$$

with

$$\frac{-2}{(2p+1)(a_p p!)^2} < c < \infty, \qquad a_p = \frac{(2p)!}{2^p (p!)^2}.$$

and the numerical flux is computed as

$$F^{\delta I} = a\left[\frac{U_+^{\delta D} + U_-^{\delta D}}{2}\right] - |a|\lambda\left[\frac{U_+^{\delta D} - U_-^{\delta D}}{2}\right], \qquad 0 \le \lambda \le 1$$

then

$$\frac{\mathrm{d}}{\mathrm{d}t}||U^{\delta D}||_{p,2}^2 \le 0$$

where

$$||U^{\delta D}||_{p,2} = \left[\sum_{n=1}^{N}\int_{x_n}^{x_{n+1}} (U_n^{\delta D})^2 + \frac{c}{2}(J_n)^{2p}\left(\frac{\partial^p U_n^{\delta D}}{\partial x^p}\right)^2 \mathrm{d}x\right]^{1/2}$$

ESFR Schemes

Dispersion and dissipation properties from von Neumann stability analysis:

- Upwind flux
- $p = 3$
- x-axis: wave number
- y-axis: real part of temporal frequency
- Range over which true dispersion relation is reasonably approximated is maximal for

$$c_{DG} < c < c_{SD}$$

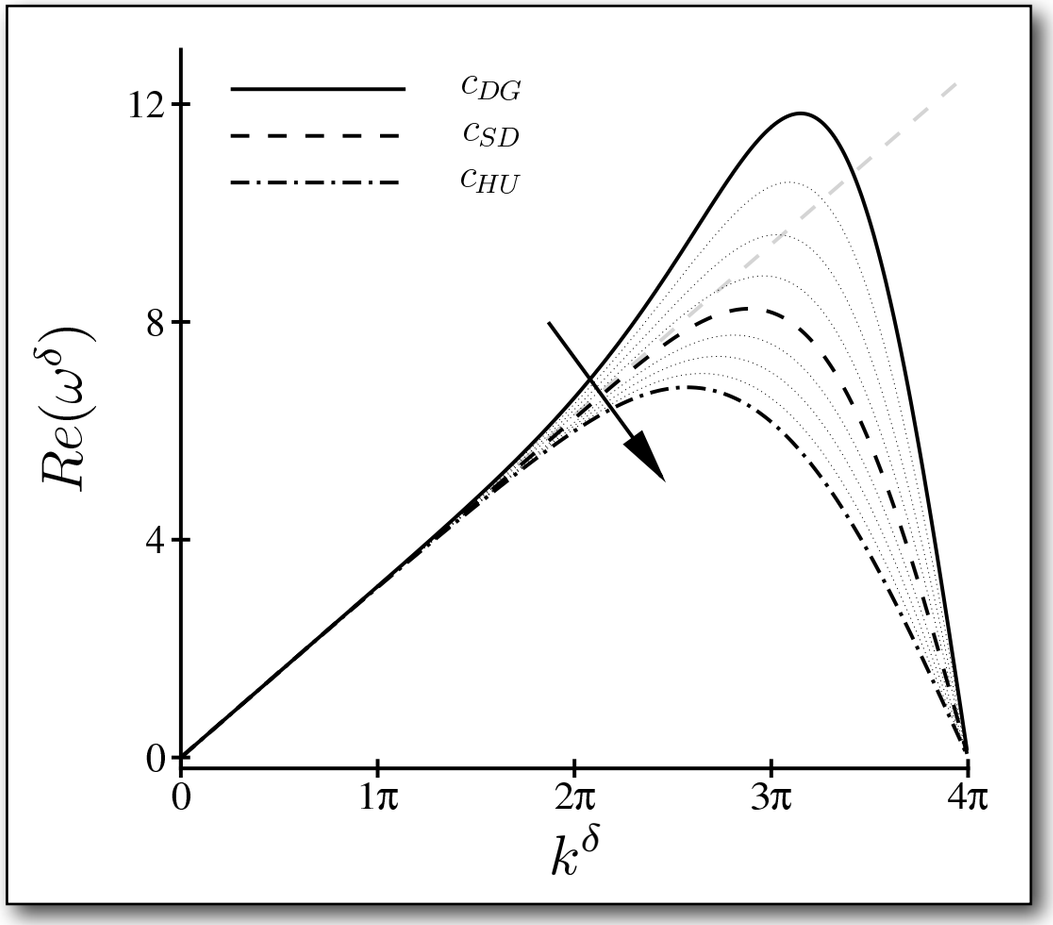

ESFR Schemes

Explicit time step limit:

- Upwind flux
- $p = 2$
- x-axis: parameter defining the ESFR scheme
- y-axis: maximum allowable time step
- there exists a value of c that maximizes the allowable time step, which will be denoted as

$$c_+$$

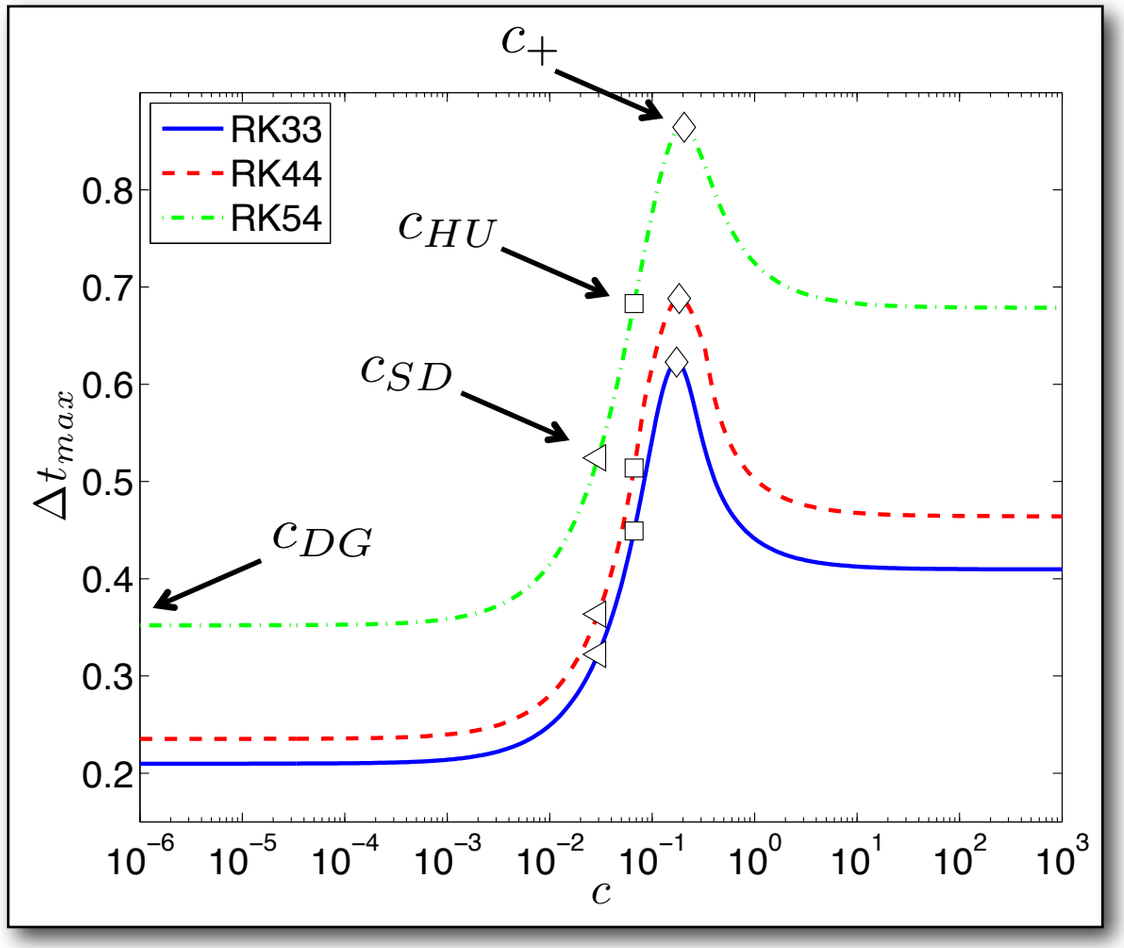

ESFR Schemes for 2nd-Order PDEs

Can extend the FR approach to 2nd-order PDEs

Main idea is to write PDE as a system of two first-order PDEs

$$\frac{\partial U}{\partial t} + \frac{\partial}{\partial x}\left[F(U, \frac{\partial U}{\partial x})\right] = 0$$

$$Q - \frac{\partial U}{\partial x} = 0 \qquad \frac{\partial U}{\partial t} + \frac{\partial}{\partial x}\left[F(U, Q)\right] = 0$$

Use FR procedure on both equations

Flux correction functions $h_L(\xi)$ and $h_R(\xi)$
Solution correction functions $g_L(\xi)$ and $g_R(\xi)$

ESFR Schemes for 2nd-Order PDEs

For the advection-diffusion equation

$$\frac{\partial U}{\partial t} + a\frac{\partial U}{\partial x} - b\frac{\partial^2 U}{\partial x^2} = 0$$

If ESFR correction functions are used on both equations, i.e.

Flux correction function: $$h_L = \frac{(-1)^p}{2}\left[\Psi_p - \left(\frac{\Upsilon_p(c)\Psi_{p-1} + \Psi_{p+1}}{1+\Upsilon_p(c)}\right)\right],$$

Sol. correction function: $$g_L = \frac{(-1)^p}{2}\left[\Psi_p - \left(\frac{\Upsilon_p(\kappa)\Psi_{p-1} + \Psi_{p+1}}{1+\Upsilon_p(\kappa)}\right)\right],$$

with

$$\frac{-2}{(2p+1)(a_p p!)^2} < c < \infty, \qquad \frac{-2}{(2p+1)(a_p p!)^2} < \kappa < \infty,$$

ESFR Schemes for 2nd-Order PDEs

The inviscid interface flux is computed as

$$F_{inv}^{\delta I} = a\left[\frac{U_+^{\delta D} + U_-^{\delta D}}{2}\right] - |a|\lambda\left[\frac{U_+^{\delta D} - U_-^{\delta D}}{2}\right],$$

The interface solution and interface viscous flux are of LDG type, i.e.

$$U^{\delta I} = \{\{U^{\delta D}\}\} + \beta[\![U^{\delta D}]\!] \qquad F_{vis}^{\delta I} = \{\{F_{vis}^{\delta D}\}\} - \beta[\![F_{vis}^{\delta D}]\!] - \tau[\![U^{\delta D}]\!]$$

where

$$[\![w]\!] = w_+ - w_- \qquad \{\{w\}\} = \frac{(w_- + w_+)}{2}$$

Then,

$$\frac{1}{2}\frac{\mathrm{d}}{\mathrm{d}t}||U^{\delta D}||_{p,c}^2 + b||Q^{\delta D}||_{p,\kappa}^2 = \sum_{e=1}^{N}\left[-|a|\frac{\lambda}{2}\left(U_{e,+}^{\delta D} - U_{e,-}^{\delta D}\right)^2 - \tau(U_{e,+}^{\delta D} - U_{e,-}^{\delta D})^2\right]$$

Castonguay, *et al.*, (2012), J. Comput. Phys., Article submitted for publication

ESFR Schemes on Triangles

- FR schemes can easily be extended to quadrilateral elements and hexahedral elements by using a tensor product formulation
- On simplex elements, such a tensor product formulation is not possible
- Extended FR approach to triangular elements
- Represent the solution inside each cell using a polynomial of degree p, using a set of $(p+1)(p+2)/2$ solution points

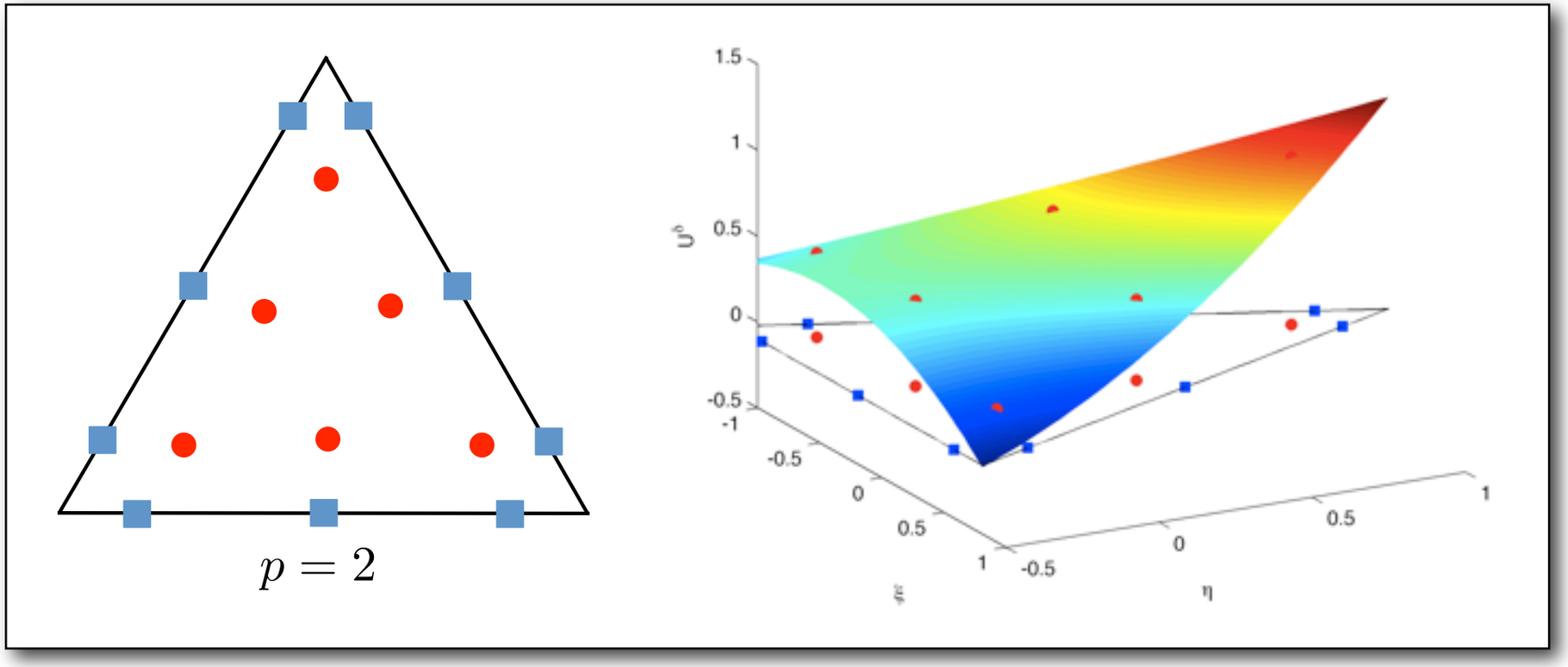

ESFR Schemes on Triangles

Total approximate flux

In 1D:

$$\hat{F}^{\delta} = \hat{F}^{\delta D}(\xi) + \Delta_L h_L(\xi) + \Delta_R h_R(\xi)$$

On triangles:

$$\hat{F}^{\delta} = \hat{F}^{\delta D}(\boldsymbol{\xi}) + \sum_{f=1}^{3} \sum_{k=1}^{p+1} \Delta_{f,k} \mathbf{h}_{f,k}(\boldsymbol{\xi})$$

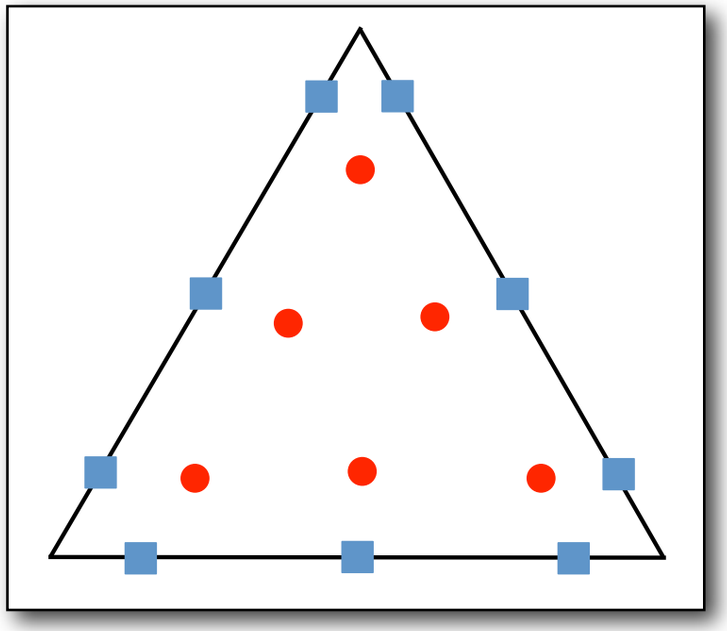

where

$$\Delta_{f,j} = \left[(\hat{\mathbf{F}} \cdot \hat{\mathbf{n}})^{\delta I}_{f,k} - (\hat{\mathbf{F}}^{\delta D} \cdot \hat{\mathbf{n}})_{f,k} \right]$$

$\mathbf{h}_{f,k}(\boldsymbol{\xi})$ is a correction function associated with flux point *f,k*

ESFR Schemes on Triangles

Associate a vector correction function $\mathbf{h}_{f,k}(\boldsymbol{\xi})$ with each flux point

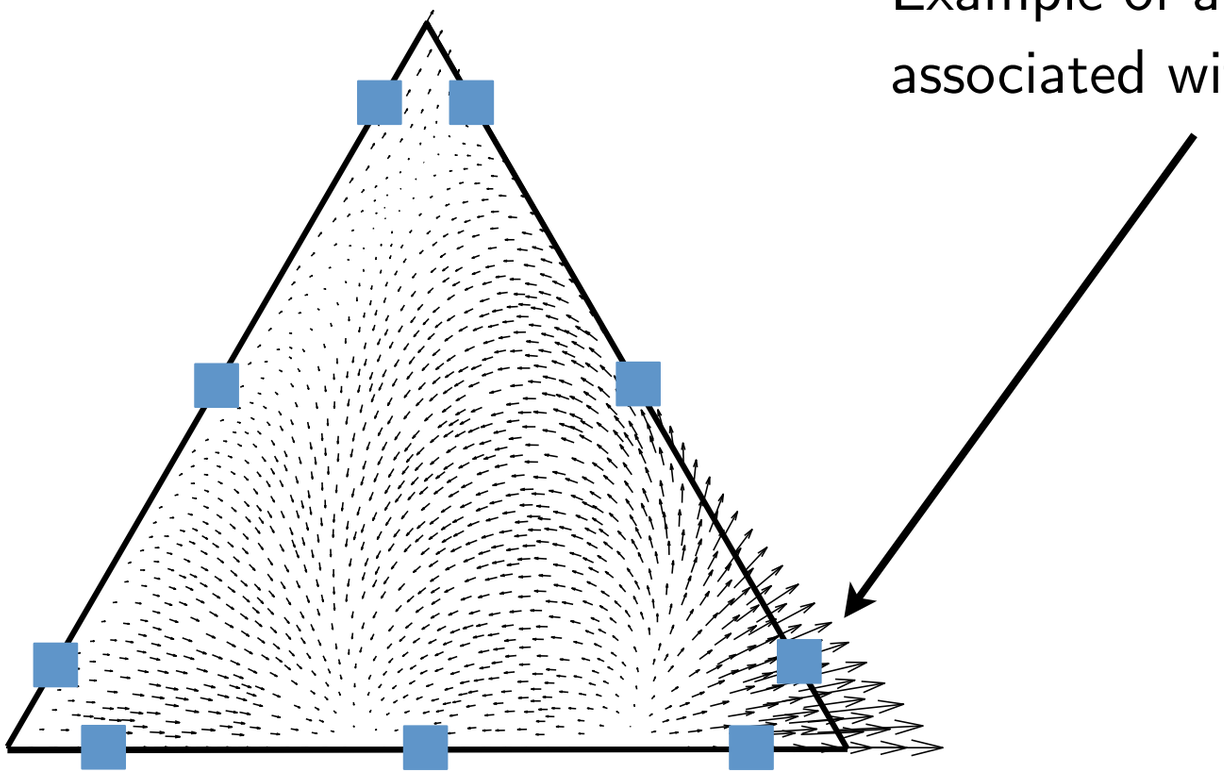

Example of a vector correction function $\mathbf{h}_{f,k}(\boldsymbol{\xi})$ associated with this flux point

ESFR Schemes on Triangles

Correction functions satisfy two important properties:

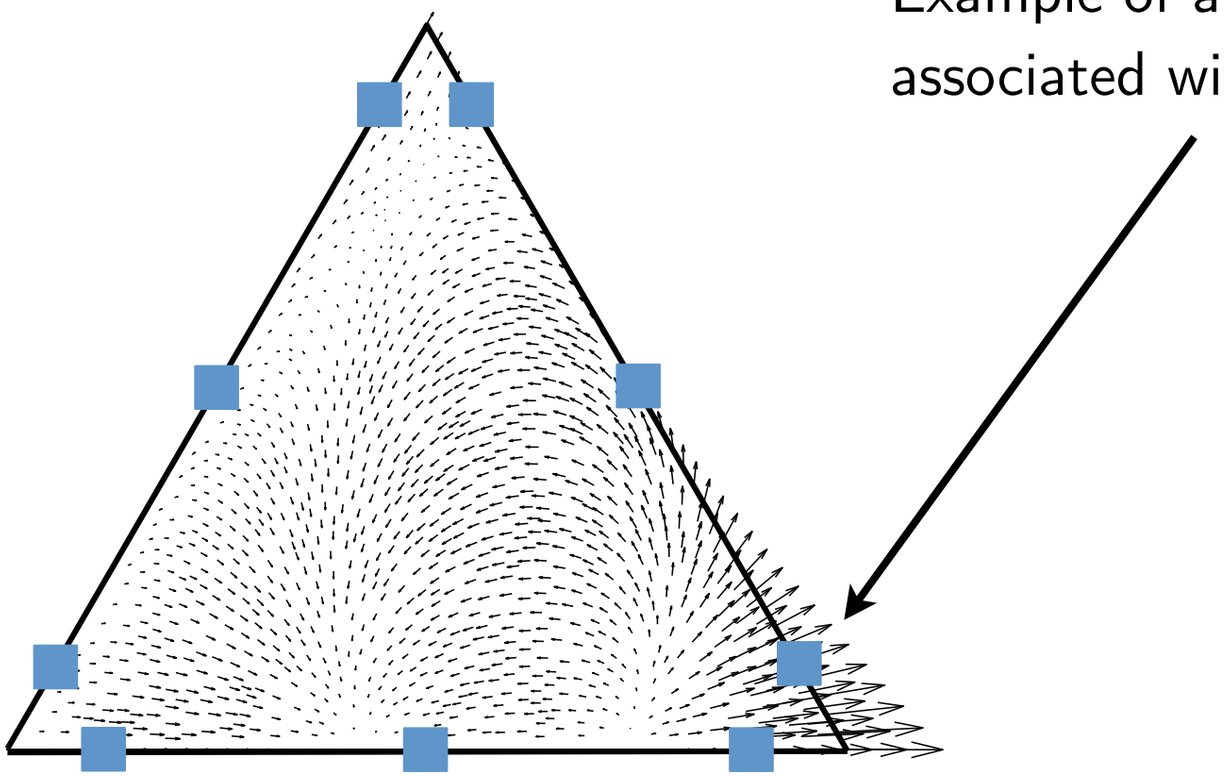

Example of a vector correction function $\mathbf{h}_{f,k}(\boldsymbol{\xi})$ associated with this flux point

ESFR Schemes on Triangles

Correction functions satisfy two important properties:

1. $$\mathbf{h}_{f,k}(\boldsymbol{\xi}_{f_2,k_2}) \cdot \mathbf{n}_{f_2,k_2} = \begin{cases} 1 & \text{if } f = f_2 \text{ and } k = k_2 \\ 0 & \text{if } f \neq f_2 \text{ or } k \neq k_2 \end{cases} .$$

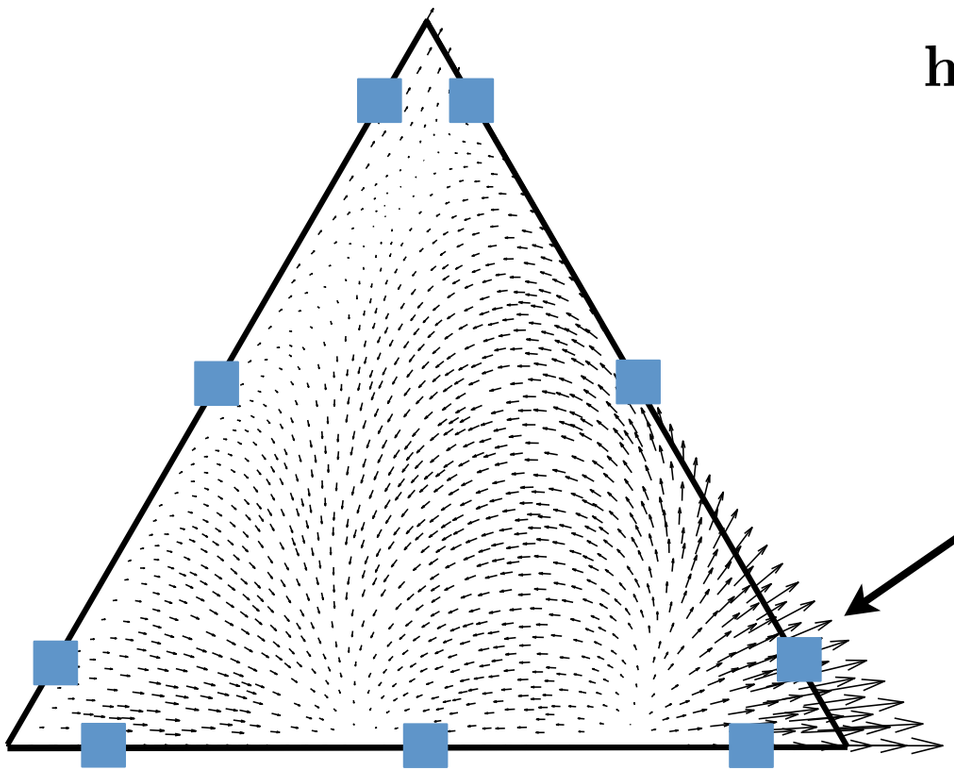

$\mathbf{h} \cdot \hat{\mathbf{n}} = 0$ at all flux points except flux point *f,k*

ESFR Schemes on Triangles

Correction functions satisfy two important properties:

2. correction functions $\mathbf{h}_{f,k}(\boldsymbol{\xi})$ lie in Raviart-Thomas space

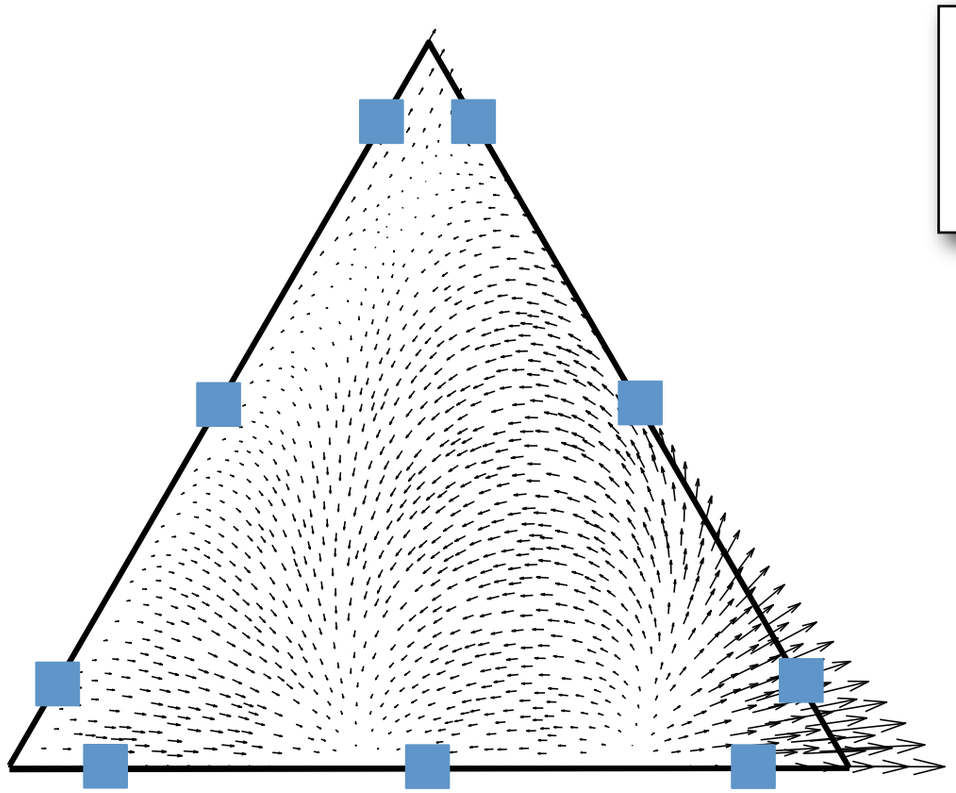

$\hat{\nabla} \cdot \mathbf{h}_{f,k}$	is a degree p polynomial
$\mathbf{h}_{f,k} \cdot \hat{\mathbf{n}}$	is of degree p on each each edge

ESFR Schemes on Triangles

Correction functions satisfy two important properties:

2. correction functions $\mathbf{h}_{f,k}(\boldsymbol{\xi})$ lie in Raviart-Thomas space

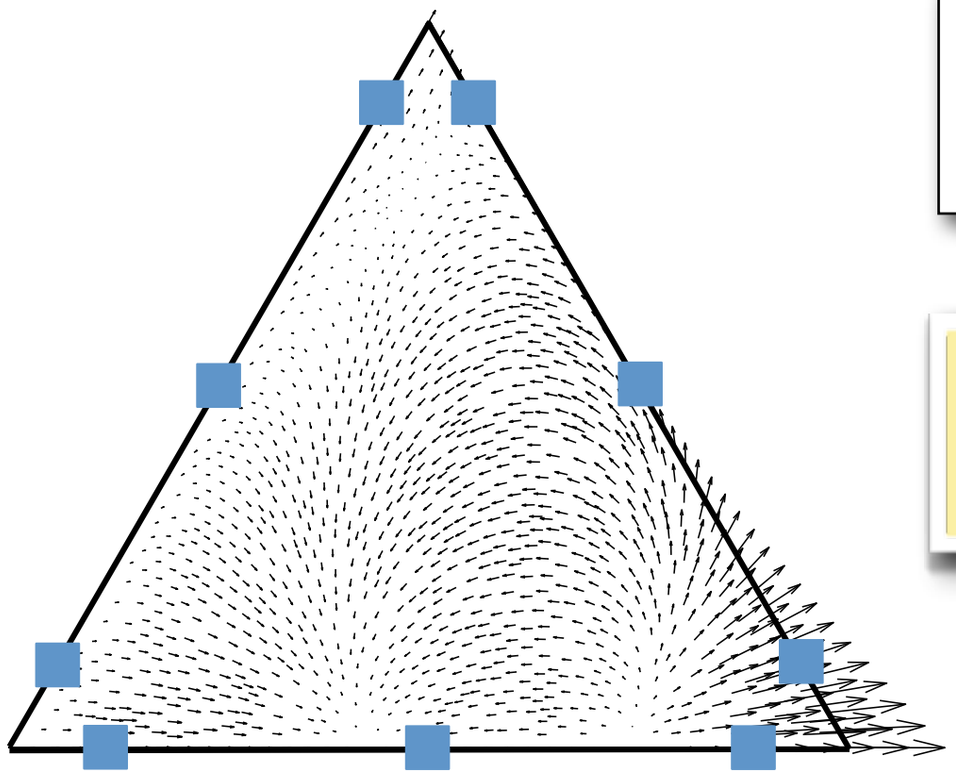

$\hat{\nabla} \cdot \mathbf{h}_{f,k}$	is a degree p polynomial
$\mathbf{h}_{f,k} \cdot \hat{\mathbf{n}}$	is of degree p on each each edge

- **Approach is conservative**
- **Divergence of total flux is of degree p**

ESFR Schemes on Triangles

Linear stability guaranteed if the vector correction functions satisfy

$$c_{tri} \sum_{m=1}^{p+1} \binom{p}{m-1} \left(D^{(m,p)} \Psi_i \right) \left(D^{(m,p)} \hat{\nabla} \cdot \mathbf{h}_{f,k} \right) = \int_S \mathbf{h}_{f,k} \cdot \hat{\nabla} \Psi_i \, d_S$$

for $1 \leq i \leq N_p$ where

$$D^{(m,p)} = \frac{\partial^m}{\partial \xi^{(p-m+1)} \partial \eta^{(m-1)}}$$

Ψ_i are members of an orthonormal basis set on the reference triangle

$\binom{p}{m-1}$ are binomial coefficients

c_{tri} is a scalar parameter that must be greater than 0

Castonguay, *et al.*, (2012). J. Sci. Comput., 51(1)

Non-Linear Properties of the ESFR Schemes

- So far, analysis done in context of linear equations, but to be practically useful, ESFR must perform well when flux is nonlinear
- ESFR schemes are **not** guaranteed to be stable for non-linear fluxes
- Instability caused by aliasing errors, which are caused by the collocation projection procedure used to compute the discontinuous flux (same instabilities afflict collocation-based nodal DG schemes)
- For first-order PDE with non-linear flux F(U), one obtains

$$\frac{1}{2}\frac{d}{dt}||U^{\delta D}||_{p,2}^2 = \Phi + \sum_{n=1}^{N} \epsilon_n$$

$$\Phi \leq 0$$

if an E-flux is used at each interface

Non-Linear Properties of the ESFR Schemes

Instabilities comes from $\sum_{n=1}^{N} \epsilon_n$

$$\epsilon_n = J_n \hat{\epsilon} \qquad \hat{\epsilon} = \sum_{i=0}^{p-1} \hat{\epsilon}_i \left[\frac{(2i+1)}{2} \int_{-1}^{1} \frac{\partial \hat{U}^{\delta D}}{\partial \xi} \Psi_i \mathrm{d}\xi \right]$$

$$\hat{\epsilon}_i = \int_{-1}^{1} \hat{F}^{\delta D} \Psi_i \mathrm{d}\xi - \int_{-1}^{1} \hat{F} \Psi_i \mathrm{d}\xi.$$

To guarantee non-linear stability, need $\hat{\epsilon}_i$ to vanish, which would require performing an exact projection, i.e.

$$\hat{F}^{\delta D} = \sum_{i=0}^{p-1} \alpha_i \Psi_i \qquad \alpha_i = \int_{-1}^{1} \hat{F} \Psi_i \mathrm{d}\xi$$

Cannot be evaluated exactly, unless $\hat{F}$ is a polynomial

Non-Linear Properties of the ESFR Schemes

Instabilities comes from $\sum_{n=1}^{N} \epsilon_n$

$$\epsilon_n = J_n \hat{\epsilon} \qquad \hat{\epsilon} = \sum_{i=0}^{p-1} \hat{\epsilon}_i \left[\frac{(2i+1)}{2} \int_{-1}^{1} \frac{\partial \hat{U}^{\delta D}}{\partial \xi} \Psi_i \mathrm{d}\xi \right]$$

$$\hat{\epsilon}_i = \int_{-1}^{1} \hat{F}^{\delta D} \Psi_i \mathrm{d}\xi - \int_{-1}^{1} \hat{F} \Psi_i \mathrm{d}\xi.$$

To guarantee non-linear stability, need $\hat{\epsilon}_i$ to vanish, which would require performing an exact projection, i.e.

$$\hat{F}^{\delta D} = \sum_{i=0}^{p-1} \alpha_i \Psi_i \qquad \alpha_i = \int_{-1}^{1} \hat{F} \Psi_i \mathrm{d}\xi$$

Cannot be evaluated exactly, unless $\hat{F}$ is a polynomial

Non-Linear Properties of the ESFR Schemes

- If a collocation projection is used

$$\hat{\epsilon}_i = \sum_{j=0}^{p} \hat{F}(\xi_j)\Psi_i(\xi_j)\omega_j - \int_{-1}^{1} \hat{F}\Psi_i \mathrm{d}\xi$$

- Should put solution points at good quadrature points (e.g. Gauss points)
  - No need to evaluate flux at new set of points
    - Computationally cheaper than DG schemes in their standard form
  - Numerical experiments suggest that no additional stabilization is required

Jameson, et al., (2012). J. Sci. Comput., 50(2)

Outline

I. Current & Future Trends
- The Current Status of CFD
- The Future of CFD (?)
- Large-Eddy Simulation

II. The Aerospace Computing Lab

III. Overview of Numerical Methods
- Typical Requirements of CFD
- Classic Numerical Methods
- A Review of the Literature
- A Review of the Literature from ACL

IV. The FR Methodology
- Introduction
- The Flux Reconstruction Scheme
- The FR Scheme Graphically Illustrated
- The Energy Stability of the FR Scheme
- ESFR Schemes
- ESFR Schemes for 2nd-Order PDEs
- ESFR Schemes on Triangles
- Non-Linear Properties of the ESFR Schemes

V. Applications
- Numerical Dissipation
- High-Order Boundaries
- Maximum Time Step *vs.* Accuracy
- 3D Unsteady Flow over a Sphere
- Transitional Flow over SD7003 Airfoil
- Study of Flapping Wing Sections

VI. Structural LES Modeling
- Explicit Filtering in the SD Element
- The Restriction-Prolongation Filter
- Discrete Filters by Gauss Quadrature
- Discrete Filters for Arbitrary Points

VII. LES Computations
- Wall-Resolved Turbulent Channel Flow
- Wall-Modeling Strategy
- Wall-Modeled Turbulent Channel Flow
- Flow past a Square Cylinder

VIII. Conclusions and Summary

Numerical Dissipation

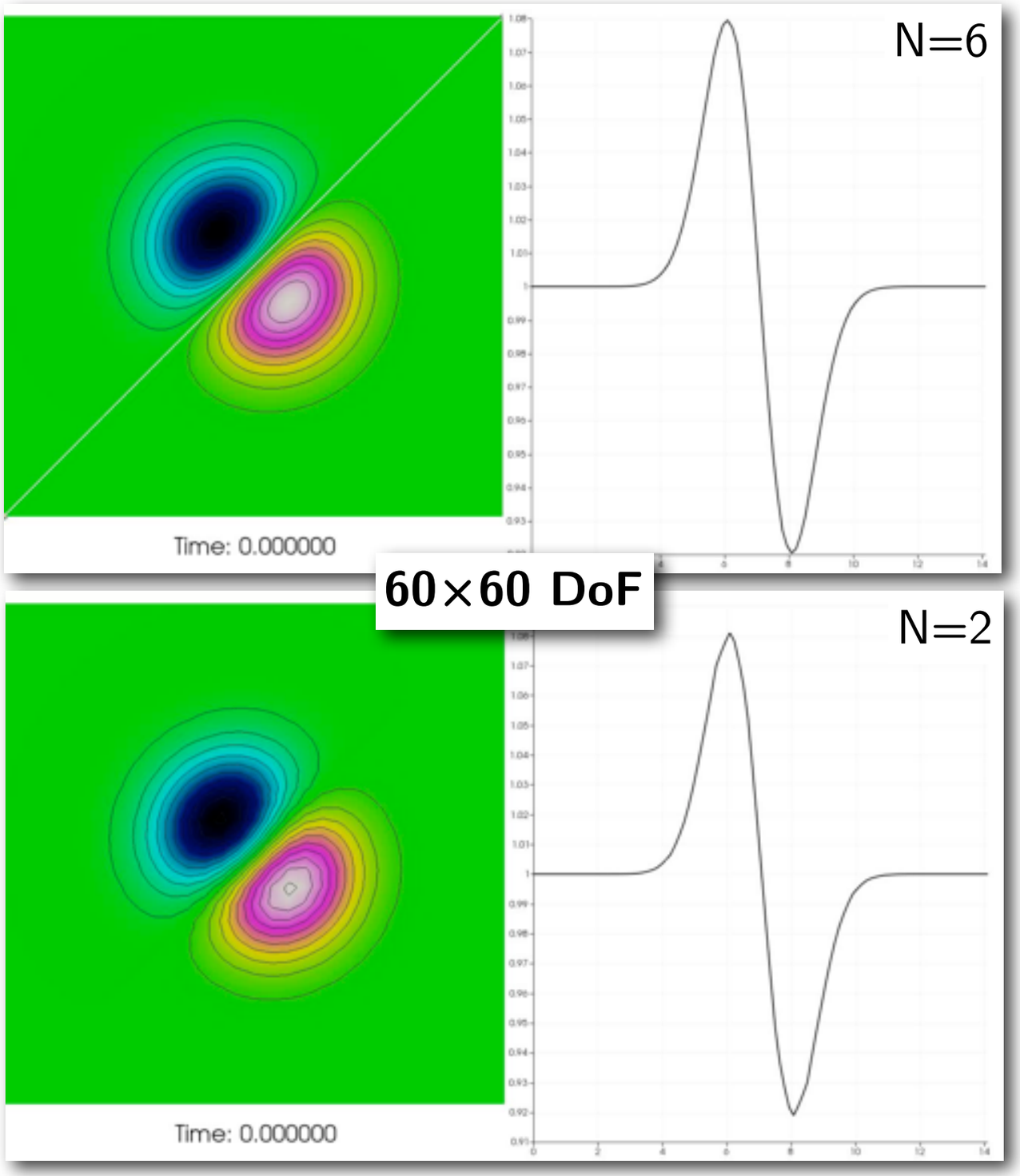

2D inviscid Euler vortex:

numerical dissipation shall not destroy the solution

Numerical Dissipation

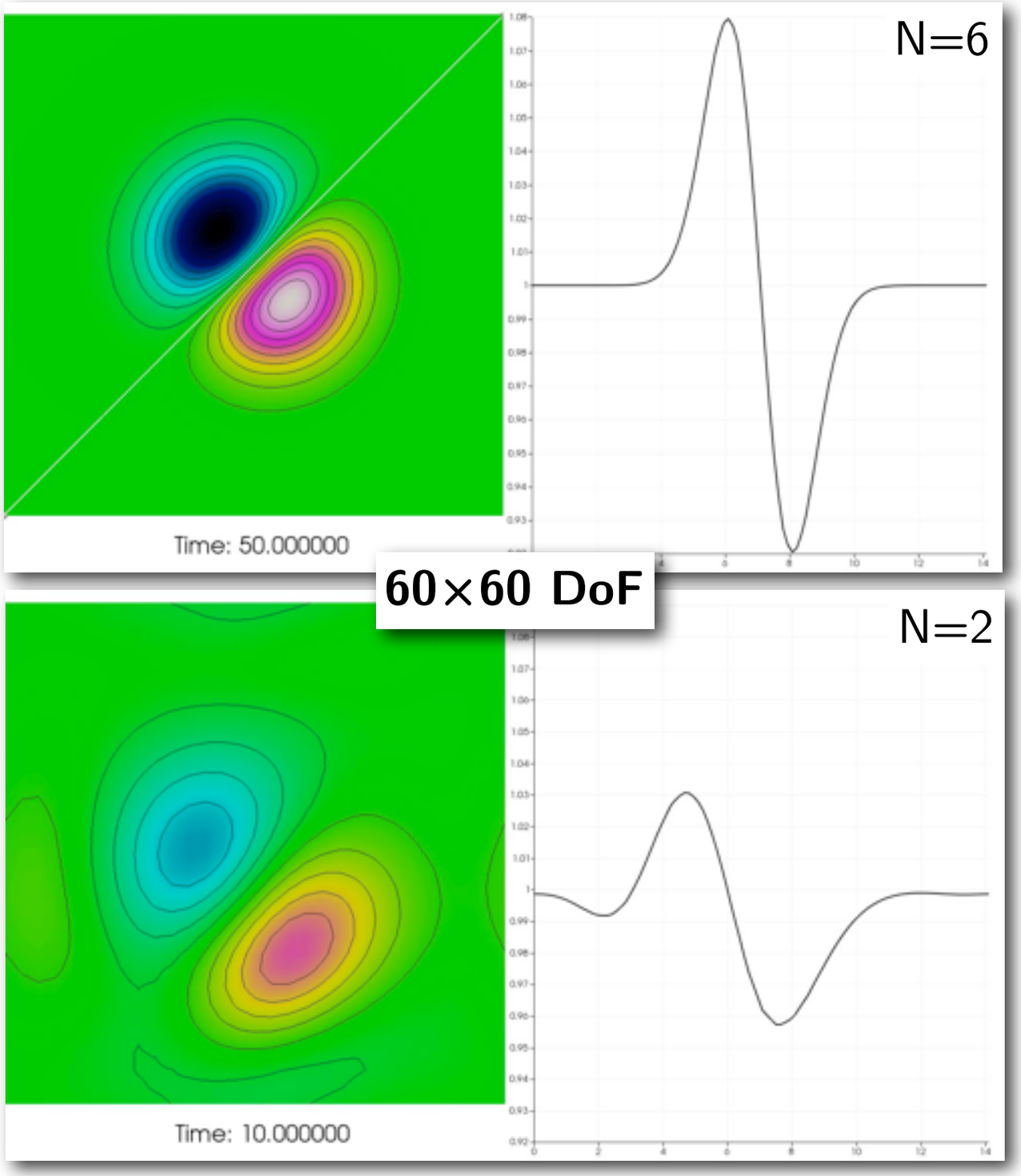

2D inviscid Euler vortex:

numerical dissipation shall not destroy the solution

Numerical Dissipation

3D inviscid Euler vortex: numerical dissipation shall not prevent transition

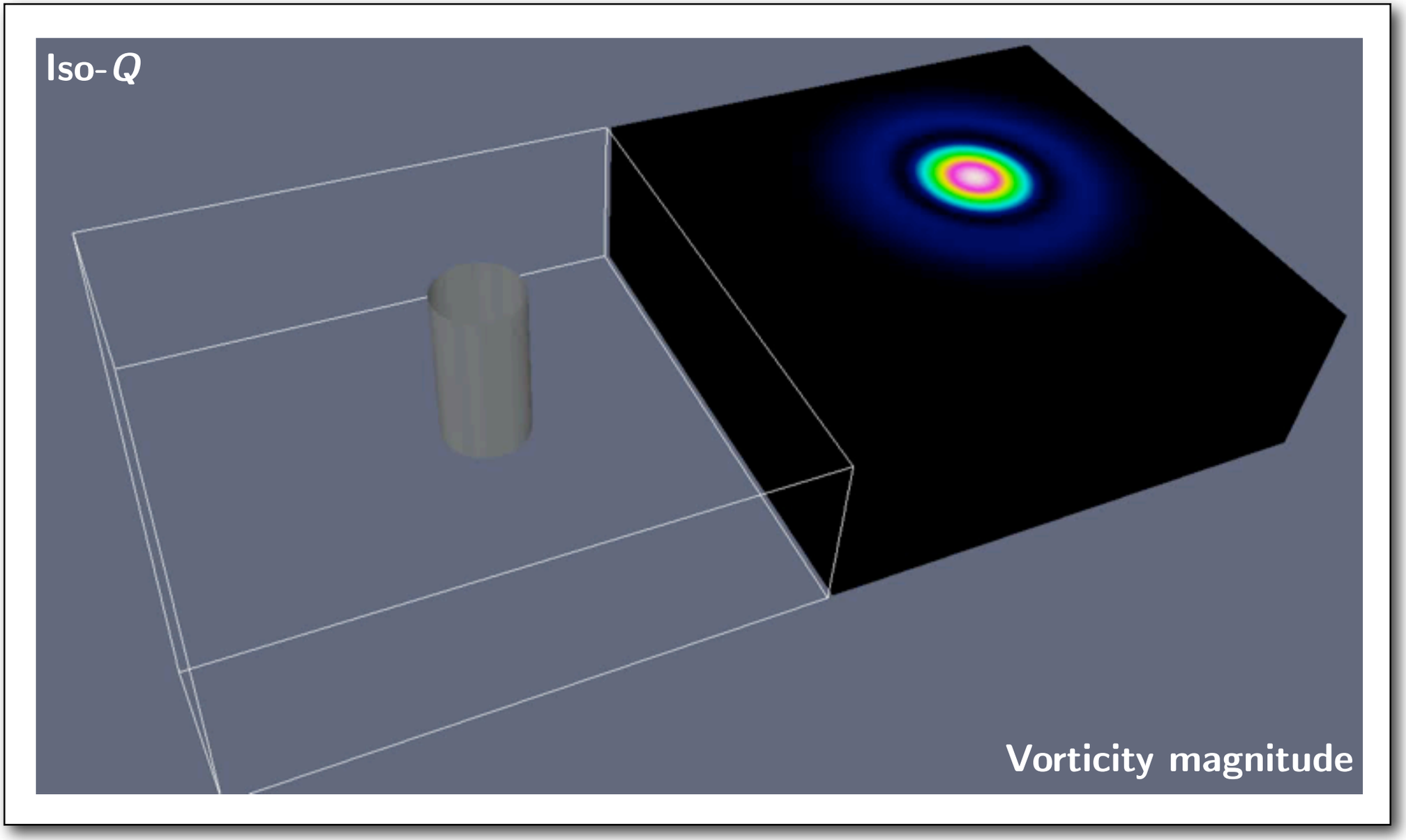

N=6, 60×60×12 DoF

Numerical Dissipation

3D inviscid Euler vortex: numerical dissipation shall not prevent transition

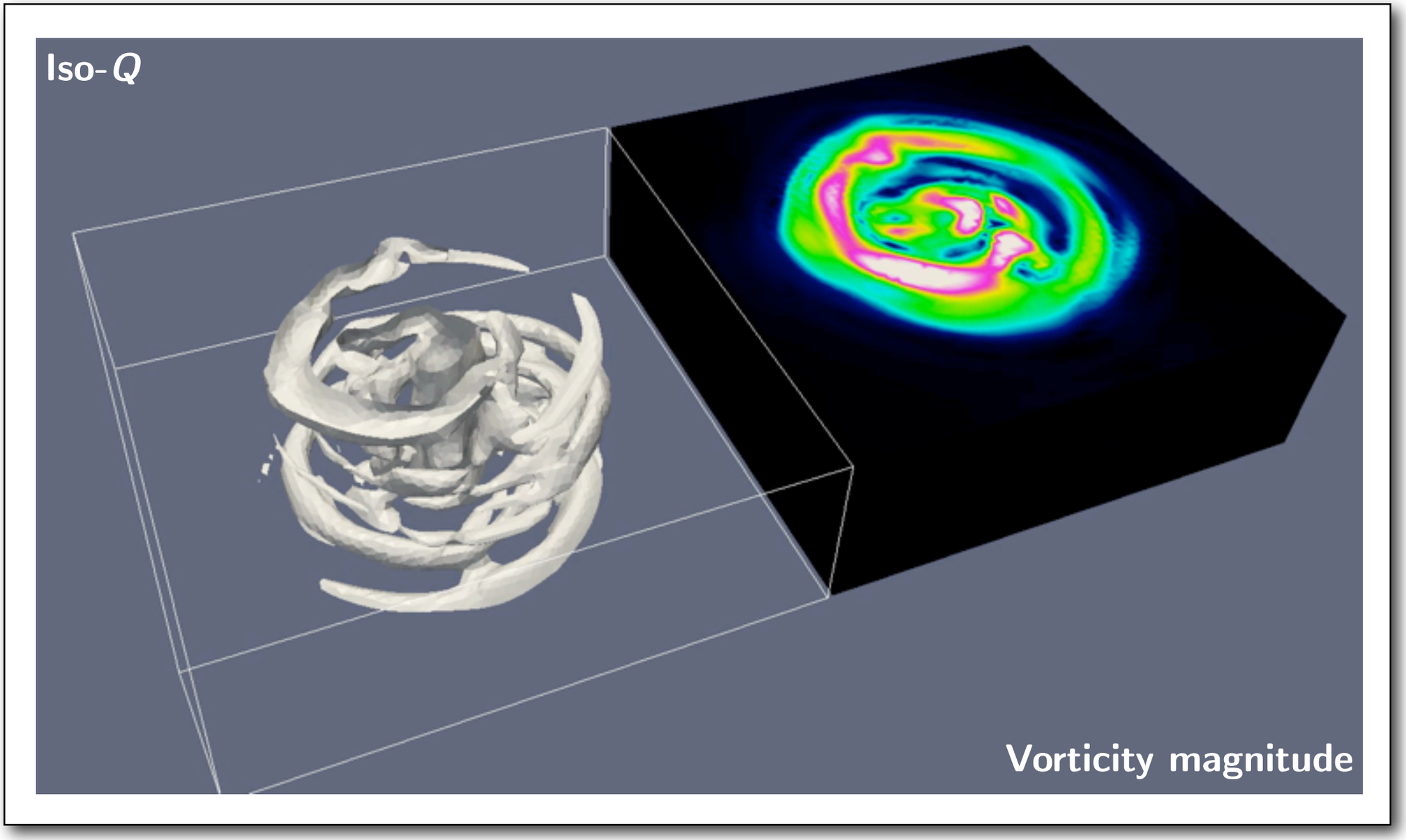

N=6, 60×60×12 DoF

High-Order Boundaries

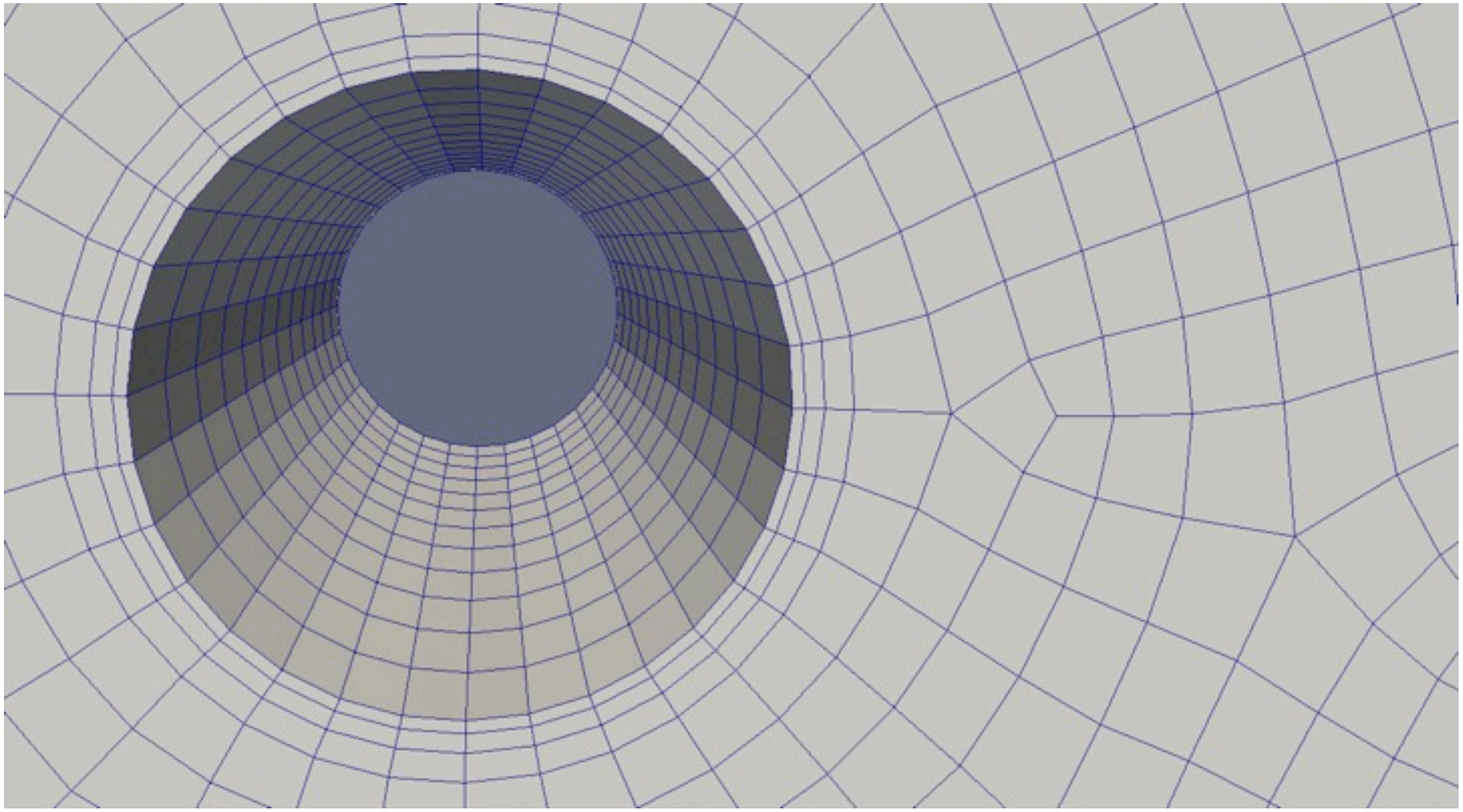

Liang, *et al.* (2009). Comput. Struct., 87; Sun, *et al.* (2007). Commun. Comput. Phys., 2(2)

High-Order Boundaries

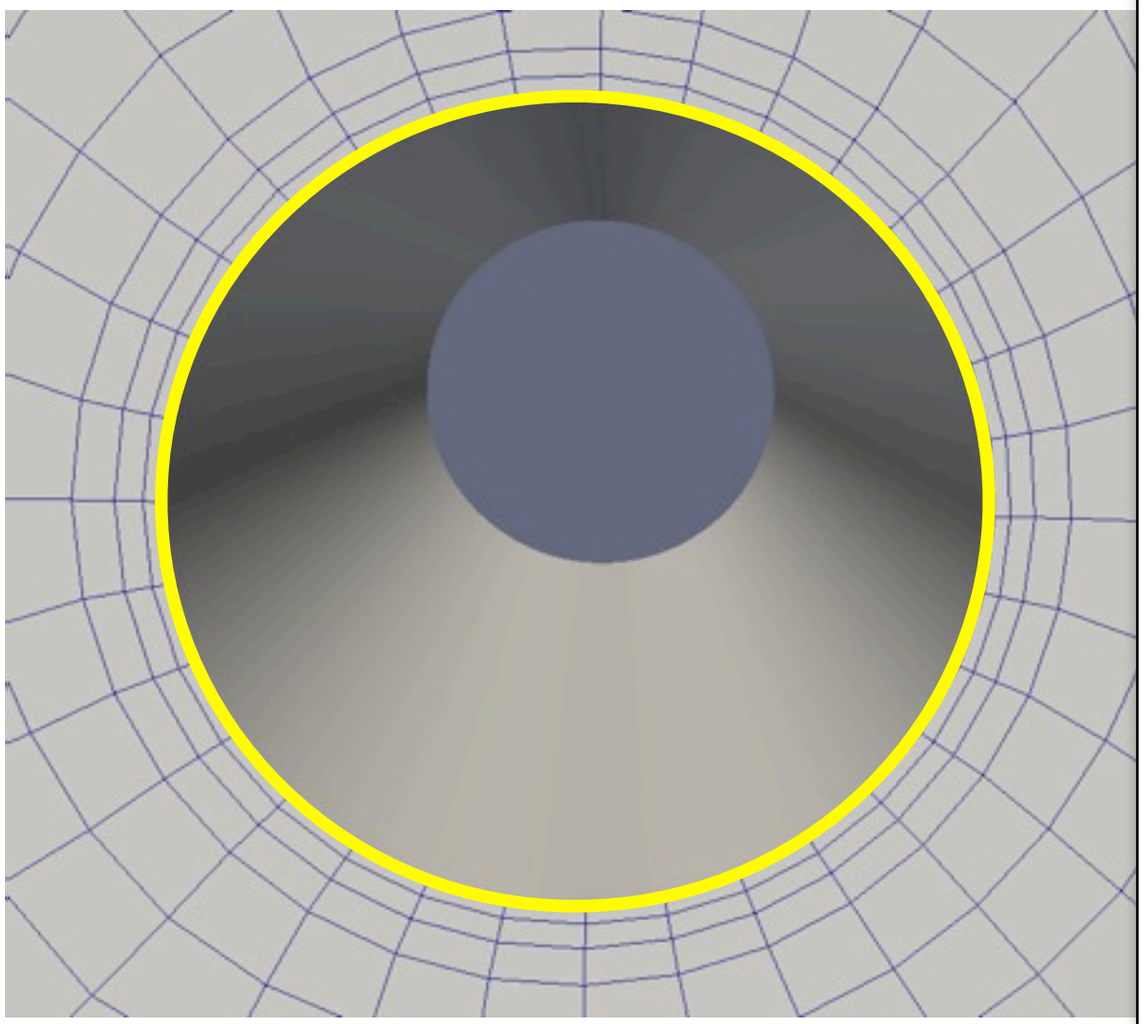

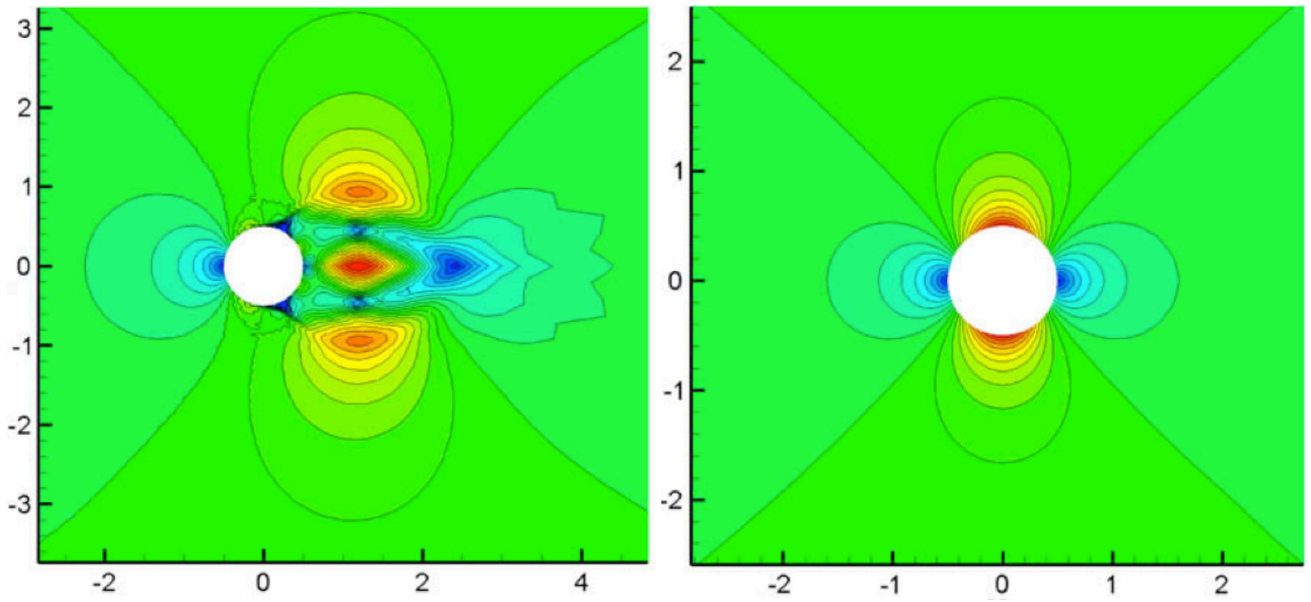

Cylinder: N=4, 32×32, linear *vs.* cubic

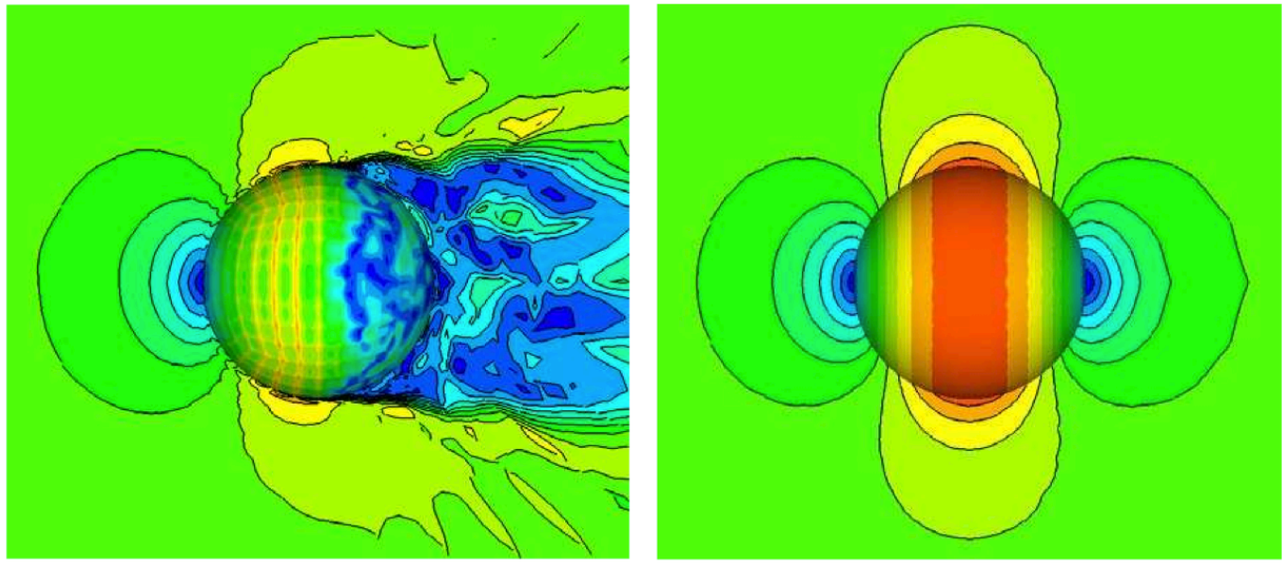

Sphere: N=3, linear *vs.* quadratic

Liang, *et al.* (2009). Comput. Struct., 87; Sun, *et al.* (2007). Commun. Comput. Phys., 2(2)

Maximum Time Step *vs.* Accuracy

- Tested ESFR schemes on a set of canonical flow problems to verify if linear properties extend to coupled non-linear problems
- For example, isentropic vortex problem on 3 different grids

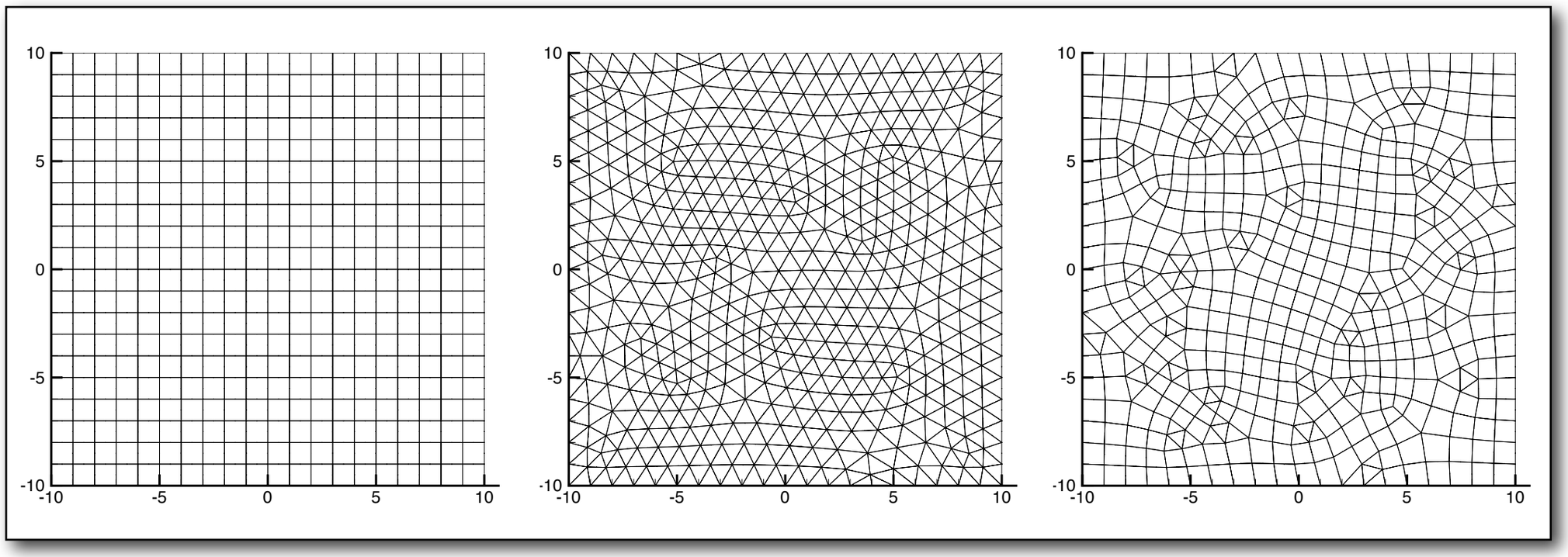

Maximum Allowable Time Step

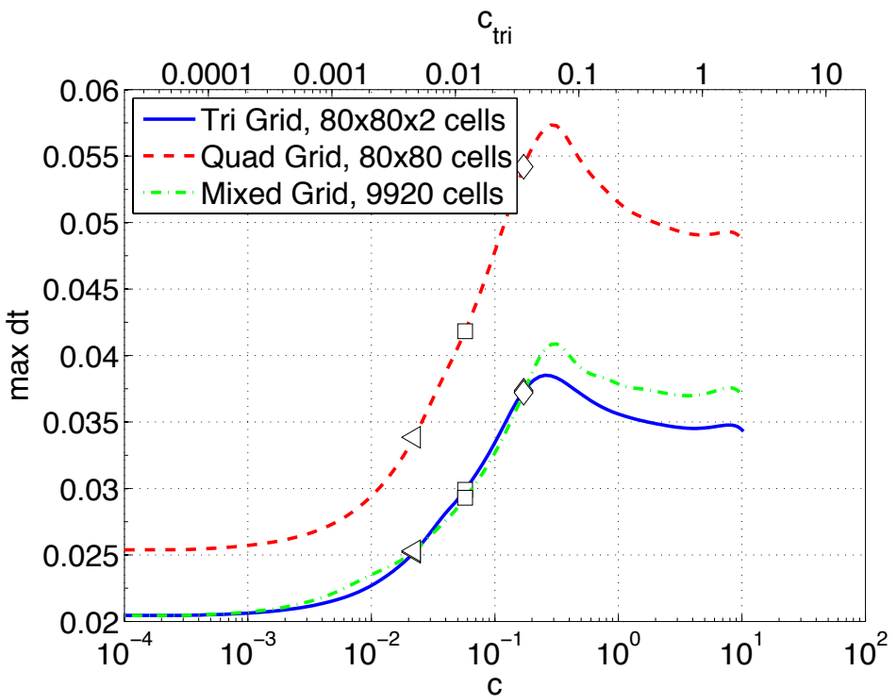

2D, mixed unstructured grid, non-linear coupled PDEs (Euler eqns), determined experimentally

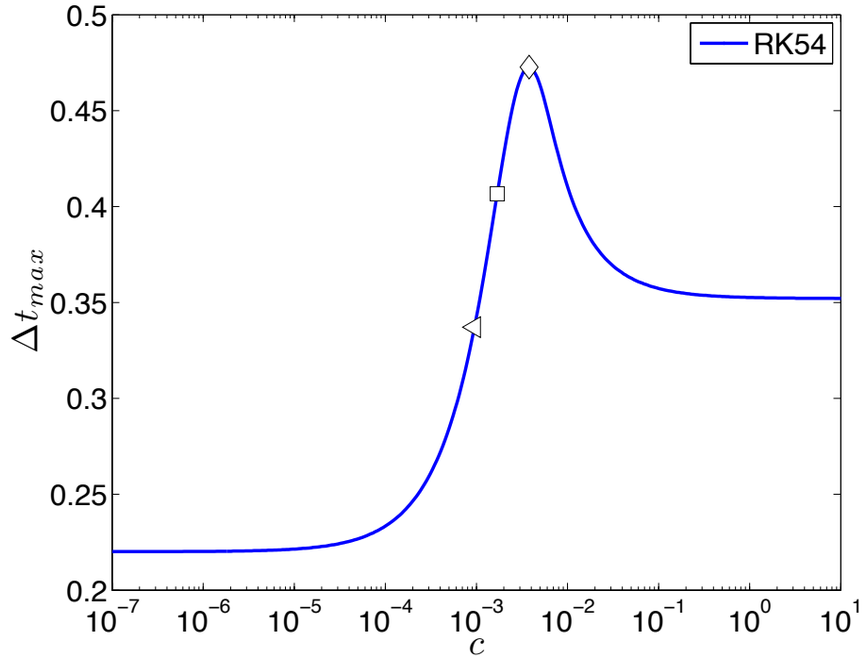

1D structured grid, uniform spacing, scalar linear advection, from von Neumann stability analysis

Symbols denote particular values of c, triangle at c_{SD}, square at c_{HU}, diamond at c_+

Accuracy

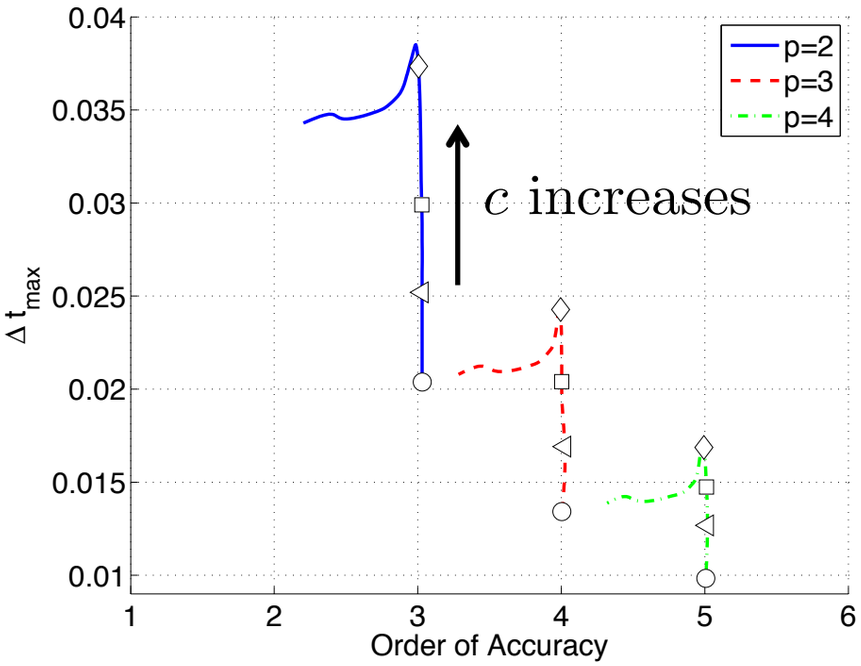

Accuracy on triangular grid

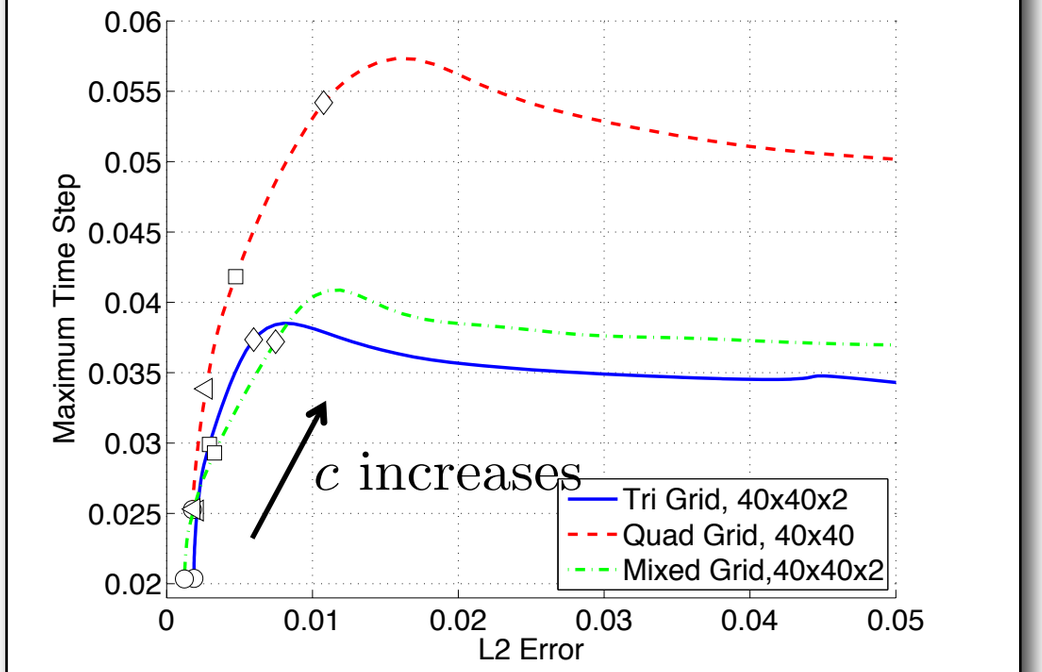

L2-Error vs Maximum time-step

Symbols denote particular values of c, triangle at c_{SD}, square at c_{HU}, diamond at c_+

3D Unsteady Flow over a Sphere

- Reynolds number 300, Mach 0.3
- Mixed grid of 28,940 prismatic elements and 258,075 tetrahedral elements
- p = 3: 6.3 million solution points
- Used ESFR scheme corresponding to c_{SD}

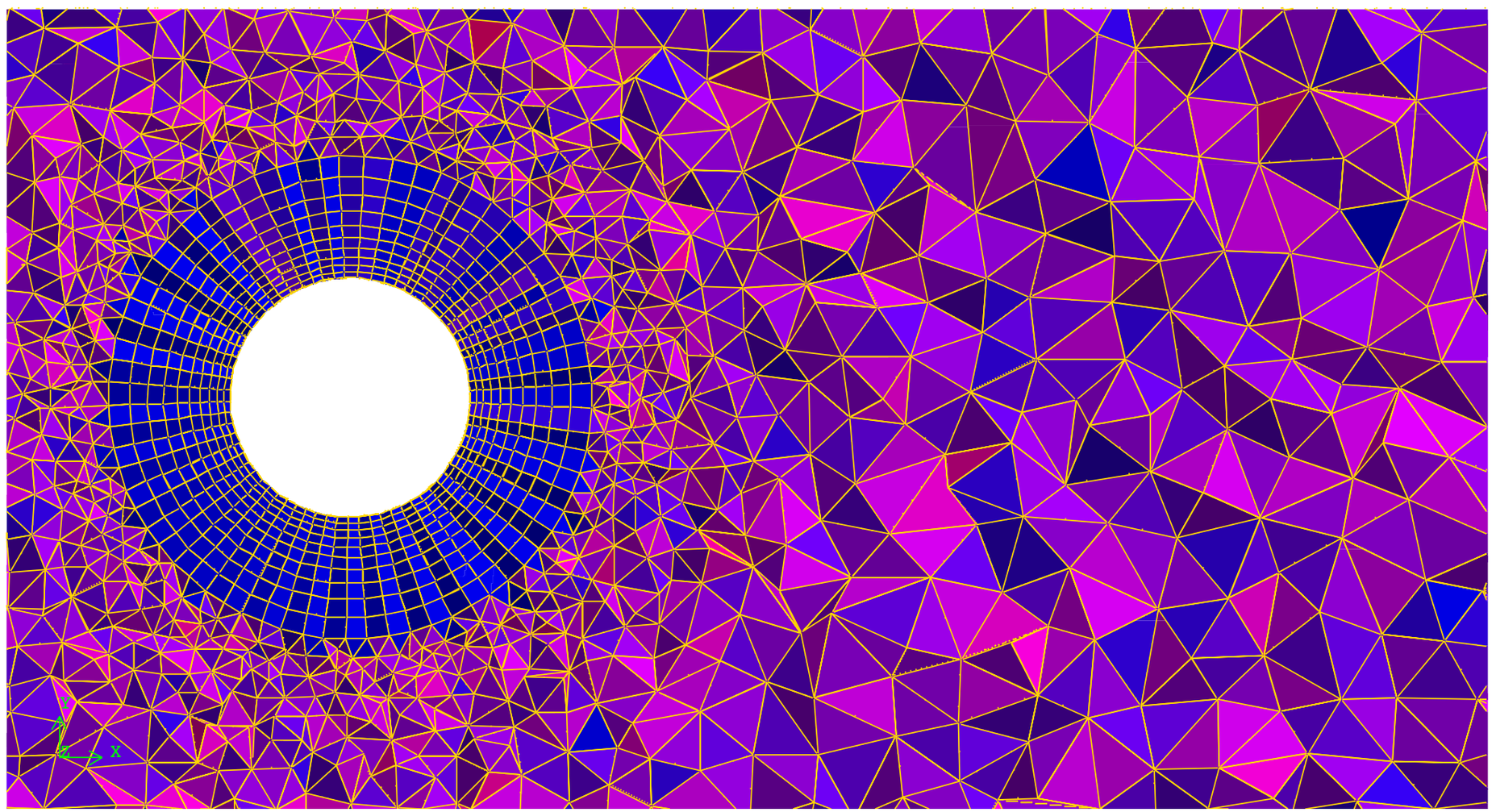

Mixed unstructured grid in the vicinity of the sphere

3D Unsteady Flow over a Sphere

- Vortical structures well captured even in coarse wake region

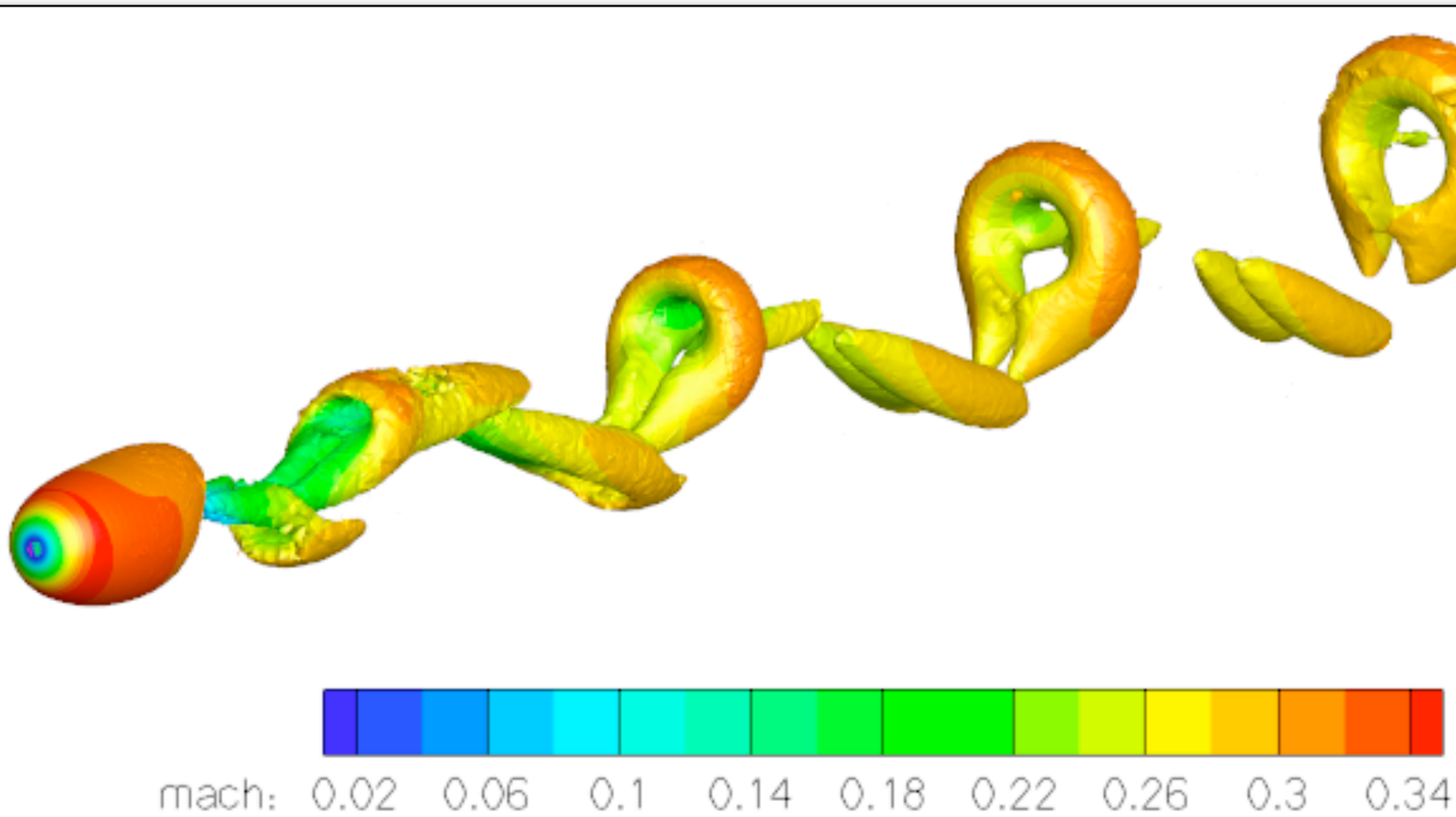

Iso-surfaces of Q criterion colored by Mach number

3D Unsteady Flow over a Sphere

Comparison with data from literature

Investigator	# Cells	p	$\bar{C}_d$	C'_d	$\bar{C}_l$	C'_l	Str
Present	287015	3	0.6724	0.00303	0.0667	0.0150	0.1313
Gassner et al.	160000	3	0.673	0.0031	0.065	0.015	0.135
Haga et al.	54312	3	0.670	0.0032	-	-	0.131
Tomboulides et al. *	-	-	0.671	0.0028	-	-	0.136
Johnson et al. *	428442	1	0.656	0.0035	0.069	0.016	0.137

Solver:

- Arbitrary orders of accuracy
- Mixed unstructured grid
- No need to apply filter to stabilize the code, no numerical quadrature
- Well understood linear and non-linear stability and accuracy properties
- Can vary a single scalar to trade-off accuracy with explicit time-step

Transitional Flow over SD7003 Airfoil

	Freestream Turbulence	Separation x_{sep}/c	Transition x_{tr}/c	Reattach. x_r/c
Radespiel et al.	0.08%	0.30	0.53	0.64
Ol et al.	0.10%	0.18	0.47	0.58
Galbraith Visbal	0%	0.23	0.55	0.65
Uranga et al.	0%	0.23	0.51	0.60
Present ILES*	**0%**	**0.23**	**0.53**	**0.64**

Experiments in green

SD scheme, N=4

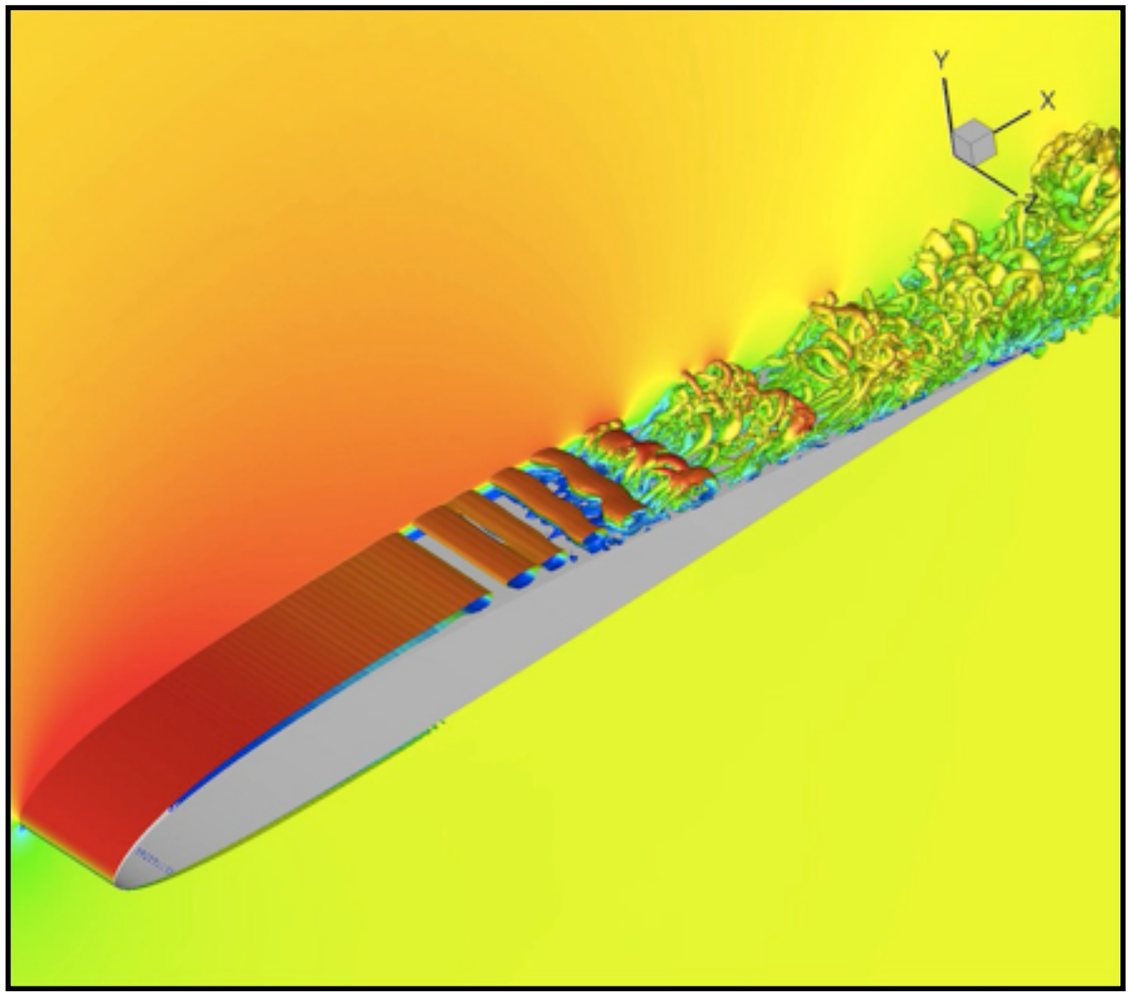

Iso-Q colored by Ma

Re=6×10^4, AoA=4°, 2.2×10^7 DoF

***1.7×10^6 DoF**

Castonguay, et al. (2010). AIAA P., 2010-4626; Radespiel, et al. (2007). AIAA J., 45(6); Ol, et al. (2005). AIAA P., 2005-5149; Galbraith, Visbal (2008). AIAA P., 2008-225; Uranga, et al. (2009). AIAA P., 2009-4131;

Transitional Flow over SD7003 Airfoil

	Freestream Turbulence	Separation x_{sep}/c	Transition x_{tr}/c	Reattach. x_r/c
Radespiel et al.	0.08%	0.30	0.53	0.64
Ol et al.	0.10%	0.18	0.47	0.58
Galbraith Visbal	0%	0.23	0.55	0.65
Uranga et al.	0%	0.23	0.51	0.60
Present ILES*	**0%**	**0.23**	**0.53**	**0.64**

Experiments in green

SD scheme, N=4

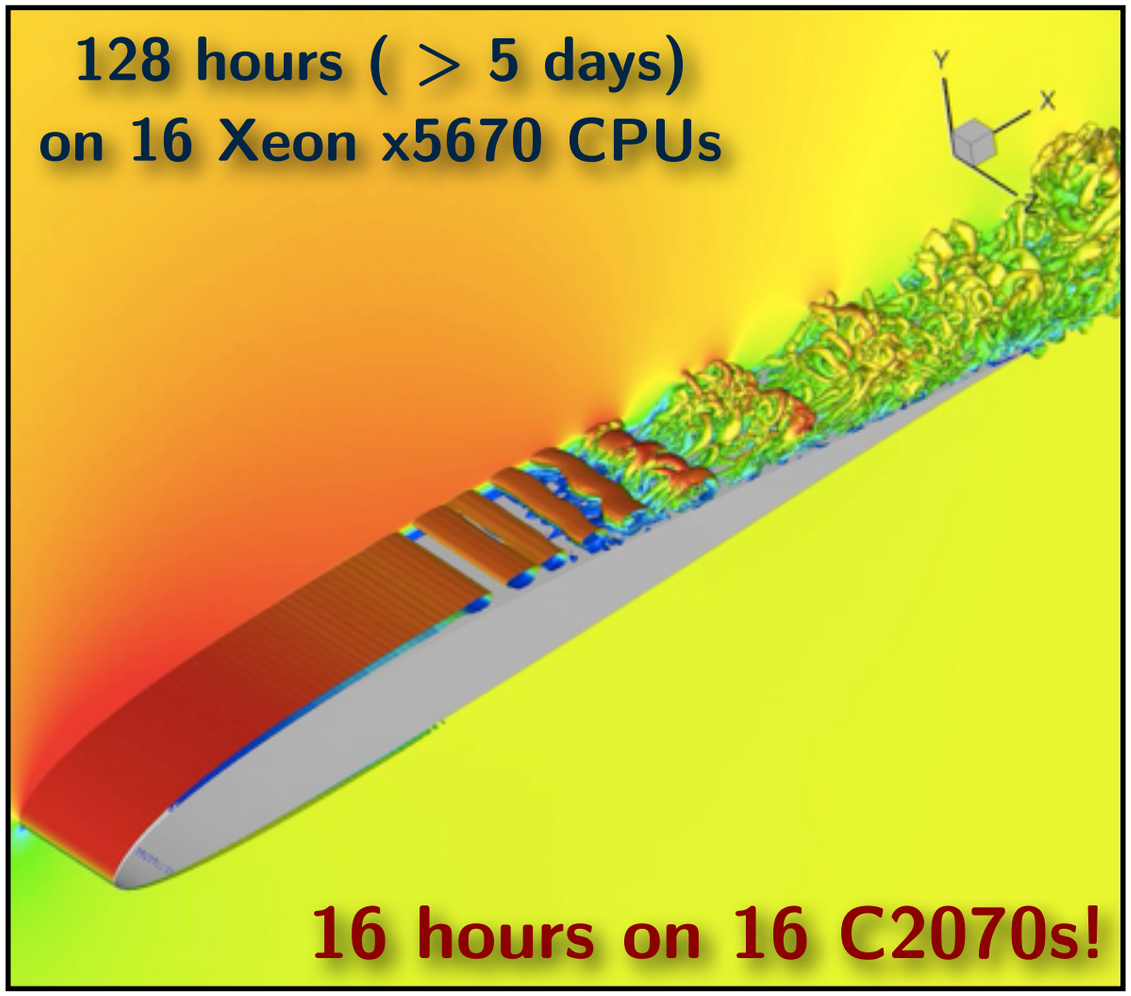

Iso-Q colored by Ma

Re=6×10⁴, AoA=4°, 2.2×10⁷ DoF

***1.7×10⁶ DoF**

Castonguay, et al. (2010). AIAA P., 2010-4626; Radespiel, et al. (2007). AIAA J., 45(6); Ol, et al. (2005). AIAA P., 2005-5149; Galbraith, Visbal (2008). AIAA P., 2008-225; Uranga, et al. (2009). AIAA P., 2009-4131;

Study of Flapping Wing Sections

SD, 2D, N=5 on deforming grid

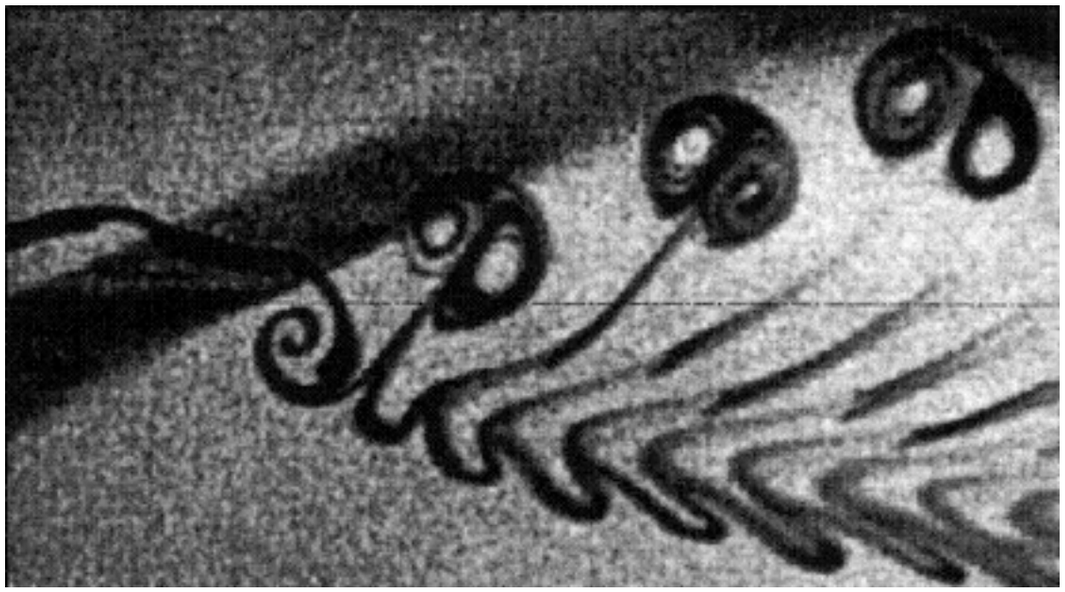

Experiment (Jones, et al.)

NACA0012, Re=1850, Ma=0.2,
St=1.5, ω=2.46, h=0.12c

Jones, et al. (1998). AIAA J., 36(7)

Study of Flapping Wing Sections

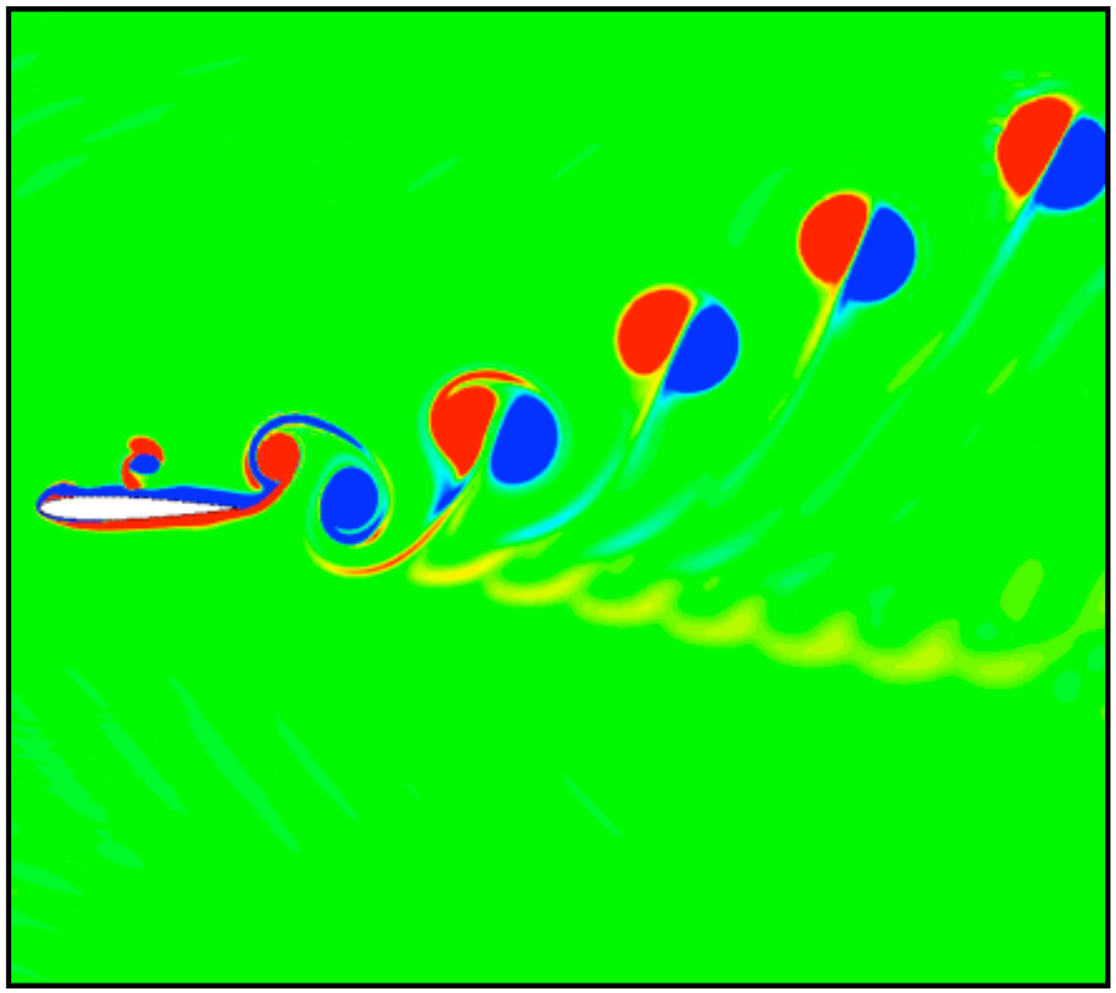

SD, 2D, N=5 on deforming grid

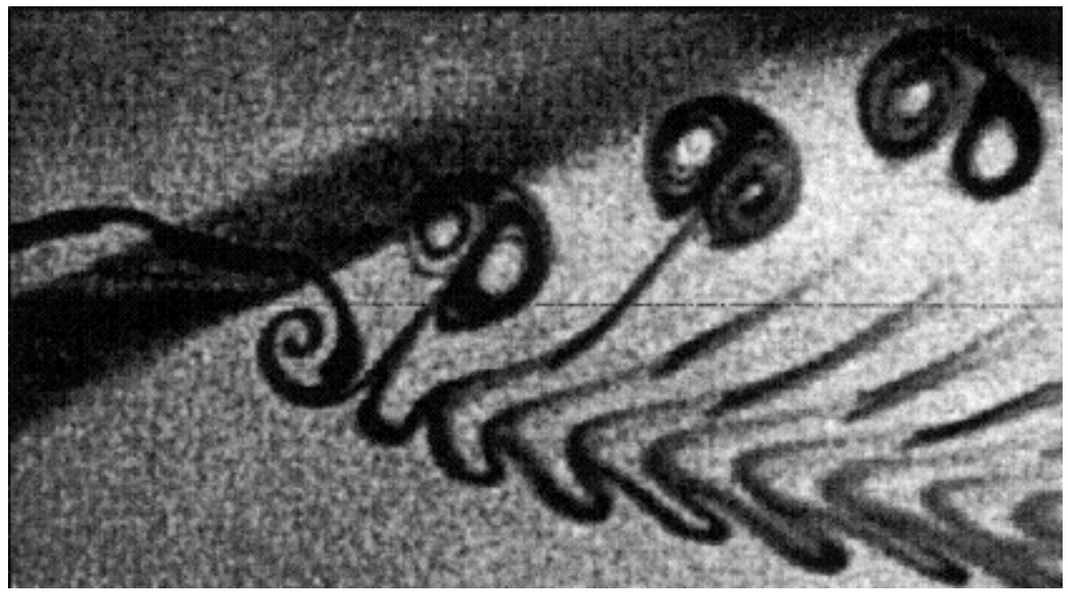

Experiment (Jones, et al.)

NACA0012, Re=1850, Ma=0.2,
St=1.5, ω=2.46, h=0.12c

Jones, et al. (1998). AIAA J., 36(7)

Outline

I. Current & Future Trends
- The Current Status of CFD
- The Future of CFD (?)
- Large-Eddy Simulation

II. The Aerospace Computing Lab

III. Overview of Numerical Methods
- Typical Requirements of CFD
- Classic Numerical Methods
- A Review of the Literature
- A Review of the Literature from ACL

IV. The FR Methodology
- Introduction
- The Flux Reconstruction Scheme
- The FR Scheme Graphically Illustrated
- The Energy Stability of the FR Scheme
- ESFR Schemes
- ESFR Schemes for 2nd-Order PDEs
- ESFR Schemes on Triangles
- Non-Linear Properties of the ESFR Schemes

V. Applications
- Numerical Dissipation
- High-Order Boundaries
- Maximum Time Step *vs.* Accuracy
- 3D Unsteady Flow over a Sphere
- Transitional Flow over SD7003 Airfoil
- Study of Flapping Wing Sections

VI. Structural LES Modeling
- Explicit Filtering in the SD Element
- The Restriction-Prolongation Filter
- Discrete Filters by Gauss Quadrature
- Discrete Filters for Arbitrary Points

VII. LES Computations
- Wall-Resolved Turbulent Channel Flow
- Wall-Modeling Strategy
- Wall-Modeled Turbulent Channel Flow
- Flow past a Square Cylinder

VIII. Conclusions and Summary

Explicit Filtering in the SD Element

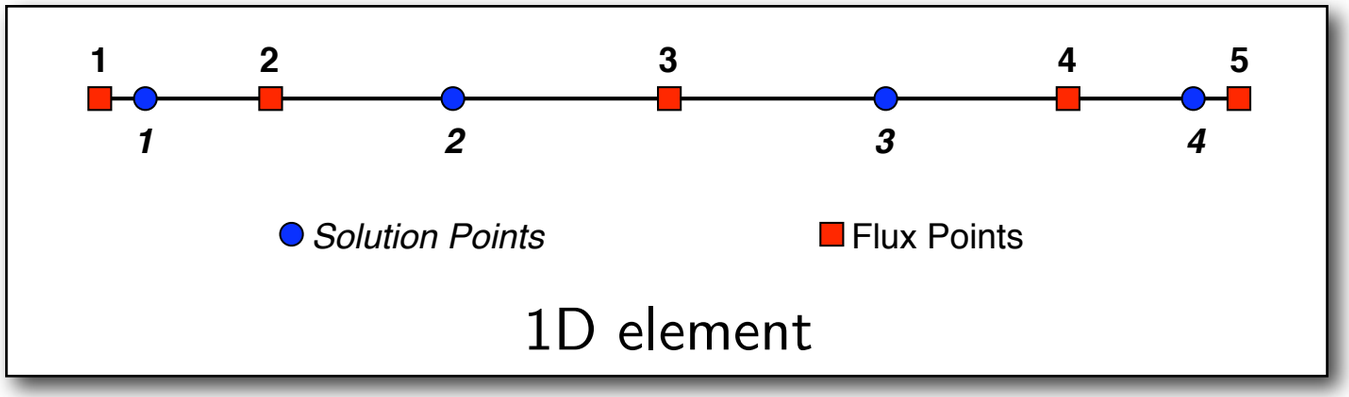

1D element

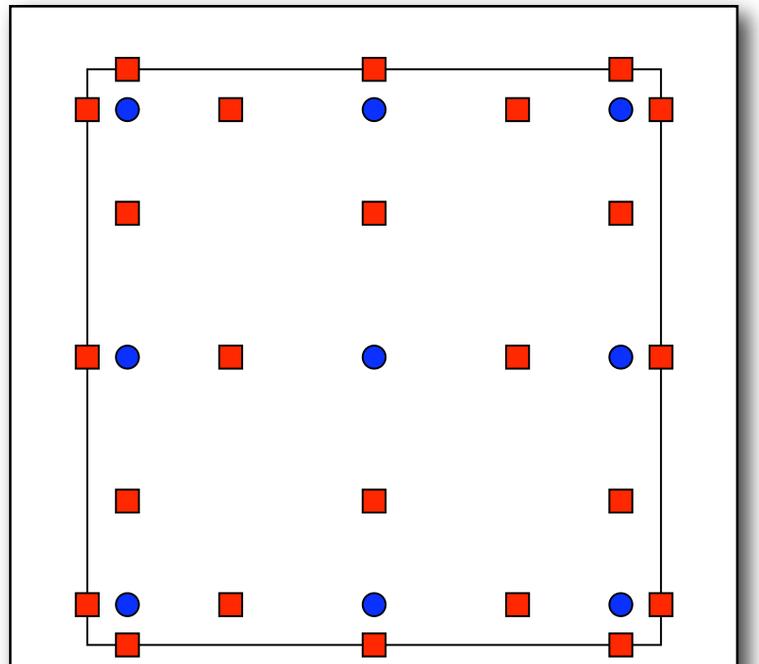

2D element

Key issues:

- non-uniform and staggered distribution of points
- the filter stencil shall not lie across elements
- filter width shall be prescribed and constant

Filtering Strategy:

1. The filtered solution is computed at solution points
2. The SGS model term is evaluated at solution points
3. The SGS model term is extrapolated at flux points via Lagrange basis

The Restriction-Prolongation Filter

Sharp cutoff in modal space:

The solution is first projected on a lower order polynomial (**restriction** step) and then extrapolated back to the original solution points (**prolongation** step)

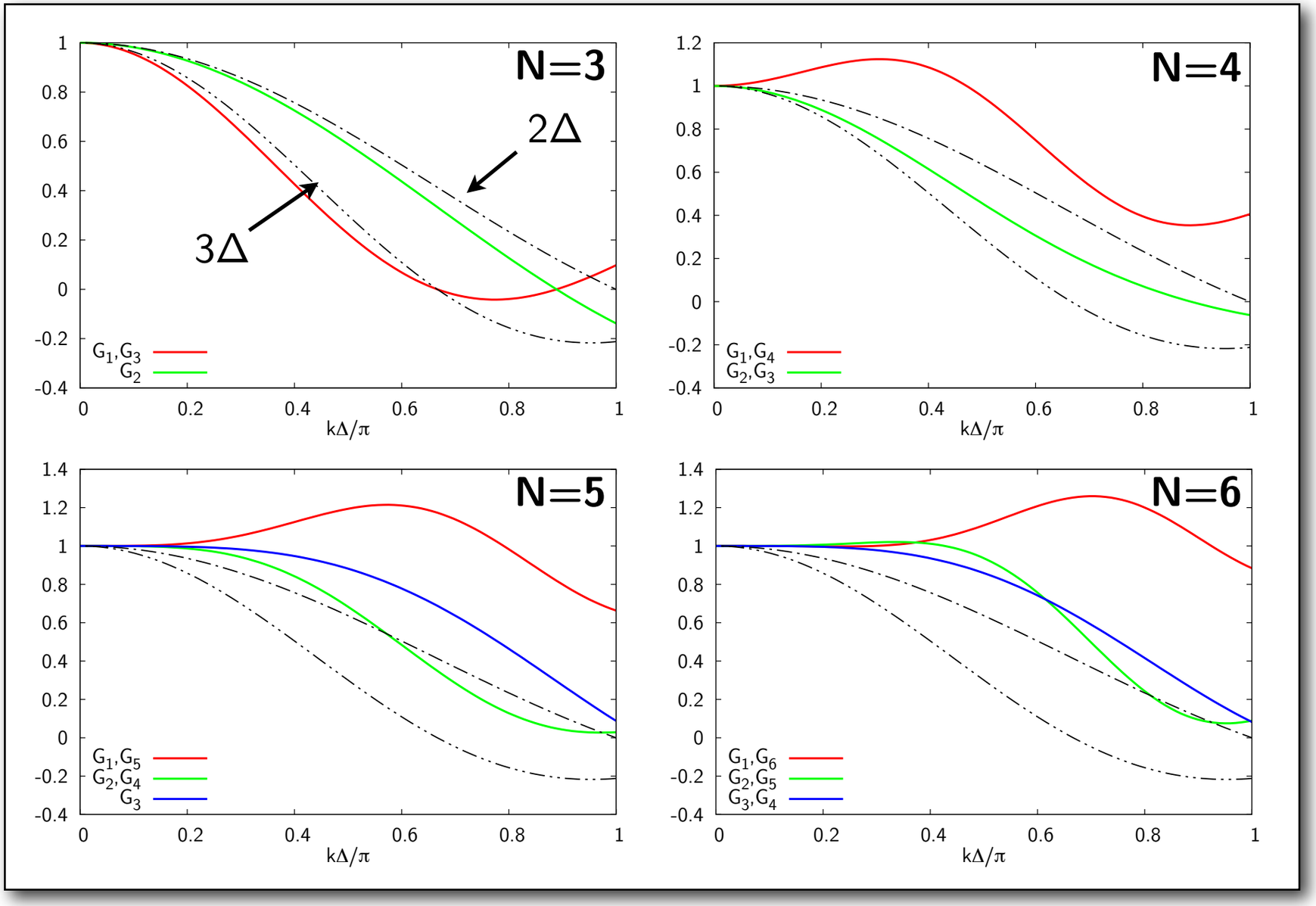

Premasuthan, et al. (2009). AIAA P., 2009-3785

The Restriction-Prolongation Filter

Sharp cutoff in modal space:

The solution is first projected on a lower order polynomial (**restriction** step) and then extrapolated back to the original solution points (**prolongation** step)

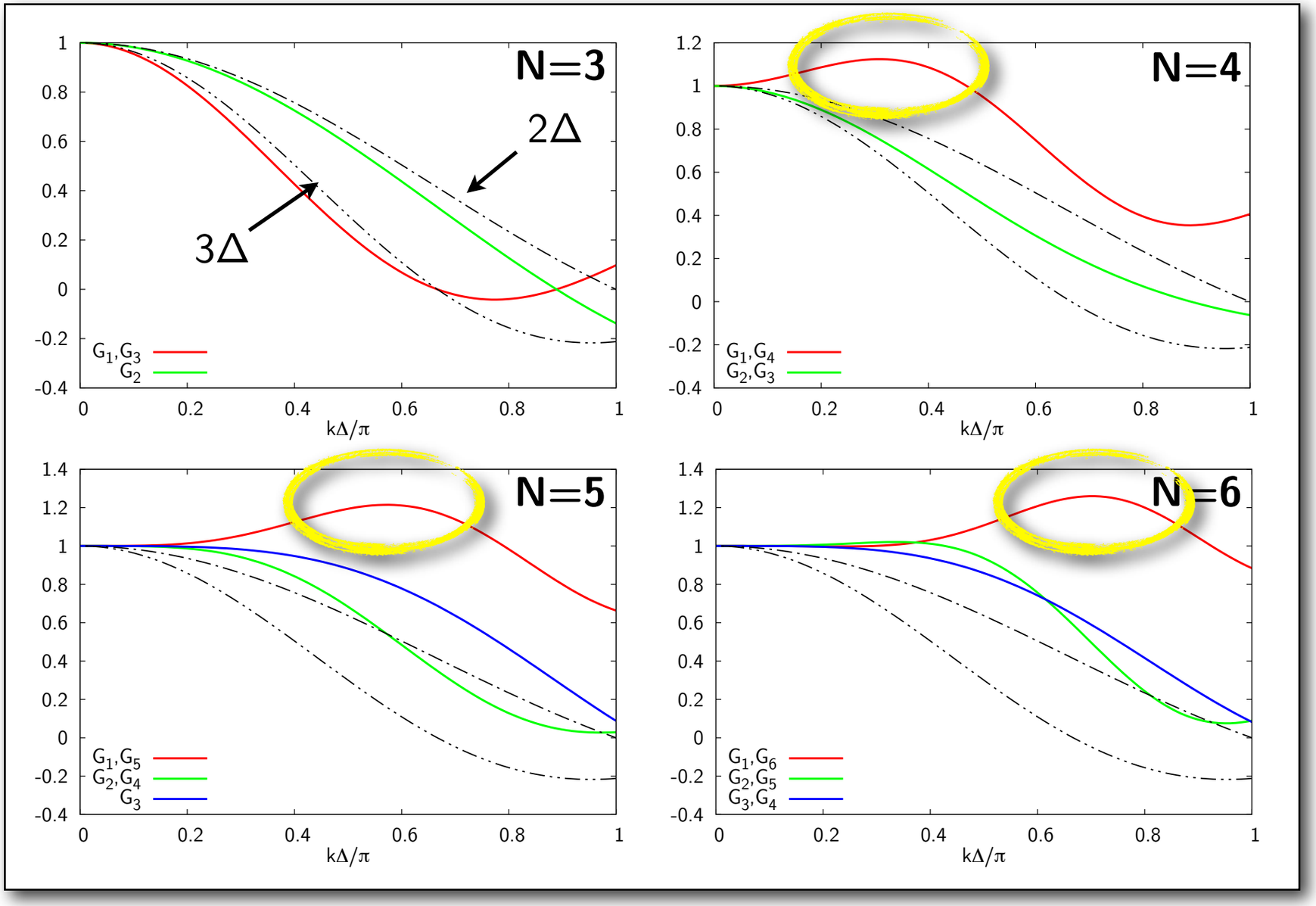

Premasuthan, et al. (2009). AIAA P., 2009-3785

Discrete Filters by Gauss Quadrature

Gauss-Legendre quadrature points:

- The discrete filter is obtained by analytical integration of a selected filter kernel
- Cutoff is enforced iteratively by checking the filter's 2nd moment in physical space

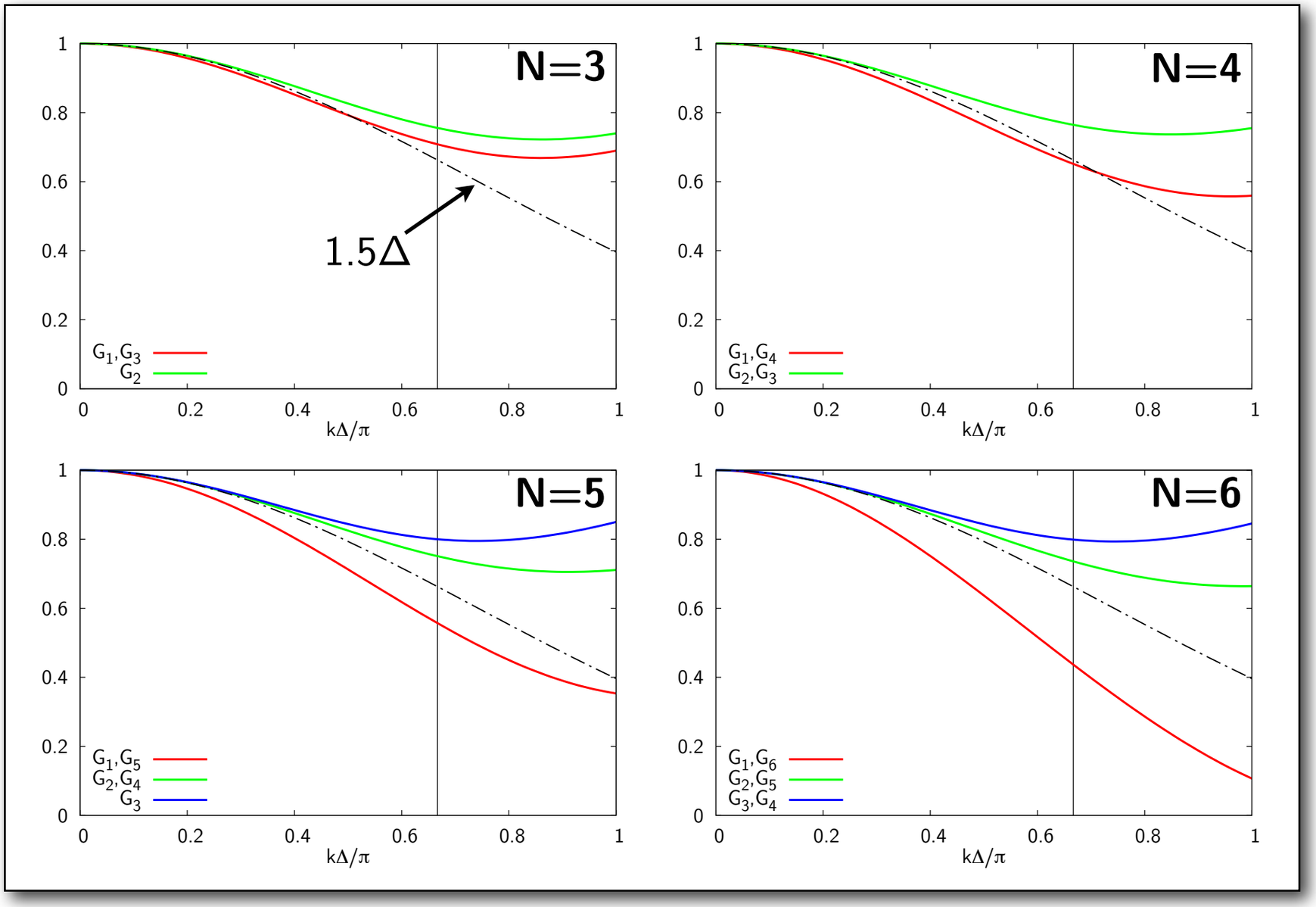

Lodato, Castonguay, Jameson (in preparation)

Discrete Filters for Arbitrary Points

Generalized method of Vasilyev et al. (1998):

- Value and slope at cutoff are enforced using a selected filter kernel (2)
- Higher moments are set to zero (N-3) + preservation of constant variable (1)

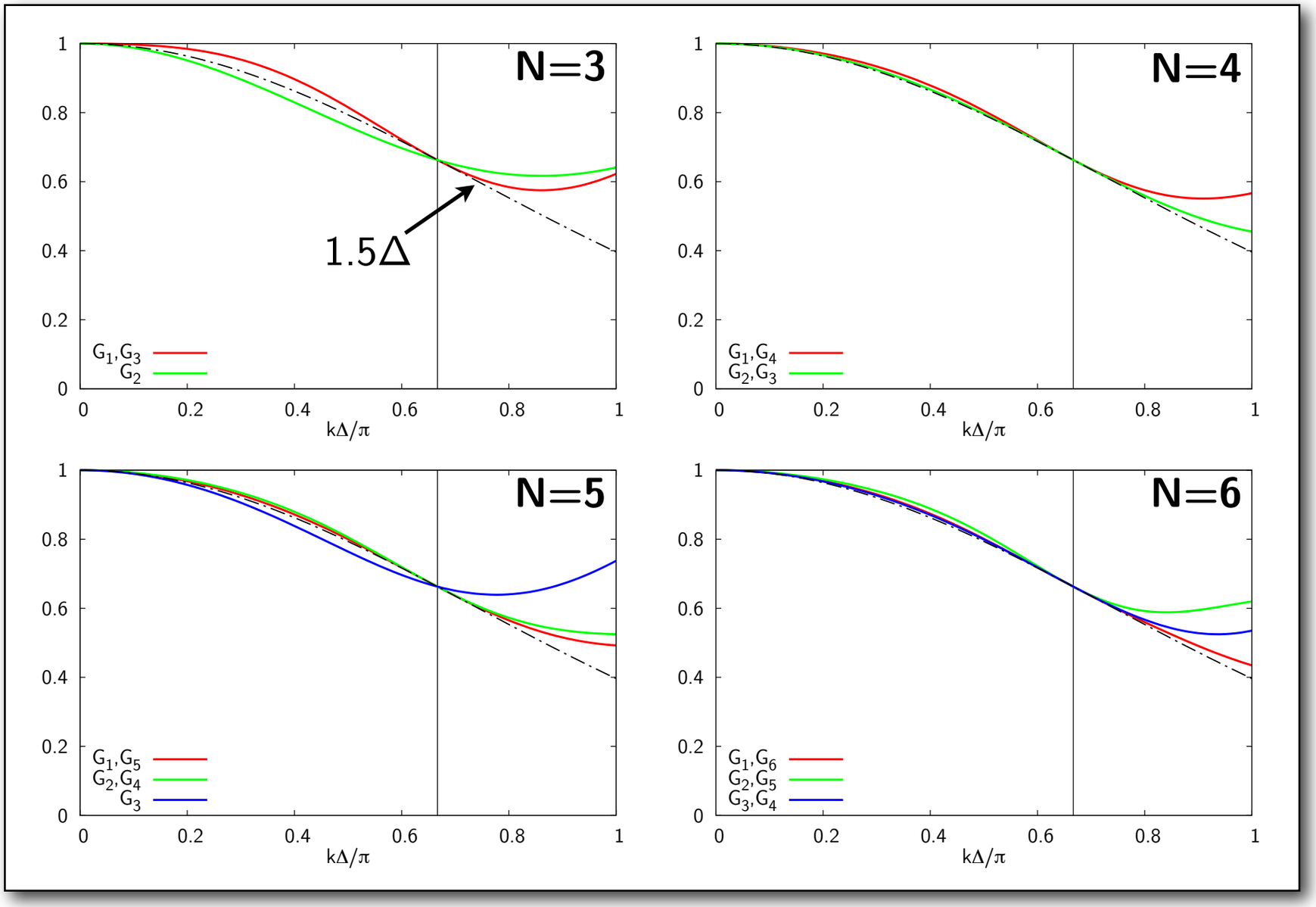

Lodato, Castonguay, Jameson (2011), CTR Annual Research Briefs; Vasilyev et al. (1998), J. Comput. Phys., 146(1)

Wall-Resolved Turbulent Channel Flow

$Re_\tau = 180$ (Δ^+: 38, 2–10, 19)

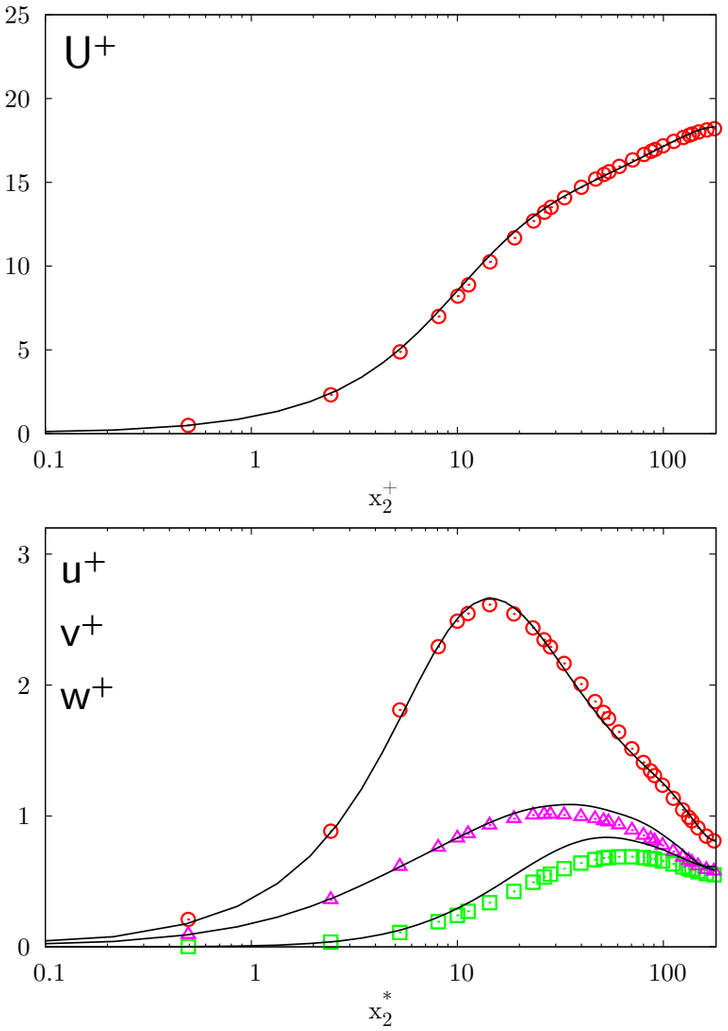

$Re_\tau = 395$ (Δ^+: 39, 1–40, 26)

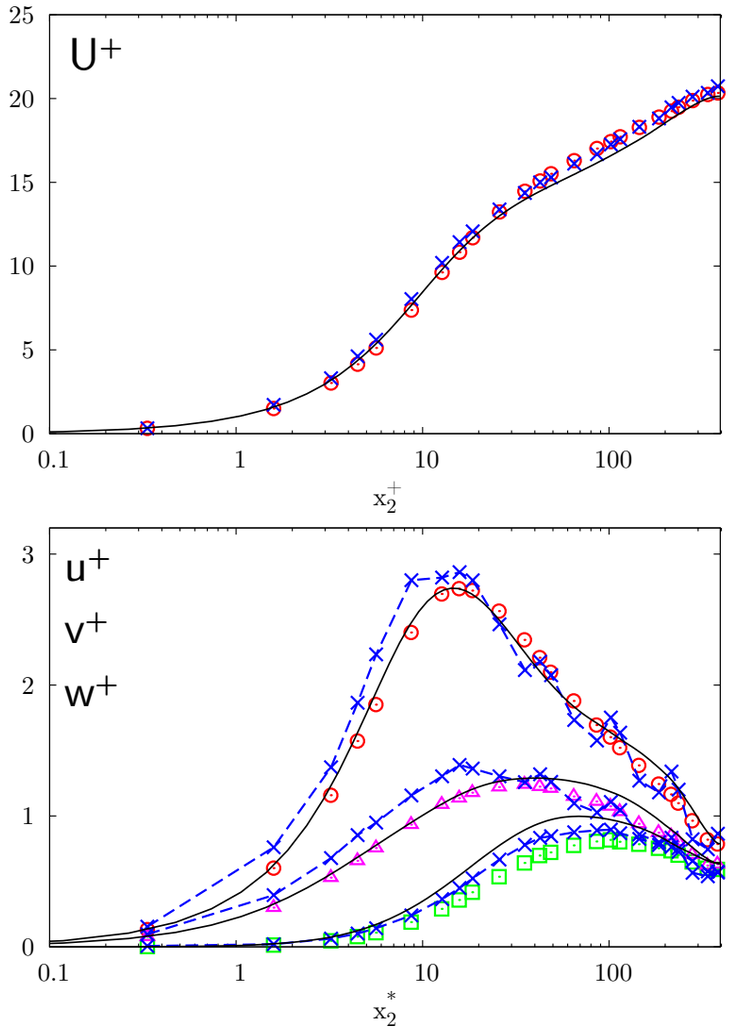

$Re_\tau = 590$ (Δ^+: 60 ,3–33 ,26)

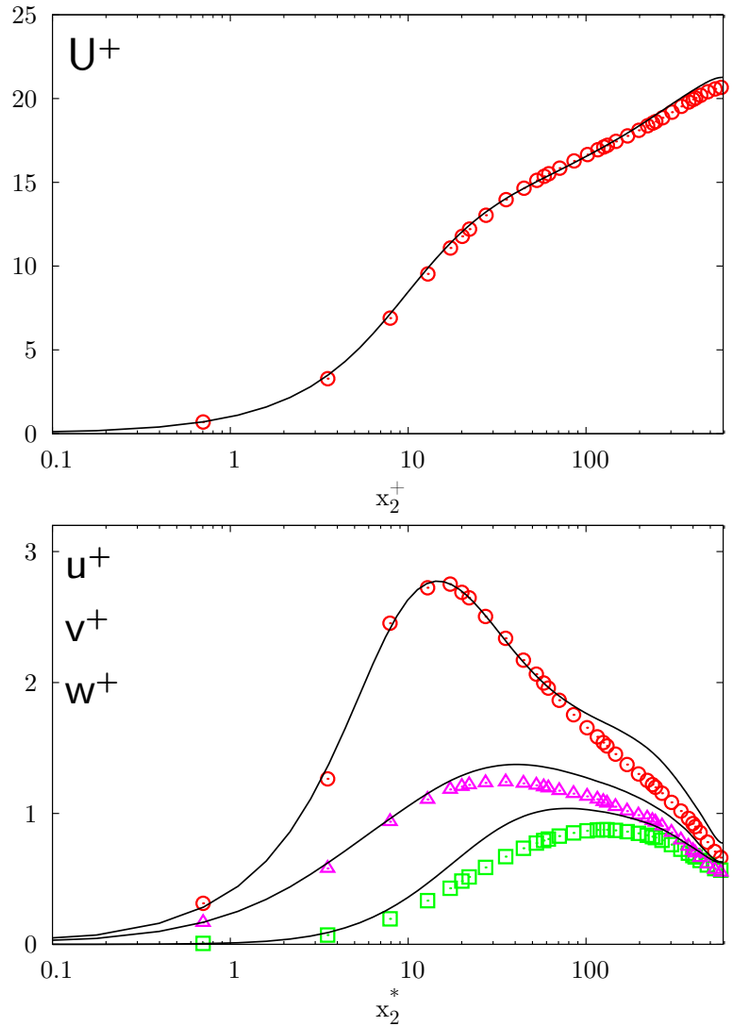

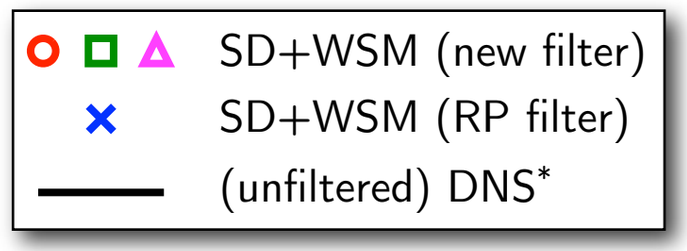

*Moser, et al. (1999). Phys. Fluids, 11(4); Lodato, et al. (2009). Phys. Fluids, 21(3); Premasuthan, et al. (2009). AIAA P., 2009-3785

Wall-Resolved Turbulent Channel Flow

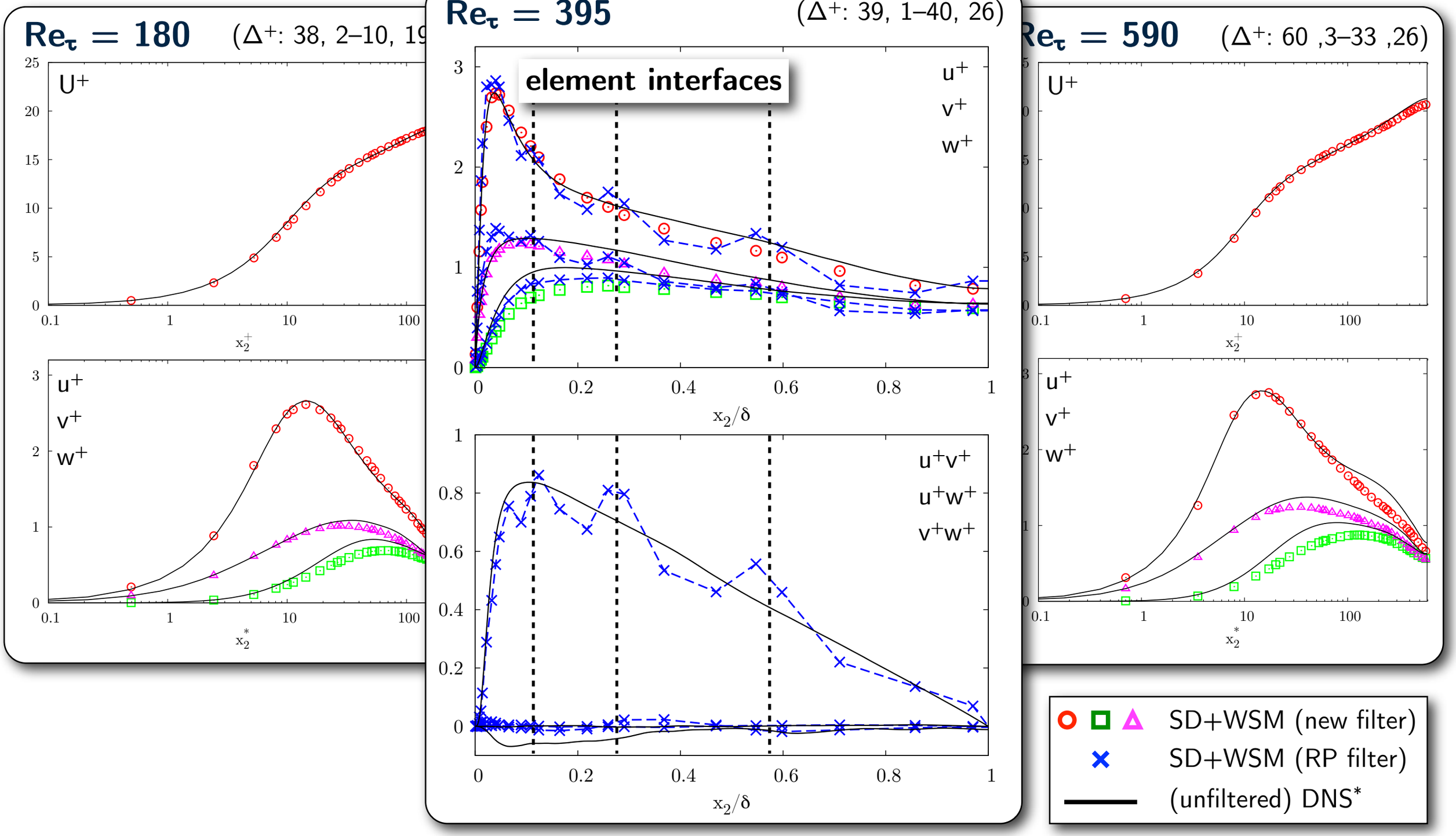

*Moser, et al. (1999). Phys. Fluids, 11(4); Lodato, et al. (2009). Phys. Fluids, 21(3); Premasuthan, et al. (2009). AIAA P., 2009-3785

Wall-Resolved Turbulent Channel Flow

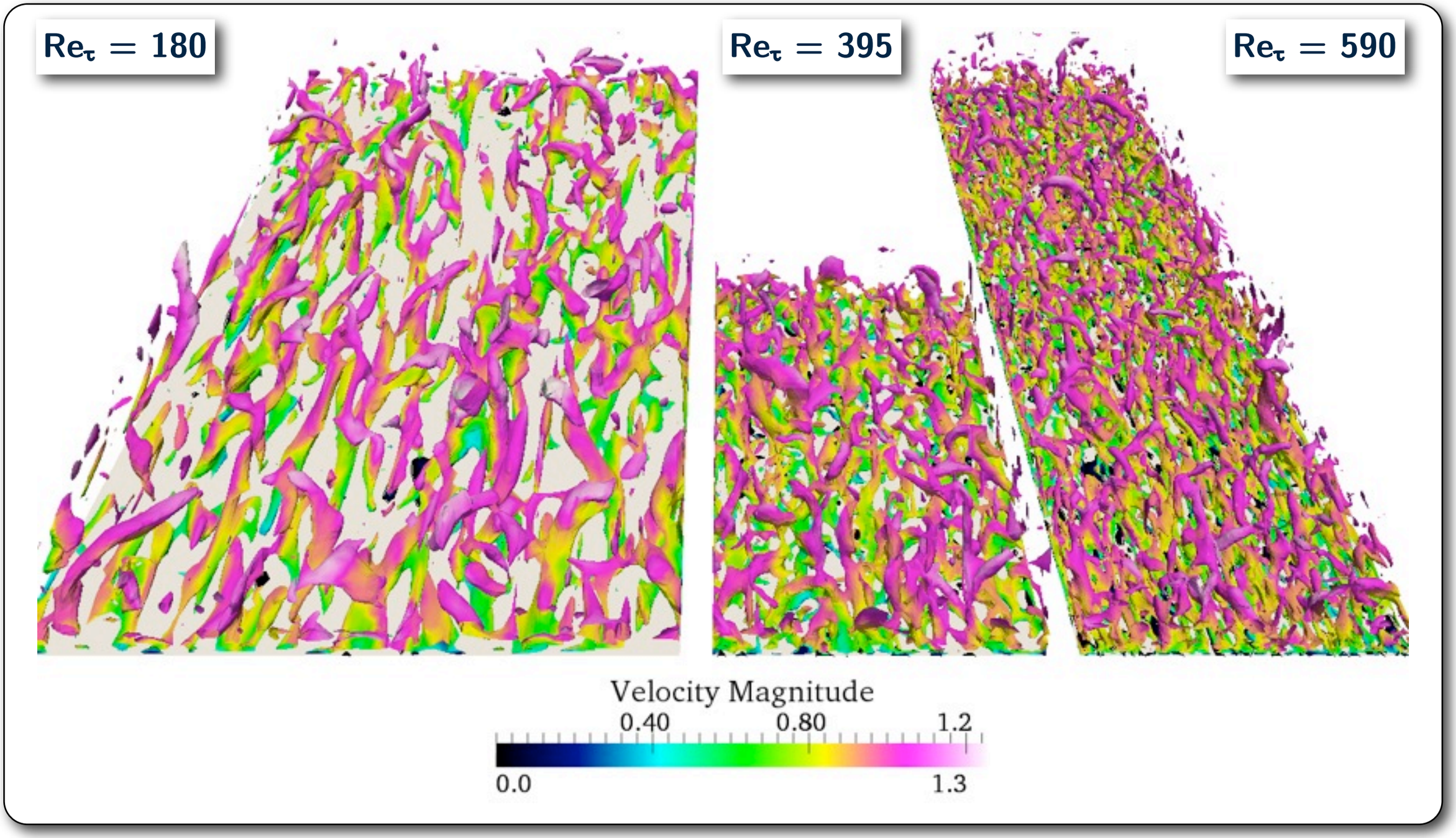

Lodato, Castonguay, Jameson (2011), CTR Annual Research Briefs; Lodato, et al. (2009). Phys. Fluids, 21(3)

Wall-Modeling Strategy

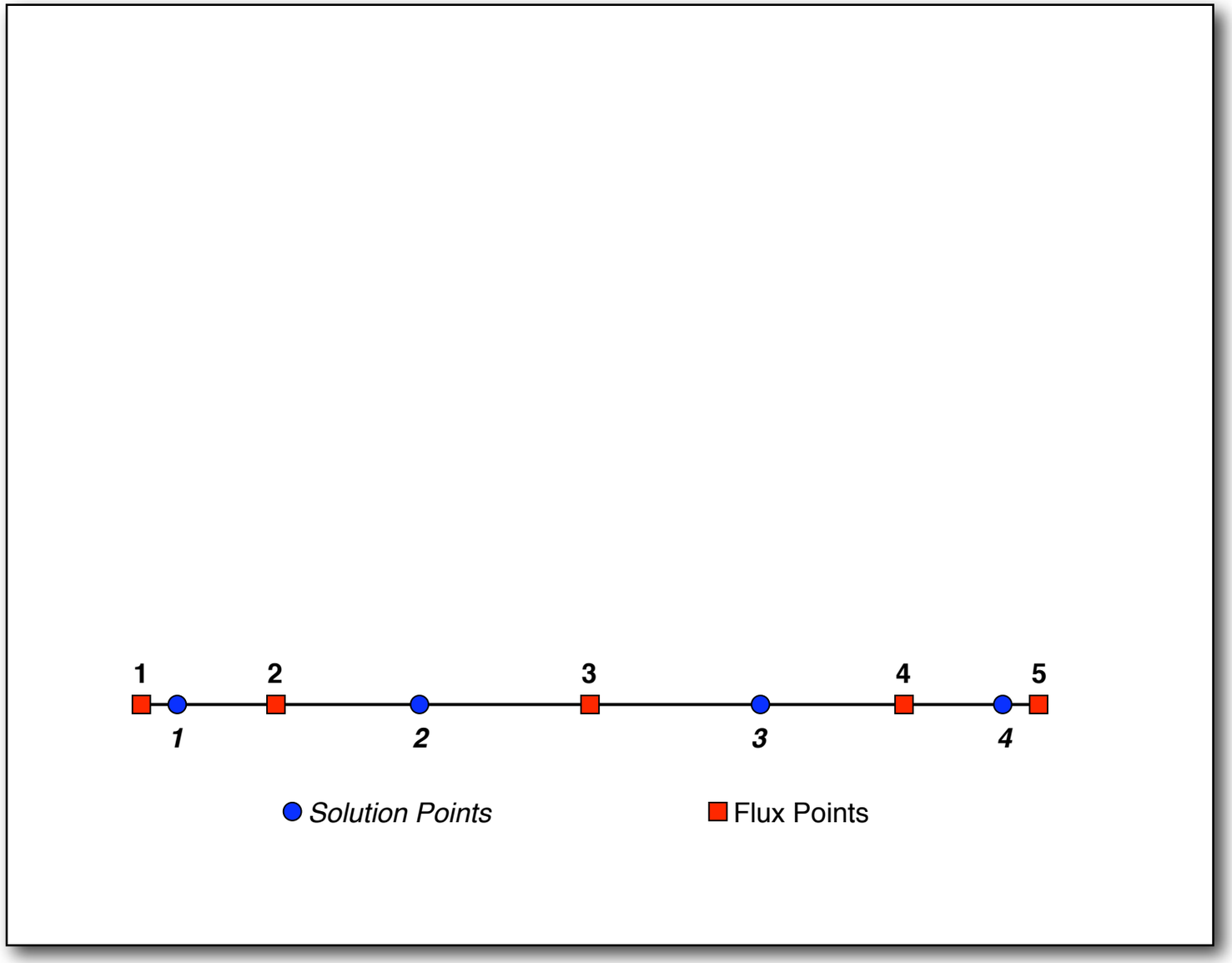

Breuer and Rodi (1996)

Wall-Modeling Strategy

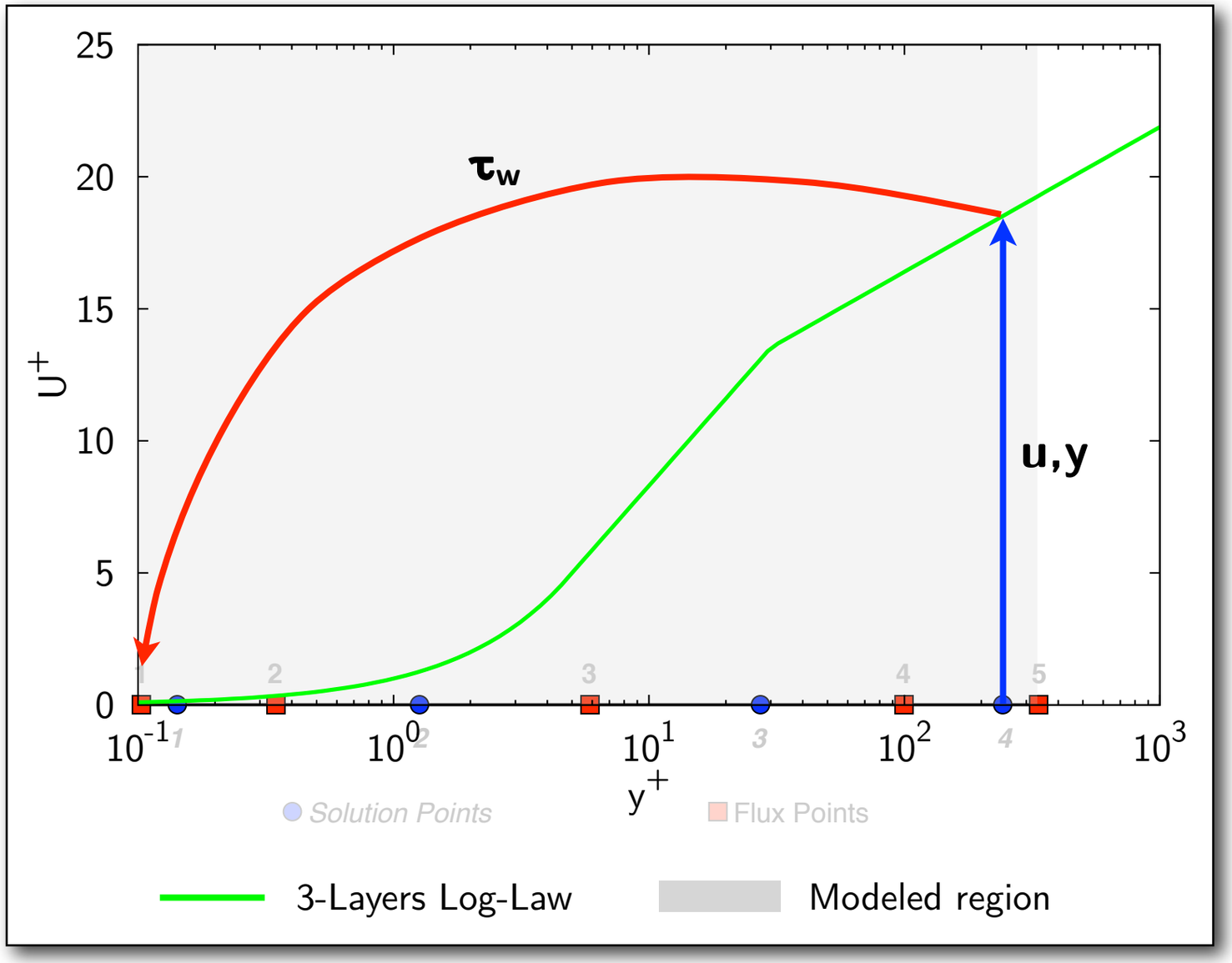

Breuer and Rodi (1996)

Wall-Modeled Turbulent Channel Flow

$Re_\tau = 590$ (Δ^+: 58, 24–47, 58)

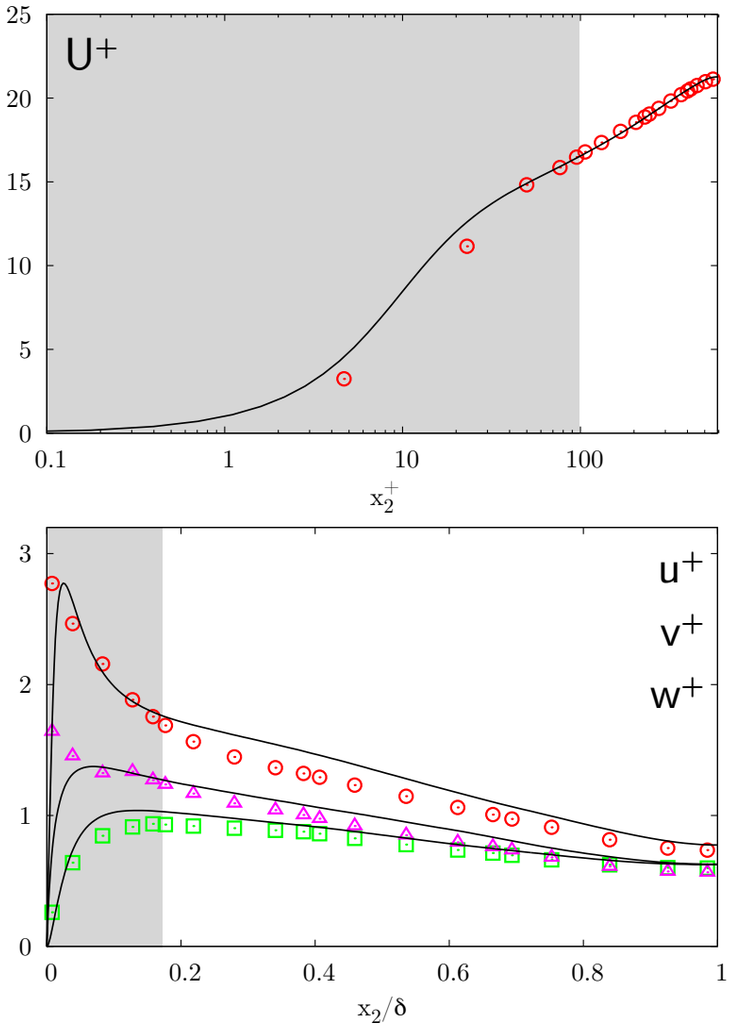

$Re_\tau = 2000$ (Δ^+: 98, 22–102, 98)

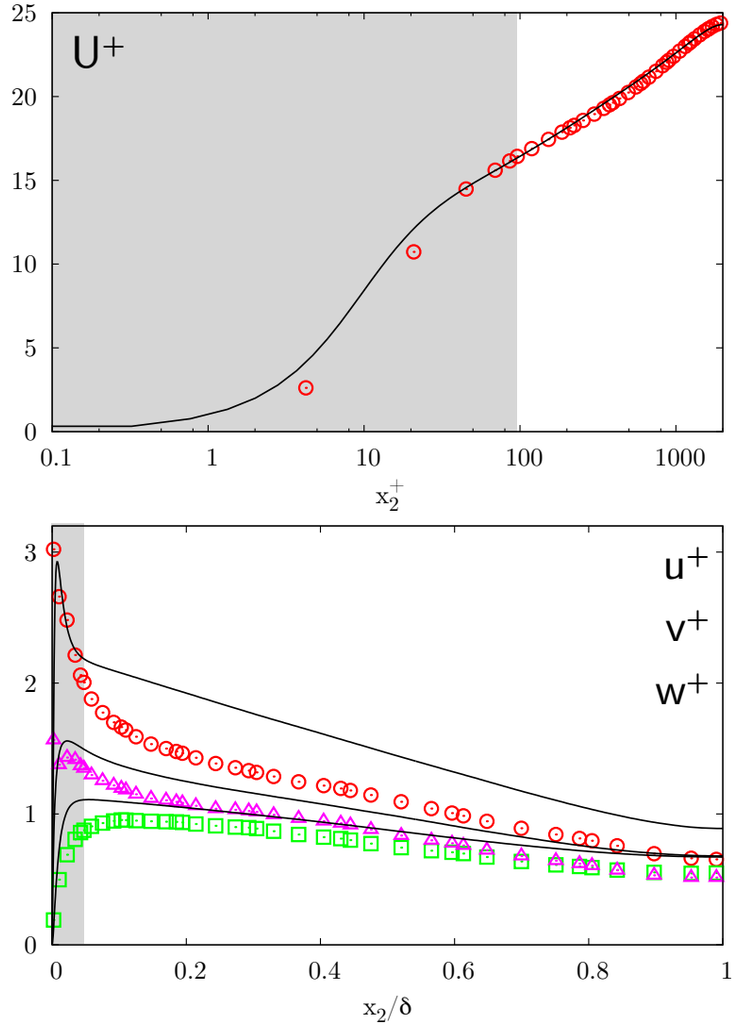

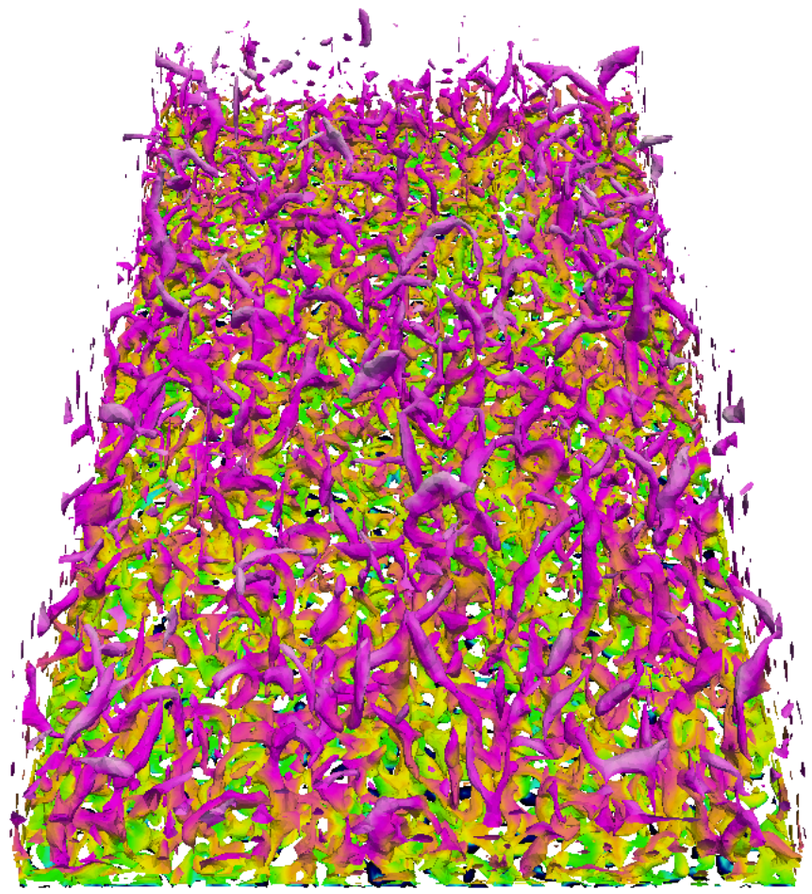

Iso-Q colored by velocity magnitude

LES with SD+WSM+LW

DNS Moser, et al., 1999 (Re_τ 590)
DNS Hoyas, Jiménez, 2006 (Re_τ 2000)

Modeled region

Moser, et al. (1999). Phys. Fluids, 11(4); Hoyas, Jiménez (2006). Phys. Fluids, 18; Breuer, Rodi (1996)

Wall-Modeled Turbulent Channel Flow

$Re_\tau = 590$

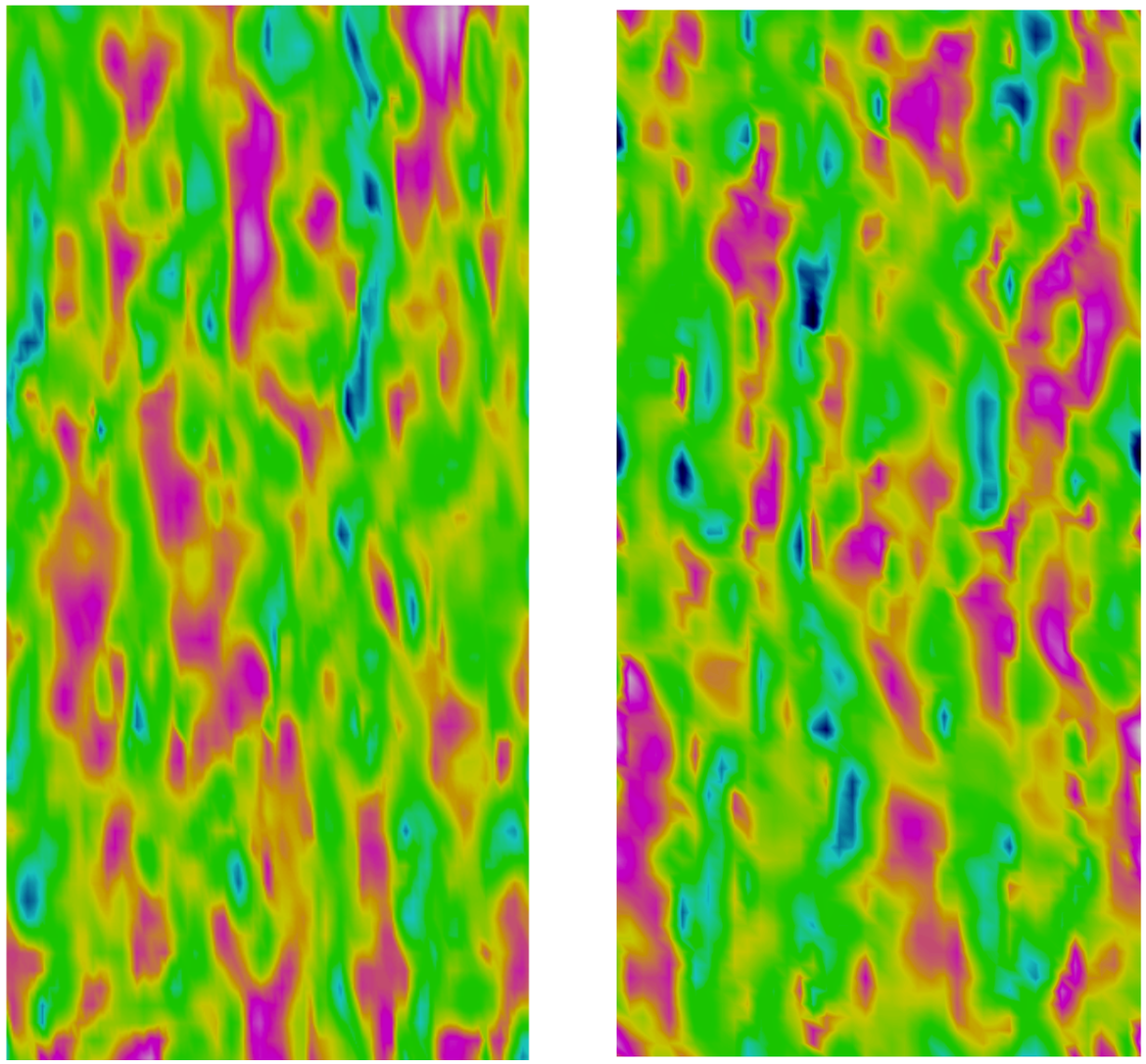

u at y^+=100

Wall-Resolved **Wall-Modeled**

$Re_\tau = 2000$

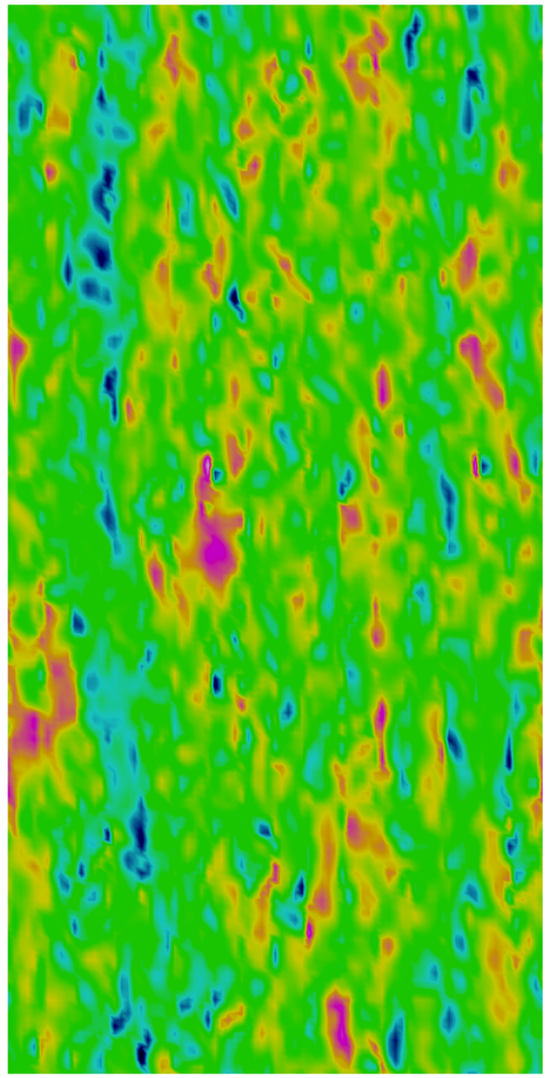

u at y^+=100

Flow past a Square Cylinder: $Re_D = 21400$

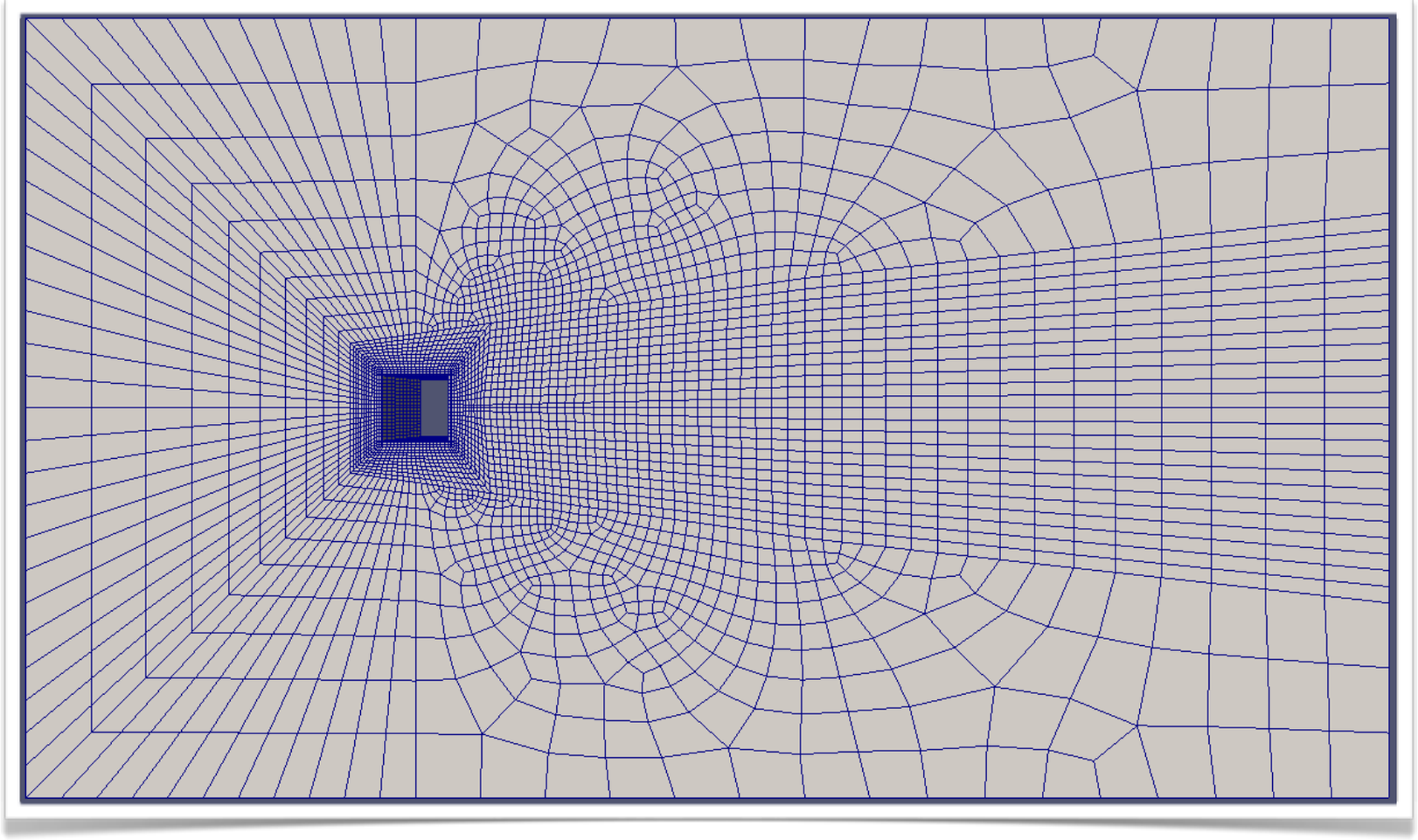

- Time integration: **RK3**
- Nº of elements: **35760** (4.5×10^6 DoF)
- Grid dimensions: **$21D \times 12D \times 3.2D$**
- Reynolds: **21400**
- Mach: **0.3**

Flow past a Square Cylinder: $Re_D = 21400$

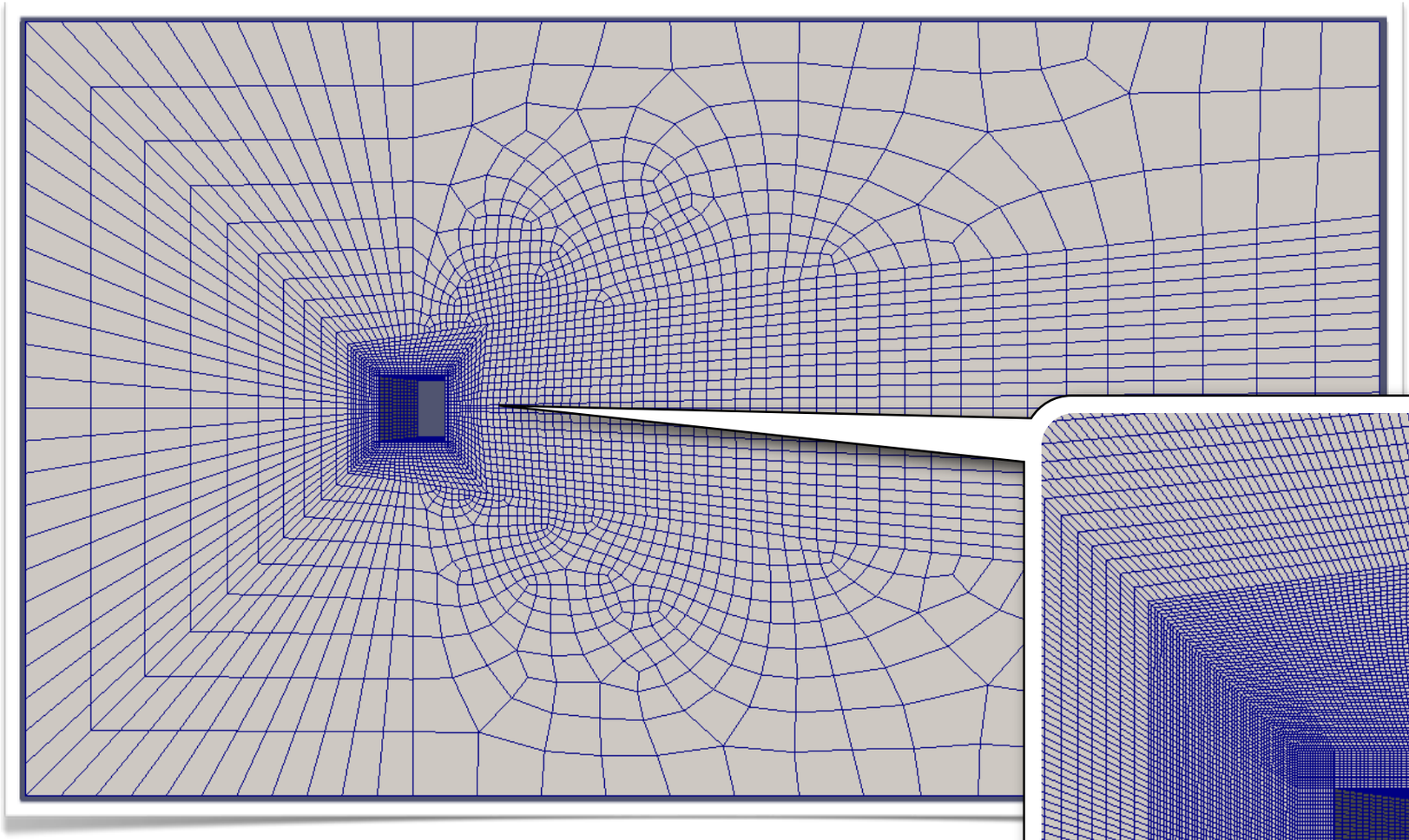

Elements

Actual resolution (N=5)

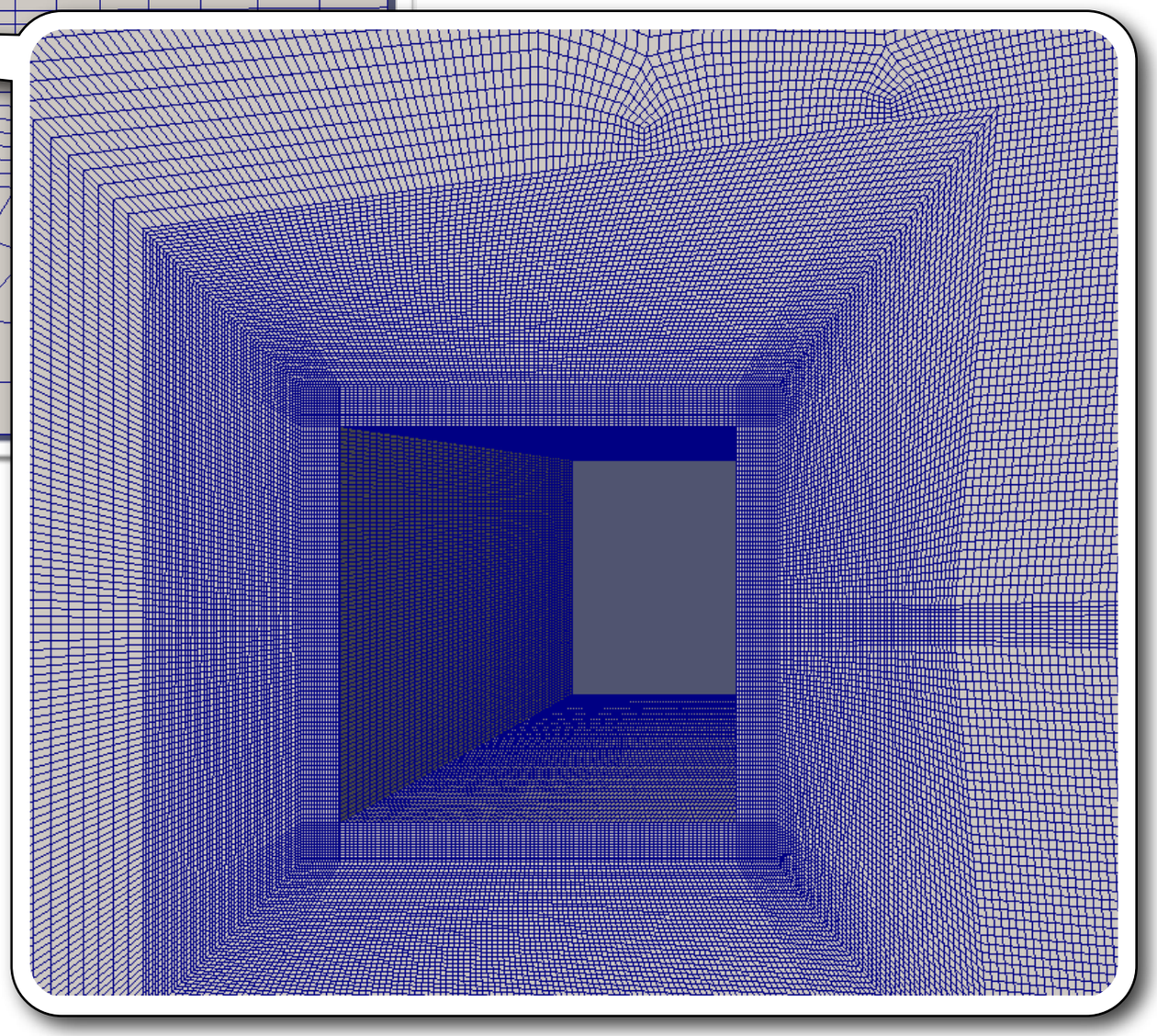

- Time integration: **RK3**
- Nº of elements: **35760** (4.5×10^6 DoF)
- Grid dimensions: **$21D\times12D\times3.2D$**
- Reynolds: **21400**
- Mach: **0.3**

Flow past a Square Cylinder: $Re_D = 21400$

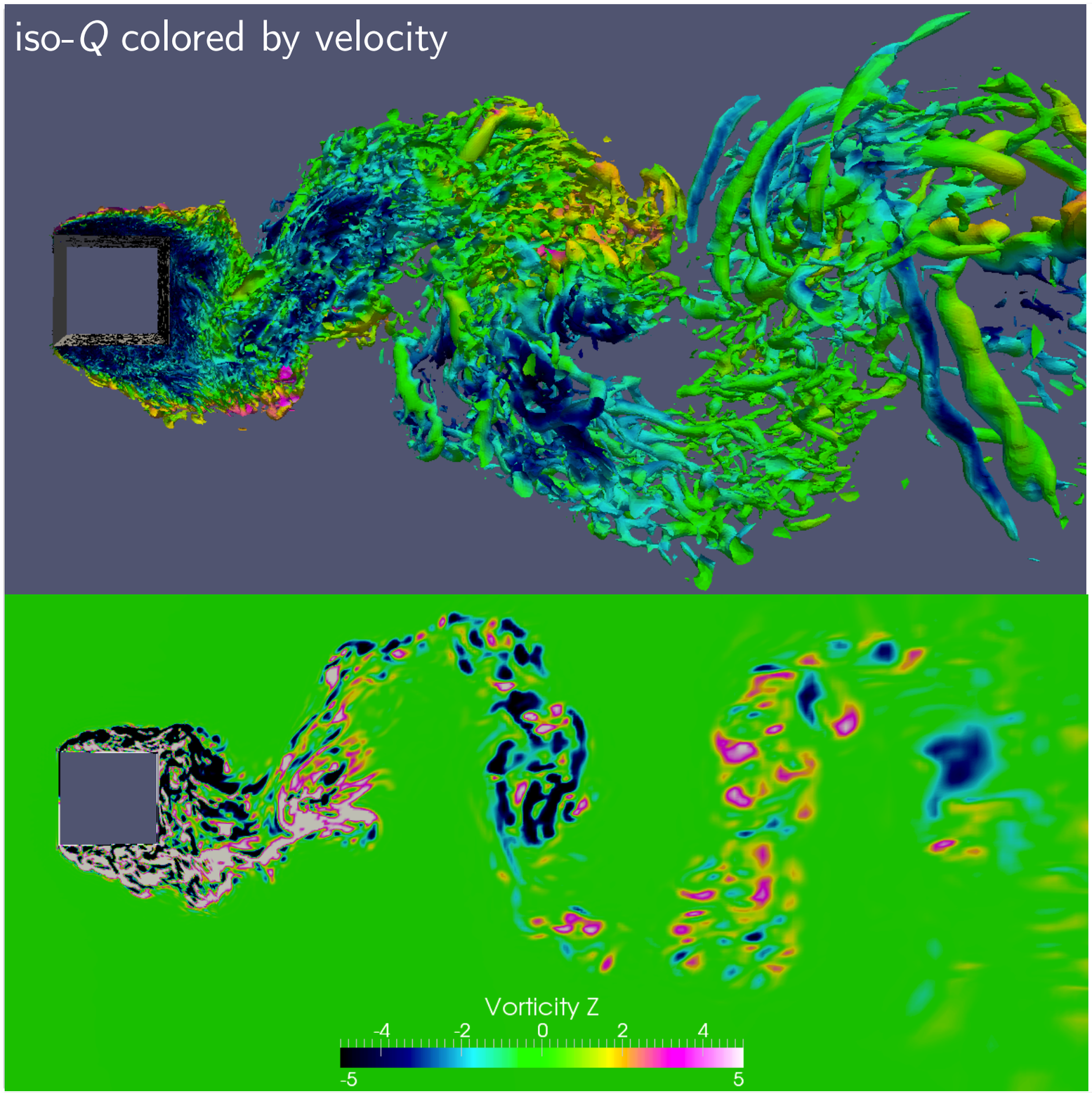

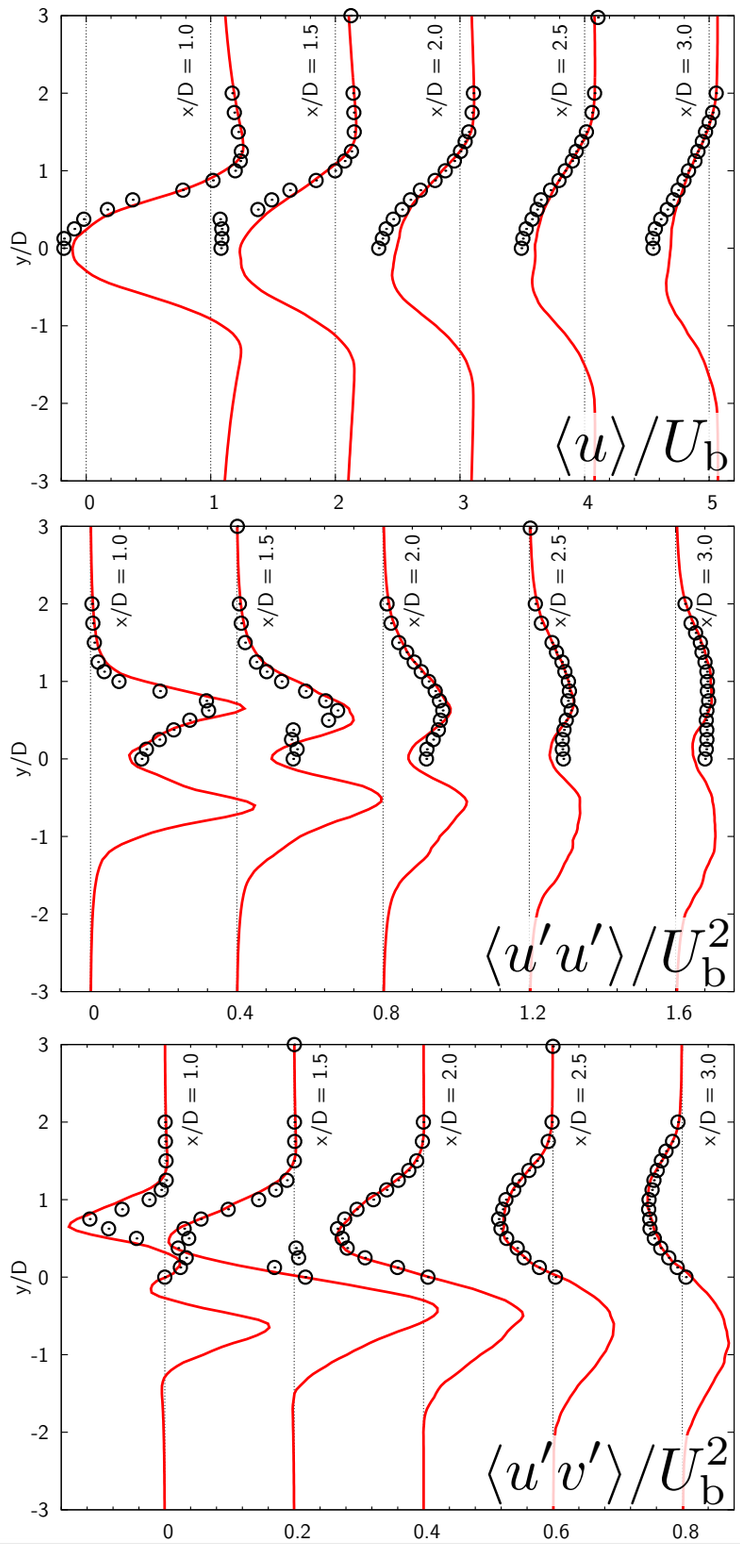

Preliminary results (work in progress)

Conclusions and Summary

- Identified a class of high-order FR schemes that are linearly stable for all orders of accuracy
- Extension to 2nd-order PDEs and triangular elements
- Thorough investigation of linear and non-linear properties of scheme
  - Identified high-order schemes with improved dispersion properties and higher explicit time-step limits compared to collocation-based DG
- ESFR schemes are:
  - Simple to implement
  - Unifying (can recover other well known high-order methods)
  - Conservative
  - Efficient (quadrature-free)

Conclusions and Summary

- Developed a 2D/3D compressible viscous flow solver based on ESFR schemes
- Verified results from theoretical analyses with numerical experiments in fluid mechanics
- Solver can handle unstructured mixed grids in 2D and 3D
- Solver can run on multiple CPUs and/or GPUs
- Efficient implementation of the schemes on GPUs allows an order of magnitude reduction in computational cost compared to traditional computer hardware
- Development of discrete filtering operators for SGS modeling
- Numerical tests on LES of turbulent channel flow and of turbulent flow past a square cylinder

A Review of the Literature from ACL

1. Castonguay, P., D. Williams, P. Vincent, M. Lopez, and A. Jameson (2011). On the development of a high-order, multi-GPU enabled, compressible viscous flow solver for mixed grids. *AIAA P.*, **vol. 2011-3229**
2. Jameson, A. (2010). A proof of the stability of the spectral difference method for all orders of accuracy. *J. Sci. Comput.*, **vol. 45**(1)
3. Jameson, A. (2011). Advances in bringing high-order methods to practical applications in computational fluid dynamics. *AIAA P.*, **vol. 2011-3226**
4. Jameson, A., P. Vincent, and P. Castonguay (2012). On the non-linear stability of flux reconstruction schemes. *J. Sci. Comput.*, **vol. 50**(2)
5. Lodato, G., P. Castonguay, and A. Jameson, Structural LES modeling with high-order spectral difference schemes. In *Annual Research Briefs* (Center for Turbulence Research, Stanford University, 2011)
6. Ou, K. and A. Jameson (2011). Unsteady adjoint method for the optimal control of advection and Burger's equations using high-order spectral difference method. *AIAA P.*, **vol. 2011- 24**
7. Vincent, P., P. Castonguay, and A. Jameson (2010). A new class of high-order energy stable flux reconstruction schemes. *J. Sci. Comput.*, **vol. 47**(1)
8. Vincent, P., P. Castonguay, and A. Jameson (2011). Insights from von Neumann analysis of high-order flux reconstruction schemes. *J. Comput. Phys.*, **vol. 230**(22)
9. Vincent, P. and A. Jameson (2011). Facilitating the adoption of unstructured high-order methods amongst a wider community of fluid dynamicists. *Math. Model. Nat. Phenom.*, **vol. 6**(3)
10. Williams, D., P. Castonguay, P. Vincent, and A. Jameson (2011). An extension of energy stable flux reconstruction to unsteady, non-linear, viscous problems on mixed grids. *AIAA P.*, **vol. 2011-3405**